Journal

of the Association of **Greek Chemists**

Issue 01

September 2024

ISSN 2945-0861

JOURNAL
OF THE ASSOCIATION OF **GREEK CHEMISTS**

Journal Scope and Aims

The Journal of Association of Greek Chemists (JAGC) aims to become an international, peer-reviewed journal, devoted to promoting the latest research and developments in a wide range of fields of chemistry. Starting in 2023 as an initiative of the Association of Greek Chemists, it is aiming to provide a unique platform for original research and scientific articles. Articles will be subjected to peer review by specialists in each field guided by distinguished Section Editors and prominent Greek researchers and academic staff.
During the initial stages, JAGC will cover primarily areas related but not limited to: Analytical Chemistry, Biochemistry- Clinical Chemistry-Biotechnology, Chemical Technology, Computational and Theoretical Chemistry, Environmental Chemistry & Technology, Forensics-Toxicology, Food Chemistry and Technology, Green Chemistry, Inorganic Chemistry, Macromolecular Chemistry, Materials Chemistry, Medicinal Chemistry, Nanochemistry, Natural Products Chemistry, Organic Chemistry, Physical Chemistry, Radiochemistry and Chemical Education.

Steering Committee of AGC

Association of Greek Chemists Headquarters
Kaningos 27, P.C. 10682 Athens,
tel: 210 3821524, 210 3829266, fax: 2103833597
info@eex.gr
www.eex.gr

Dear colleagues

With this first issue we are launching our new scientific journal, the Journal of the Association of Greek Chemists (JAGC), a pioneering platform dedicated to advancing the frontiers of science by providing a robust outlet for the dissemination of cutting-edge research, novel methodologies, and insightful reviews. The Journal of Association of Greek Chemists (JAGC) aims to become an international, peer-reviewed journal, devoted to promoting the latest developments in a wide range of fields of chemistry. Articles will be subjected to peer review by specialists in each field guided by distinguished Section Editors and prominent Greek researchers and academic staff.

During these initial stages, JAGC will cover primarily areas related but not limited to: Analytical Chemistry, Biochemistry- Clinical Chemistry-Biotechnology, Chemical Technology, Computational and Theoretical Chemistry, Environmental Chemistry & Technology, Forensics-Toxicology, Food Chemistry and Technology, Green Chemistry, Inorganic Chemistry, Macromolecular Chemistry, Materials Chemistry, Medicinal Chemistry, Nanochemistry, Natural Products Chemistry, Organic Chemistry, Physical Chemistry, Radiochemistry and Chemical Education.

The Journal of the Association of Greek Chemists is committed to the highest standards of scholarly excellence and rigor. We aim to foster innovation and collaboration across disciplines by publishing significant, high-quality contributions that reflect the latest advancements and address the most pressing challenges in chemistry.

Key features of the Journal of the Association of Greek Chemists include:

Open Access: Ensuring that all published articles are freely accessible to researchers, practitioners, and the public worldwide, promoting the widest possible dissemination and impact of the research.

Rigorous Peer Review: Maintaining a thorough and fair peer-review process to uphold the quality and integrity of the published work.

Interdisciplinary Focus: Encouraging submissions that transcend traditional disciplinary boundaries, fostering a holistic approach to scientific inquiry.
Innovative Content: Featuring original research articles, comprehensive reviews, rapid communications, and special issues on emerging topics.

We cordially invite you to explore our inaugural issue, which showcases a diverse array of pioneering studies and thought-provoking articles from leading experts in the field.

Our section editors are integral to our mission of advancing scientific knowledge and fostering innovation. Their expertise and dedication ensure that the Journal of the Association of Greek Chemists will publish high-quality, impactful research. Each editor brings a wealth of expertise and a deep commitment to advancing scientific knowledge in their respective fields. Together, they form a robust editorial board dedicated to maintaining the highest standards of scholarly excellence. Creating a strong team of section editors for a scientific journal is crucial for maintaining the journal's quality and reputation.

We are also actively seeking submissions for future issues and welcome contributions from researchers at all stages of their careers. We look forward to receiving your valuable contributions and to working with you to disseminate impactful research within our scientific community.
Detailed submission guidelines and information about the journal can be found on our website:
www.eex.gr/library/journal-of-the-association-of-greek-chemists
We are excited to embark on this journey with you and believe that the Journal of the Association of Greek Chemists will become an indispensable resource for the scientific community. Thank you for your support and engagement.
Sincerely,

The chief editor, Professor Victoria Samanidou
The publishing manager, Dr Spiros Kitsinelis

Rapid detection of soil carbonates by means of NIR spectroscopy, deep learning methods and phase quantification by powder X-ray diffraction.

Lykourgos Chiniadis[a*], Petros Tamvakis[b]

[a] Athena Research and Innovation Centre, ILSP Xanthi's Division, Xanthi 67100, Greece,
b Hellenic Open University, School of Sciences and Technology, 26335 Patras, Greece
e-mail: Lykourgos Chiniadis: lykchiniadis@gmail.com and Petros Tamvakis: tamvakis.petros@ac.eap.gr
*Corresponding author
ORCID(s): LC 0000-0002-7118-9942, PT 0000-0001-9514-8283
DOI: 10.62579/JAGC0001

Authorship contribution statement

Lykourgos Chiniadis: Conceptualization, Data acquisition, Writing – review and editing, Validation, Formal analysis, Supervision.
Petros Tamvakis: Conceptualization, Data curation, Writing – review and editing, Validation, Programming, Formal Analysis, Visua

ABSTRACT

In this study we propose a novel rapid and efficient way to predict carbonates content in soil by means of Fourier Transform Near-Infrared (FT-NIR) reflectance spectroscopy and by use of deep learning methods. In addition to using traditional machine learning algorithms, we exploited multiple deep learning methods, such as: 1) a Multi-Layered Perceptron Regressor (MLP) and 2) a Convolutional Neural Network (CNN) in an attempt to compare their performance with other classical machine learning algorithms, which up until now were considered the field's standards, such as Partial Least Squares Regression (PLSR), Cubist and Support Vector Machines (SVM) on the combined dataset of two NIR spectral libraries: Kellogg Soil Survey Laboratory (KSSL) of the United States Department of Agriculture (USDA), a dataset of soil samples reflectance spectra collected nationwide, and Land Use and Coverage Area Frame Survey (LUCAS) TopSoil-2015 (European Soil Library) which contains soil sample absorbance spectra from all over the European Union, and use them to predict carbonate content on never-before-seen soil samples. In this study, absorbances in the NIR spectral region (1150-2500 nm) were utilized in two different ways: a) as one-dimensional data and b) as two-dimensional spectrograms which, to our knowledge, is a completely novel approach that has rarely been researched. Quantification of carbonates by means of X-ray-Diffraction is in good agreement with the volumetric method and the MLP prediction. Our work contributes to rapid carbonates content prediction in soil samples in cases where: 1) no volumetric method is available and 2) only NIR spectra absorbance data are available.

1. Introduction

NIR spectroscopy is a rapid, non-destructive method of low cost that provides excellent correlation of observed and predicted values when regression algorithms are applied in spectral data and especially in large datasets (1–3). Early research studies in soil properties are using minimal input in terms of soil samples collected and considering minimal geographical areas and locations (4,5). These studies typically modeled total carbon (tC) and soil organic carbon (SOC) (2,5–8), soil organic matter (SOM) (9,10), soil inorganic carbon and carbonates (SIC) (11), total nitrogen (tN) (12–18), phosphorous content (12), potassium content (12), clay (18,19), pH (15,16), moisture content (6,20,21) and cationic exchange capacity (CEC) (18,22). Some studies had also modeled other properties specific to their objectives, such as total elemental content e.g., in (15). Computational progress and especially new algorithms applied in the spectral data are nowadays efficient to predict soil properties for larger datasets and fields, acquiring hundreds and thousands soil samples over locations of interest to generate large databases of spectral and physicochemical properties. Recently, hyperspectral NIR spectral data acquisition is even possible using satellites with high resolution data acquired (23).

Graphical Abstract

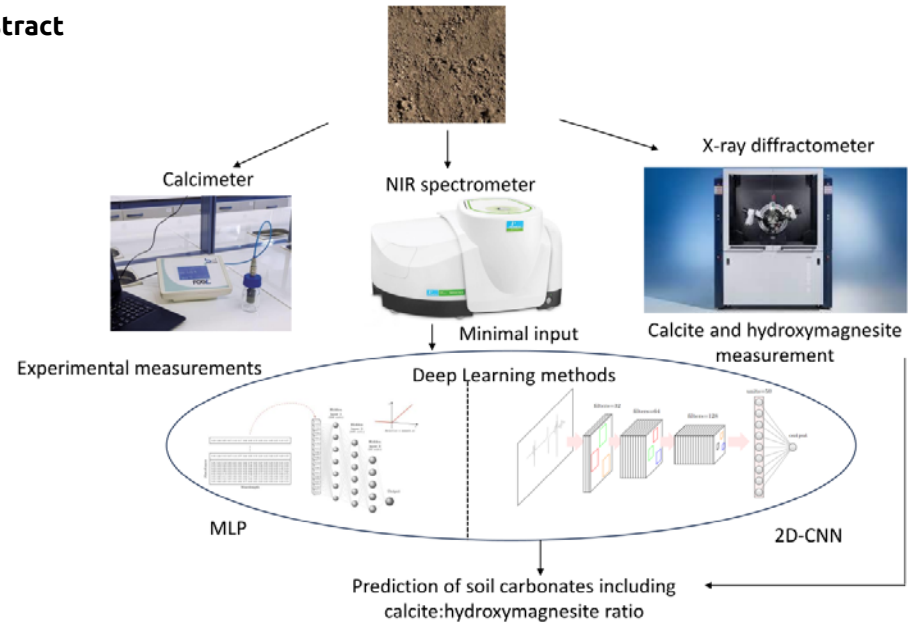

***Figure 1**: The pipeline of collection of soil samples, experimental and theoretical assessment, and prediction of carbonates. Soil samples were collected from two distinct areas in Xanthi and Alexandroupolis fields and were sieved to >250μm. Furthermore, NIR spectra were acquired and calcimetry was applied in addition to calibration dataset generated by large spectral libraries (KSSL, USDA and LUCAS-2015-TopSoil). This calibration dataset, with spectra in the NIR region, was utilized for applying different regression models (namely PLSR, SVM, Cubist, MLP and 2D-CNN). MLP method outperformed other methods in prediction of carbonates in soil samples. Saliency map from 2D-CNN deep learning method, also indicated hydromagnesite peaks in the samples and XRD verified the presence of hydromagnesite quantitatively. It should be noted that apparatus is utilized exactly as appeared in this figure.*

2. Related Work

Machine Learning (ML) techniques were introduced in chemometrics and soil spectroscopy as a means for information extraction and soil properties prediction. Both traditional ML and Deep Learning (DL) approaches have been extensively adopted (1,6,28) because of their intrinsic property to handle high dimensional data such as spectra. Deep neural networks, in particular, are capable of handling data in almost every form e.g. tabular data, text, images and audio, coupled with recent increases in computational power and the expansion of system memory capabilities, now make possible the use of spectral data to perform spectrogram-based analysis for soil properties predictions. As there are usually thousands of predictor variables (reflectance values), neural networks make an excellent choice for such a task because of their intrinsic trait to handle well data that suffer from high dimensionality. Convolutional Neural Networks (CNN) (29) have been used in image recognition with remarkable success and constitute one of the most powerful DL techniques for modeling complex processes such as pattern recognition in image based applications. Recently, Tsakiridis et al., (2020) utilized CNNs to predict multiple soil properties (30). The successful use of CNNs for soil property prediction without the use of pre-processed spectra was demonstrated in (31). They proposed the representation of raw spectral data as a two-dimensional (2D) spectrogram and showed its superior performance over traditional ML techniques such as Partial least squares regression (PLSR) (32) and Cubist regression trees (33). Ng et al., (2019)laboratories have become equipped with various spectrometers. By fusing output from different spectrometers, better prediction outcomes are expected than using any single spectrometer alone. In this study, model performance from a single spectrometer (visible-near-infrared spectroscopy, vis-NIR or midinfrared spectroscopy, MIR used the combined spectra of soil samples to train 1D and 2D CNNs that both outperformed traditional ML techniques (34)laboratories have become equipped with various spectrometers. By fusing output from different spectrometers, better prediction outcomes are expected than using any single spectrometer alone. In this study, model performance from a single spectrometer (visible-near-infrared spectroscopy, vis-NIR or midinfrared spectroscopy, MIR.

In our study, we compare different methodologies and techniques based on both computational regression techniques on NIR spectral data and experimental methods that usually apply on soil samples. Neural Networks algorithms outperformed the linear models for the soil carbonates content prediction as one term, and secondly, in the prediction of important NIR peaks. Classic mineralogical and analytical methods were also applied in soil samples establishing the feasibility of introducing neural networks regression methods in soil NIR spectra.

Much effort is given towards elucidating soil properties in all continents and all recorded data is valuable knowledge for today and future research. Moreover, data science applied to spectral and physicochemical libraries for the construction of calibration libraries is a novel approach redefining universal scientific effort. Non-destructive and scientific effective methods are a new path in modern soil research and is adding value from a spectroscopic point of view.

3. Methodology

This research introduces a novel and efficient and expeditious method for forecasting soil carbonates content utilizing non-destructive Fourier Transform Near-Infrared (FT-NIR) reflectance spectroscopy and advanced deep learning techniques. The study assesses the performance of two deep learning models—namely, a Multi-Layered Perceptron Regressor (MLP) and a Convolutional Neural Network (CNN. Model training is performed on the consolidated dataset from two Near-Infrared (NIR) spectral libraries: the Kellogg Soil Survey Laboratory (KSSL) of the United States Department of Agriculture (USDA) (https://ncsslabdatamart.sc.egov.usda.gov/), which is a service agency that has been collecting spectral and other data, measuring physicochemical soil properties and location characteristics to vis-NIR and MIR spectra across the United States of America, uploading and sharing the data, since 80 and more years until nowadays and the Land Use and Coverage Area Frame Survey (LUCAS) European Topsoil dataset (25)2009–2012 and 2015. A new sampling series will be undertaken in 2018, with new measurements included. The organization for the 2018 sampling campaign represents an opportunity to summarize past LUCAS Soil achievements and present its future objectives. In 2009–2012 and 2015, LUCAS Soil surveys targeted physicochemical properties, including pH, organic carbon, nutrient concentrations and cation exchange capacity. Data from 2009–2012 (ca. 22 000 points (https://esdac.jrc.ec.europa.eu/content/lucas2015-topsoil-data). Other similar spectral libraries include the Brazilian Soil Spectral Library (BSSL) (26) global soil datasets (1) and the Chinese vis–NIR soil spectral library (CSSL) (27).

The prediction models are trained on these extensive datasets and are then applied to predict carbonate content in previously unobserved soil samples collected from Xatzisavva wine fields in Alexandroupolis, Greece and Vourvoukelis vineyards in Avdira, Greece. We compare predictions with the predictions of more conventional machine learning algorithms like Partial Least Squares Regression (PLSR), Cubist, and Support Vector Machines (SVM) which are considered the standards in this research field. To validate models' accuracy and performance, we also evaluate all models' results against the results of our laboratory volumetric methods (Figure 1).

3.1. Study Area

The investigated area falls within the so-called areas of wine fields of Vourvoukelis winery in Avdira in Xanthi, Greece (40° 54' 20'' N, 25° 48' 24''E) and of organic wine fields of Xatzisavva winery in Alexandroupolis, Greece (41° 00' 09'' N, 24° 55' 00'' E).

3.2. Sample pretreatment

The diffuse NIR reflectance spectra of air-dried and (<250 μm) sieved soil samples were measured in the laboratory. Before spectral measurements, the samples were placed in glass Petri dishes and spectral acquisition was performed with thickness of the sample of ~3-4 cm to avoid transmission effects, for all samples. Background spectra was subtracted from all acquired NIR spectra.

3.3. Spectral acquisition

A Perkin-Elmer Spectrum N Two FT-NIR spectrophotometer (quartz beamsplitter and $LiTaO_3$ NIR detector based on diode array) was used for spectral measurements in the spectral region of 1150–2500 nm. The spectral data was screened to ensure percentage reflectance measurements did not exceed theoretical limits, from 0.0 to 100.0. All spectra were exported to wavelength intervals of 0.5 nm. Absorbance spectra were calculated by means of equation (1).

3.4. Pretreatment of spectral libraries as calibration dataset

The soil spectra were transformed using three pretreatment methods prior to chemometric modeling, as the best treatment was not known a priori. This technique included the (pseudo) absorbance transformation, normalization of spectra between values 0-1, Savitzky-Golay smoothing filtering with a window size of 11, polyorder of 2 for the differentiating SG-1 and window size of 13, polyorder of 2 for the differentiating SG-2 (35) were applied to the spectral data to reduce noise and enhance spectral features to all calibration data of both KSSL-LUCAS 2015 TopSoil libraries combined, in order to reduce undesirable variance of the data to improve the predictive capacity of the calibration models. These procedures were applied to the original reflectance spectra (R) for KSSL (USDA) and TopSoil 2015 (Europe) and transformed to Absorbance (A) by the following equation:

$$A = \log_{10}(1/R) \quad (1)$$

No transmission (T) is observed due to the large thickness of the sample measured with the NIR spectrophotometer. Data screening resulted 28,615 samples for modeling with PLSR, Cubist, SVM, MLP and CNN models. Spectra of KSSL-USDA spectral library were transformed from percent reflectance

to absorbance, by means of equation (1). The values of $CaCO_3$ were normalized to g/100g since LUCAS-TopSoil laboratory measurement unit of $CaCO_3$ is in g/kg.

In machine learning applications, it is a well-known fact that the size of the training set plays a crucial role in generalization. Generalization is the ability of the model to perform well on never-before-seen data. Typically, we aim for a large, diverse training set and to that end a decision was made to merge the two spectral libraries into a larger one. Before merging, we compare both spectral datasets based on the Wasserstein metric which is a common way to compare the probability distributions of two variables:

$$W_p(P,Q) = \left(\frac{1}{n}\sum_{i=1}^{n}\left|\left|X_{(i)} - Y_{(i)}\right|\right|^p\right)^{\frac{1}{p}} \quad (2)$$

where ***P, Q*** are probability distributions (one-dimensional) and ***p*** is the number of moments. The results show that the two libraries are similar enough to be merged (Wasserstein distance=1.78). Comparison of the new combined training dataset with the test set shows low similarity between them (Wasserstein distance=6.48), which raises a concern of how well our model will perform on the test set.

3.5. Laboratory carbonates measurement

Results throughout this study are given as CO_3^{2-} equivalents. The measurement is based on measuring the gaseous CO_2 released from carbonate reacting with 6M HCl and is expected to be equally effective at measuring soil carbonates released from the full range of carbonate soil minerals including common forms such as calcite, magnesite, and dolomite and their hydrous compounds.

Carbonates equivalents were determined at both locations by pressure calcimeter method treating the <250 µm soil fraction with 6M HCl in a closed vial. At KSSL this was volumetric method 4E1a1a1 (https://www.nrcs.usda.gov/sites/default/files/2023-01/SSIR42.pdf, accessed on 20 November 2022), and at LUCAS-Topsoil this method was similar volumetric method with ISO 10693:1995 (https://esdac.jrc.ec.europa.eu/public_path/shared_folder/dataset/66/JRC121325_lucas_2015_topsoil_survey_final_1.pdf, accessed on 21 November 2022).

3.6. Model Accuracy Evaluation

In order to evaluate the model accuracy, four statistical metrics were applied, namely the coefficient of determination (R2), the Root Mean Square Error of calibration (RMSE), the Residual Prediction Deviation (RPD), and the Ratio of Performance to Inter-Quartile distance (RPIQ) as shown in the following equations (2)-(5). The R^2 measures the percentage of variance of the dependent variable as influenced by the independent variable. The RPD is explained as the ratio of standard deviation of the measured reference values to RMSE and it is used for NIR spectra in soil science as a value of correctness of the model. Also, RPIQ is explained as the ratio of the standard deviation of the inter-quartile distance of the measured reference data to RMSE.

A combination of the R^2 and RPD statistical metrics is allowing predictions to be favored or not. In more details, when $R^2 > 0.90$ and RPD > 3.0, excellent prediction is provided by the model. When $0.82 < R^2 < 0.90$ and 2.5 < RPD < 3.0 a good approximation is feasible by the model. In addition, moderate approximation is made when $0.66 < R^2 < 0.82$ and 2 < RPD < 2.5. Finally, poor distinction of high and low values are performed when R2 < 0.66 and RPD < 2 as shown in (3).

$$\boldsymbol{R^2}(y,\hat{y}) = 1 - \frac{\sum_{i=1}^{n}(y_i-\hat{y}_i)^2}{\sum_{i=1}^{n}(y_i-\bar{y})^2} \quad (3)$$

where y_i and $\hat{y}_i$ are measured values and predicted values, respectively; n is the number of samples in the training set,

$$\mathbf{RMSE} = \sqrt{\frac{1}{N}\sum(y_{pred} - y_{obs})2} \quad (4)$$

where N is the sample size, y_{pred} is the predicted value, and y_{obs} is the observed value. Typically, the model with the lowest RMSE is chosen.

RPD = STDEV(yobs)/RMSE (5)

RPIQ is the ratio of performance to inter-quartile distance of the reference data in the external validation set). RPIQ is proposed to be applied instead of RPD in soil samples sets, for which often show a skewed distribution. As a result, RPIQ is a better way to standardize the RMSE in terms of population spread compared to RPD. RPIQ is based on quartiles representing the Q1 as the value below which 25% of the samples is found, Q2 as the value below where 50% of the samples are found and Q3 as the value below where 75% of the samples are found. Such an approach as described in equation 5 is useful to determine equivalent ranges of population spread (3).

RPIQ = IQ/RMSE (6)
where IQ = (Q3-Q1)

3.7 XRD Quantification

The samples were measured in a Bruker D8 Focus diffractometer with Bragg– Brentano configuration, operating at a voltage of 40 kV and an intensity of 40 mA. It contains a primary monochromator, working with a copper anti-

cathode, Cu $K\alpha_1$ monochromatic radiation (λ = 1.54056 Å). Acquisition was performed in 2θ scanning mode covering the 5-90° range with steps/sec of 0.02°. Samples were grinded until the fine powder was less than 20 μm. The powder was mounted in a circular quartz holder. The phases included in the refinement were all the minerals that were identified by Profex and BGNM libraries according to their peak intensities.

The Rietveld method (Rietveld, 1969) is a method that theoretically adjusts the structural and experimental parameters to the complete powder diffractogram profile of the sample, considering it as the sum of the Bragg reflections that appear at respective angular positions form crystalline material in the sample. It is considered as a total approach to mineralogical quantification. In addition, $x^2 < 5$ was considered as acceptable refinement statistics based on the complexity of soil samples examined in this study and based on previous similar work of clay material XRD analysis (36).

4. Algorithms and implementation

4.1 Partial Least Squares Regression

PLSR is a linear chemometric technique used for analysis of spectroscopic data for different applications. In our study, PLSR is used for the determination of soil carbonate content and is presented as a common modelling technique for quantitative spectroscopic analysis in soil mapping and classification as found in the literature (7,32,37) large amounts of diffuse cadmium (Cd. Decomposition of the spectral data into features (namely collective variables) is performed. The collective variables include most of the variance that exists in the reflectance NIR spectral data and thus linear models of the most correlated features are created.

$$X=T \cdot P^T+Residuals(E) \quad (7)$$

$$Y=T \cdot C+Error(f) \quad (8)$$

In PLSR, a decomposition of the ***X*** and ***Y*** variables with finding new latent variables and a selection of orthogonal factors that is maximizing the relation between prediction variables (X-soil reflectance) and response variables (Y-laboratory measured data) is performed. Components T that allows the decomposition of the predictors are searched by the PLSR (eq.1) and prediction of the response variables is also performed (equation 2). ***P*** and ***C*** are the factor loadings, and ***E*** and ***f*** are the residuals and errors matrices, respectively (38).

In our study, the PLSR was performed with the optimum 22 collective variables (CV's) in the existing NIR reflectance spectra acquired by the KSSL-USDA combined to LUCAS-TopSoil libraries (Figure 2).

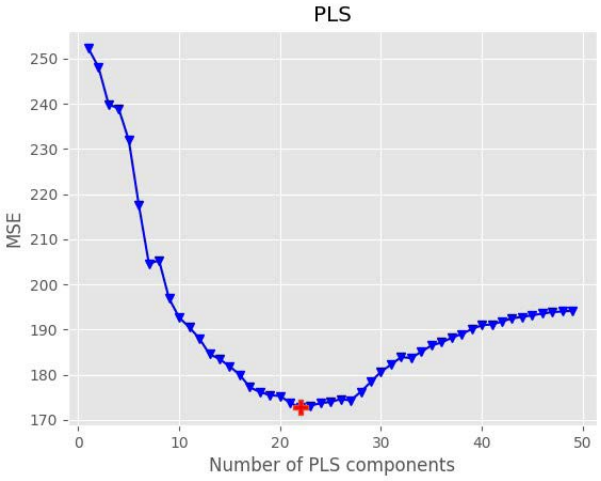

Figure 2: *Evolution of Mean Square Error (MSE) in progressing number of PLS components (collective variables, CV's) is showing the optimum selection of 22 collective variables (CV's) to best contribute to our PLSR model.*

4.2 Cubist

The Cubist chemometric technique is based on the M5 algorithm of Quinlan (33) and is widely and successfully applied in vis-NIR spectroscopy analysis. Thus, the Cubist method is considered as a competitive method to other methods of multivariate regression in terms of prediction accuracy.

The Cubist model is based on a regression tree construction with intermediate linear models extracted at each step of the procedure. It splits the original dataset that has similar attributes into subsets of sample and then generates multi-linear regression rules by optimal predictor variables selected from all spectral variables.

To optimize our Cubist model, we experimented on the number of committees (boosting). The results of our tests

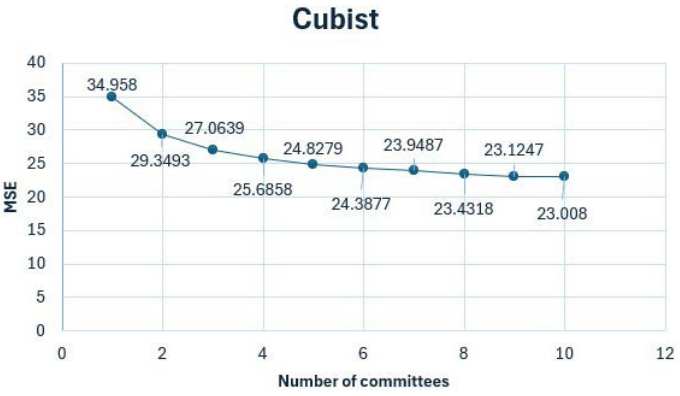

Figure 3: *Evolution of Mean Square Error (MSE) in progressing number of committees is showing the optimum selection of 10 committees to best contribute to our Cubist model.*

showed that after 10 committees, model performance saturates and we get diminishing returns (see Figure 3). Regarding the number of neighbors, it was kept to zero, based on our decision to not develop a composite model because the main focus of this research was on the novel deep learning methods. Furthermore, the number of trained models was ample enough for our research interest.

4.3 Support Vector Machines

Support vector machines (SVM) is a method that incorporates in its algorithm, linear equations for the regression analysis of multivariate cases (39,40).

The input parameters used for training the SVM are the NIR features that will be derived from the CV's calculated from the PLS regression model (CV's = 22). A linear kernel was used, and all spectra were normalized using a standard scaler (all values truncated between 0-1).

4.4 Multi-Layer Perceptrons

Multi-layer perceptrons (MLPs) or deep feedforward networks are machine learning models that use intermediate computations to transform their input to the output and in doing so evaluate a function :

$$\boldsymbol{y} = f(\boldsymbol{x}; \boldsymbol{\theta}) \qquad (9)$$

The transformations (linear and non-linear) that each model's layer implements to the data is parameterized by its weights $\boldsymbol{\theta}$. In this context, the model's goal is to find the set of values for the weights $\boldsymbol{\theta}$ of all layers in the network that correctly map inputs instances to their corresponding targets. Put in another way, the weights $\boldsymbol{\theta}$ that minimize the difference between the distribution of the output $\boldsymbol{y}$ and the true underlying distribution of the targets.

In contrast to linear models and to extend them to represent nonlinear functions of $\boldsymbol{x}$, MLPs apply the linear model to a transformed input $\boldsymbol{\phi}$(x) and not to $\boldsymbol{x}$. The ultimate goal is to learn $\boldsymbol{\phi}$:

$$y = f(\boldsymbol{x}; \boldsymbol{\theta}; \boldsymbol{w}) = \boldsymbol{\phi}(\boldsymbol{x}; \boldsymbol{\theta})\text{^}(\mathsf{T}\boldsymbol{w}) \qquad (10)$$

where $\boldsymbol{\theta}$ are parameters used to learn $\boldsymbol{\phi}$ from a broad family of functions and parameters $\boldsymbol{w}$ that map from $\boldsymbol{\phi(x)}$ to the desired output. The choice of how to represent the output determines the form of the cost function which usually expresses the difference between the predicted and the true distribution. In most cases the parametric model defines a distribution p($\boldsymbol{y} \mid \boldsymbol{x};\boldsymbol{\theta}$) and the principle of maximumm likelihood is used:

$$J(\theta) = -E_{x,y\sim\widehat{p_{data}}} log p_{model}(y|x) \qquad (11)$$

In such cases, the cost function is the negative log-likelihood between targets and model's predictions. A simpler approach is to merely predict a statistic of conditioned on . Note that the cost function will often combine a regularization term such as weight decay or dropout layers in order to avoid overfitting.

Our MLP model consists of three layers of 500, 200 and 50 units respectively (Figures 4, 5). Since we are predicting only one soil attribute ($CaCO_3$) the model has a single output. To introduce non-linearity we apply the Rectified Linear Unit (ReLU) activation function and as a measure to mitigate overfitting L_1 and L_2 regularizers are applied to the third layer. We use the Adam optimizer (41)an algorithm for first-order gradient-based optimization of stochastic objective functions, based on adaptive estimates of lower-order moments. The method is straightforward to implement, is computationally efficient, has little memory requirements, is invariant to diagonal rescaling of the gradients, and is well suited for problems that are large in terms of data and/or parameters. The method is also appropriate for non-stationary objectives and problems with very noisy and/or sparse gradients. The hyper-parameters have intuitive interpretations and typically require little tuning. Some connections to related algorithms, on which Adam was inspired, are discussed. We also analyze the theoretical convergence properties of the algorithm and provide a regret bound on the convergence rate that is comparable to the best known results under the online convex optimization framework. Empirical results demonstrate that Adam works well in practice and compares favorably to other stochastic optimization methods. Finally, we discuss AdaMax, a variant of Adam based on the infinity norm.","DOI":"10.48550/ARXIV.1412.6980","license":"arXiv.org perpetual, non-exclusive license","note":"publisher: arXiv\nversion: 9","source":"DOI.org (Datacite with a decaying learning rate. Savitzky-Golay second derivative smoothing filter is applied to the spectral dataset before being fed to the network.

To train a neural network, usually one has to split their dataset in three smaller datasets: a) a training set that will be used to train the network and fix its weights (training sets are usually large in size and preferably diverse because training set diversity contributes to better generalization) b) a validation set which size is typically ~20% of training's set size, and is used to test the model's performance c) the unknown set which contains data samples that the model has never "seen" before. The performance of the model on the unknown dataset is the key objective.

In our study, we performed an 80/20 training/validation dataset split and used 10-fold validation. K-fold validation is a technique typically used when the training set is relatively small, however, it has been proved that it yields slightly better predictive results even for larger datasets.

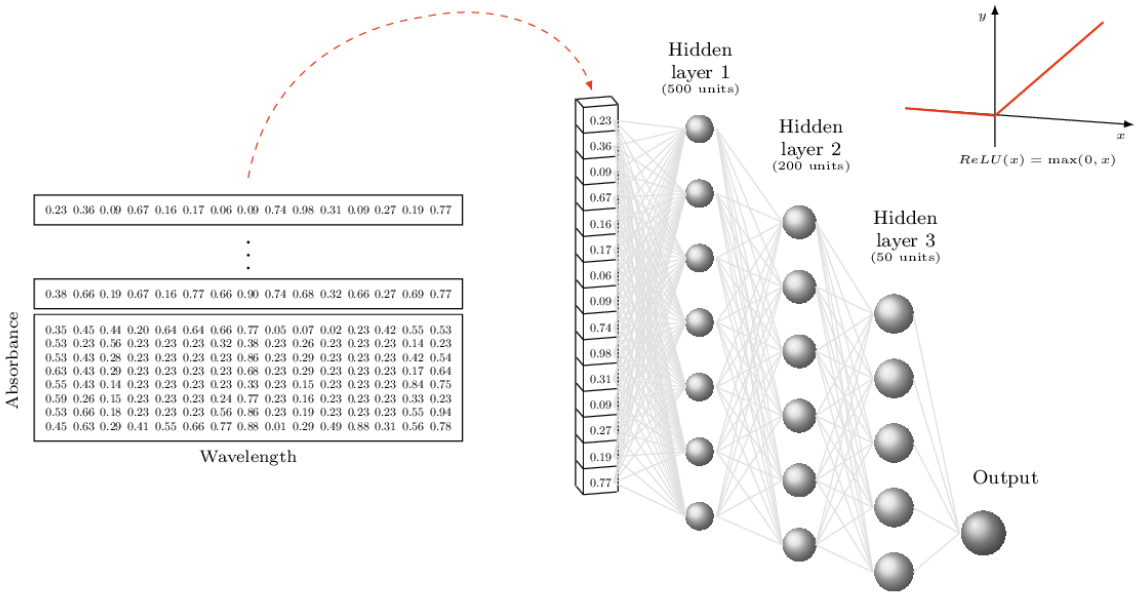

Figure 4: *MLP architecture. Three consecutive hidden layers (with 500, 200, 50 units) are filtering the combined spectral dataset in the NIR region, to a final output. An activation function ReLU is applied to facilitate training of the MLP model.*

For our experiments we combined both KSSL and LUCAS datasets. Before merging the two datasets, the Wasserstein test statistic was performed to gain insight on the "resemblance" of the two datasets. The result showed that the two datasets are very similar to each other (Wasserstein distance=1.78). High dataset similarity is often considered a good indicator for dataset merging. On the other hand, a training set should be diverse and present a relatively high degree of variability to avoid overfitting.

4.5 Convolutional Neural Networks

Convolutional neural networks (CNN) are neural networks specialized in grid-like topology data i.e. images that are represented as 2D grid of pixels. Their architecture consists of stacked convolutional layers of multiple filters that convolve with their input to produce a series of feature maps. Generally, a convolution is an operation on two functions:

$$s(t)=\int(x*w)(t) \qquad (12)$$

where is the input function and , also known as the kernel (or filter), needs to be a valid density function for the output to be a valid weighted average of over time .

When an instance passes through a CNN layer it usually undergoes three stages: first, the layer applies several convolutions in parallel to produce a set of linear activations. Then, each linear activation passes through a nonlinear activation function, such as a rectified linear unit. Finally, the output is further modified by a pooling function which serves both as a downsampling technique to reduce statistical and computational burden (42) as means to make the representation become approximately invariant to small translations of the input (42). Besides being translation invariant, CNNs learn spatial hierarchies of patterns: lower layers learn smaller patterns whereas layers near the output learn more complex patterns and abstract visual concepts (43).

These traits make CNNs an excellent choice for machine vision tasks such as object detection, image classification and semantic segmentation. Although designed for multi-dimensional data e.g. images and CT scans, CNNs perform equally good on one-dimensional inputs. In fact, CNNs have been used with relative success in tasks that involve sequences e.g. time-series. However, in our case we applied CNNs to the sample spectrograms (2D images) although we trained a CNN on spectra which yielded results on par with the MLP Regressor.

Our CNN model is made of three convolutional layers of 32, 64 and 128 filters respectively, each succeeded by a max-pooling layer (F). All convolutional and max-pooling kernels are 3X3 size. A dense layer of 50 units sits on top of the convolutional stack which in turn is connected to the network's single output. As in the MLP approach, we use ReLU activation function and Adam optimizer. In this approach, the network's input is not spectra but their respective spectrograms, each with dimensions 244X488 pixels. It is easy to convert NIR spectral absorbances into two-dimensional plots: NIR wavelengths represent the x-axis of the plot and absorbance values the y-axis. After conversion, the plots are stored as images and fed to the convolutional network. It should be considered that axis scale must be the same for all the plots.

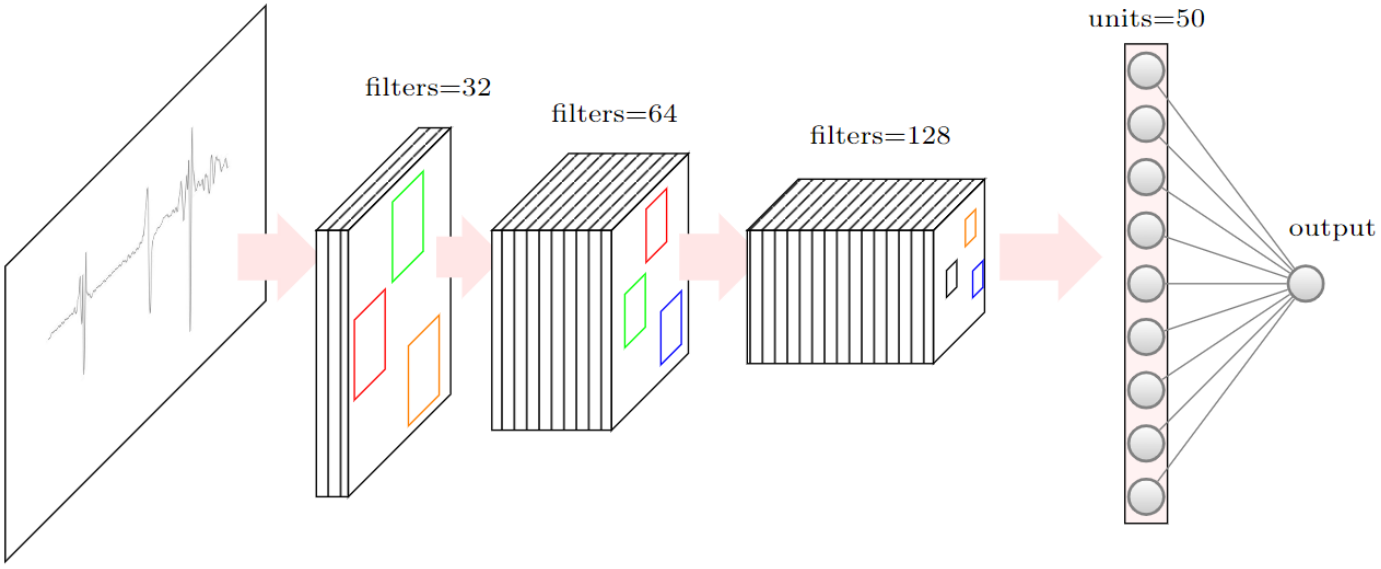

Figure 5: *CNN architecture. Three consecutive convolutional layers (with 32, 64, 128 units) are filtering the combined spectral dataset as images in the NIR region, with dimensions 244x488 pixels, to a final output. An activation function ReLU is also applied to facilitate training of the CNN model.*

5. Results

Our predictive machine learning models, classical (PLSR, Cubist, SVM) and deep learning ones (MLP and CNN), trained on the combined two large spectral databases, achieve high performance results (R^2 = 0.84, RPD = 2.14 for MLP) when applied to the unknown set: R^2 = 0.68 and RPD = 1.47 for CNN, for the prediction accuracy of soil carbonates, in the second derivative of NIR spectra (Figure 7).

Soil samples (no.45) of both Xatzisavva (SAM-1) wine fields in Alexandroupolis in Greece and Vourvoukelis (SAM-2) in Avdira in Greece were collected and samples (no.19) from SAM-1 and SAM-2 groups exhibited non-zero values in carbonate content, using the volumetric method as described in the methods section and were recorded (g/100g). As shown in Table 1, at least one soil sample from SAM-1 group is rich in carbonates (highest content = 18.14%) and the poorest carbonates content is in SAM-2 group (lowest content = 0.04%).

a **b**

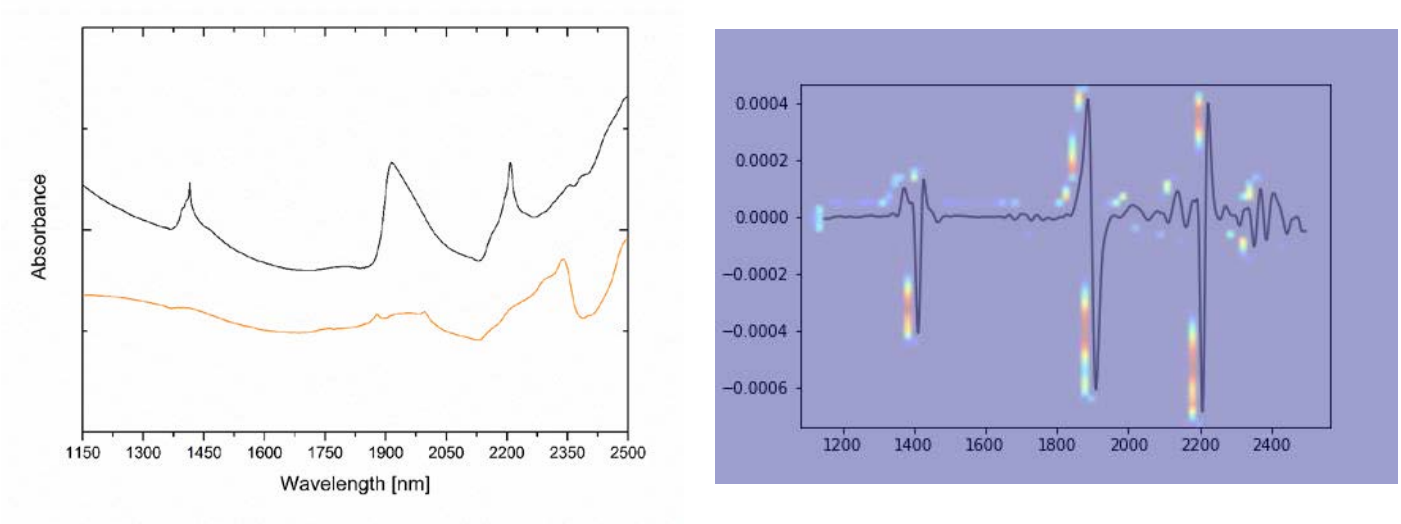

Figure 6: *On the top (a) absorbance spectra of an indicative soil sample (s03) (black) of Asyrtiko species from the Xatzisavva wine field in Alexandroupolis and calcium carbonate (Sigma, 239216) white powder spectrum (orange). Indication lines of carbonates vibration peaks are also shown as dashed lines. (b) a saliency map from CNN model in second derivative spectra, is showing the most favorable peaks that are considered to trigger the CNN model in a color gradient from red (most favored peaks) to light blue (less favored peaks).*

Table 1: *Experimental values of diverse soil samples (no.19) using the volumetric method in comparison with the predicted carbonates values from MLP model. Two groups of soil samples (SAM-1 and SAM-2) were measured and predicted.*

S/no	Exp g/100g	Pred g/100g	
S01	7.85	11.53	
S02	1.83	0.86	
S03	8.56	8.80	
S04	10.84	5.85	
S05	9.32	8.37	
S06	4.63	1.64	
S07	3.39	1.52	
S08	5.75	3.31	**SAM-1**
S09	1.18	1.07	
S10	18.14	13.44	
S11	11.28	14.18	
S12	17.32	14.38	
S13	17.00	18.57	
S14	1.12	1.80	
S15	0.07	0.60	
S16	0.13	0.59	
S17	0.13	0.53	**SAM-2**
S18	0.09	0.51	
S19	0.04	0.51	

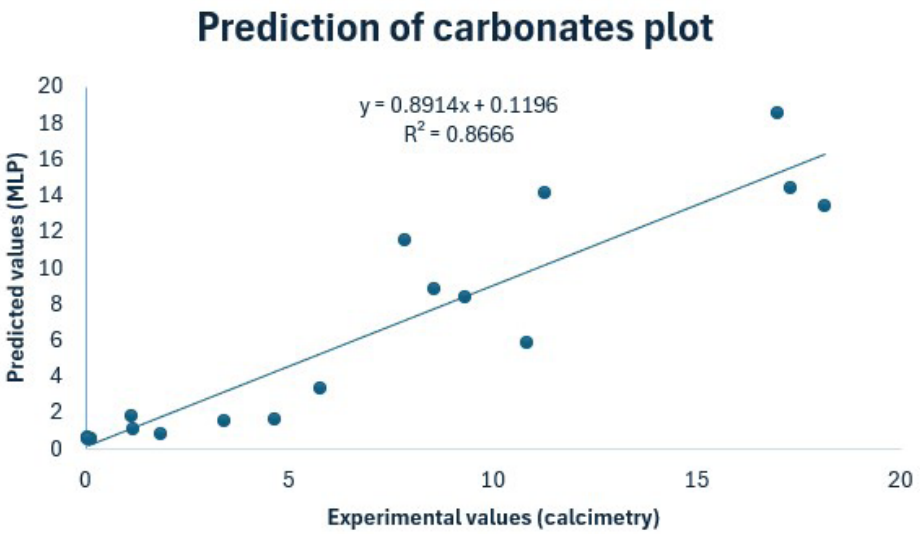

Figure 7: *Plot of carbonates prediction with MLP vs Calcimetry (Volumetric method) of Table 1, exhibits R^2 = 0.87. MLP deep learning methods calibrated throughout the combined dataset of KSSL-USDA NIR spectral library and LUCAS-2015-TopSoil NIR spectral library out-performed other regression methods utilized in our work. MLP performs well, even below the Limit of Detection of the Volumetric method that is 2.5 g/100g. All values reported are in g/100g.*

Table 2: *Regression prediction models applied to all data for carbonates (two spectral libraries, firstly 6,833 NIR spectra from KSSL (USA) combined with 21,782 NIR spectra from Lucas TopSoil (all European fields) for carbonates). Statistics of R^2, Root Mean Square Error (RMSE), Residual Prediction Deviation (RPD) and Ratio of Performance to Inter-Quartile distance (RPIQ) are shown. From all pretreatments, the second derivative outperformed the other two methods of absorbance and first derivative spectra.*

	PLSR	**SVM**	**Cubist**	**MLP**	**CNN (images)**
Second Derivative	R^2 = -1.43	R^2 = -0.19	R^2 = 0.86	R^2 = 0.87	R^2 = 0.68
	RMSE = 13.11	RMSE = 6.59	RMSE = 4.80	RMSE = 2.11	RMSE = 4.11
	RPD = 0.54	RPD = 0.91	RPD = 2.70	RPD = 2.14	RPD = 1.47
	RPIQ = 0.82	RPIQ = 1.43	RPIQ = 2.13	RPIQ = 3.33	RPIQ = 2.29

In order to describe in full detail, the carbonates content of the SAM-1 (sample S03), and SAM-2 (S18) we took insight in the quantification of the minerals by means of powder X-ray diffraction (XRD) method. Diffractograms were acquired in an in-house diffractometer, as mentioned in the methods section. Rietveld refinement using structural models was then performed (Figure 8).

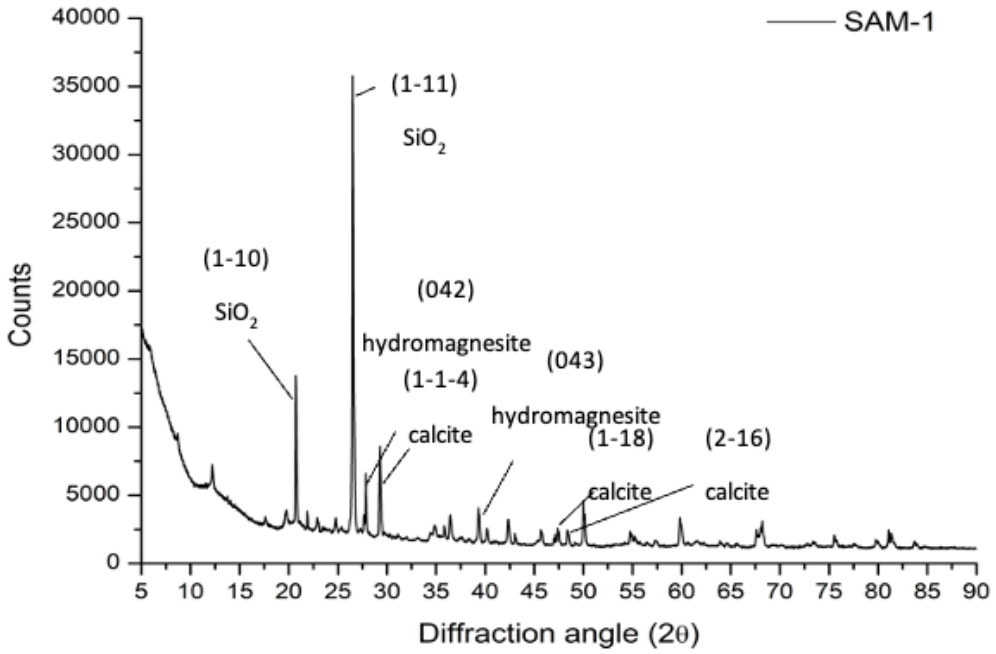

Figure 8*: XRD diffractogram shows that peaks of characteristic planes of calcite, and hydromagnesite are present in SAM-1, among other distinct minerals peaks. Crystalline Index (CI) is calculated to 0.72.*

Quantification of carbonates minerals in crystalline phase, in the representative soil sample (S03) of SAM-1 group, shows that total carbonates are contained in 6.07 % (w/w) with a crystalline index = 0.72. The total carbonates content is then calculated to 8.43 % (w/w). The minerals found were firstly calcite 3.88 % (w/w), and also hydromagnesite 2.19 %, as shown in Table 3. A total of 8.43 % (w/w) in ratio of total minerals and in specific of both their crystalline phases of SAM-1 group and amorphous content based on crystalline index, is in good agreement with both volumetric method and MLP prediction of NIR spectra based on the calibration libraries of KSSL (USA) and LUCAS-Topsoil (EU).

Table 3: *Comparison of total carbonates content of S03 from SAM-1 group by volumetric method, MLP prediction and XRD phase quantification of both calcite and hydromagnesite minerals shows a very good values agreement.*

SAM-1	**Molecular formula**	**Phase quantification from XRD (wt-%)**	**Volumetric method (wt-%)**	**MLP (wt-%)**
Calcite	$CaCO_3$	3.88	-	-
Hydro-magnesite	$Mg_5(CO_3)_4(OH)_2 \cdot 4H_2O$	2.19	-	-
Total carbonates	CO_3^{2-}	6.07 (Crystalline Index = 0.72) **Total = 8.43**	**8.56**	**8.80**

In SAM-2 group, the carbonates content is negligible, as shown in Figure 9 and the XRD diffractogram where all peaks of calcite are absent, at 29.4° for (1-1-4) calcite plane and around 47.4° and 48.5° for (2-2-2) and (1-18) planes, respectively. Also, hydromagnesite is absent at 27.7° for (042) and at 39.2° for (080).

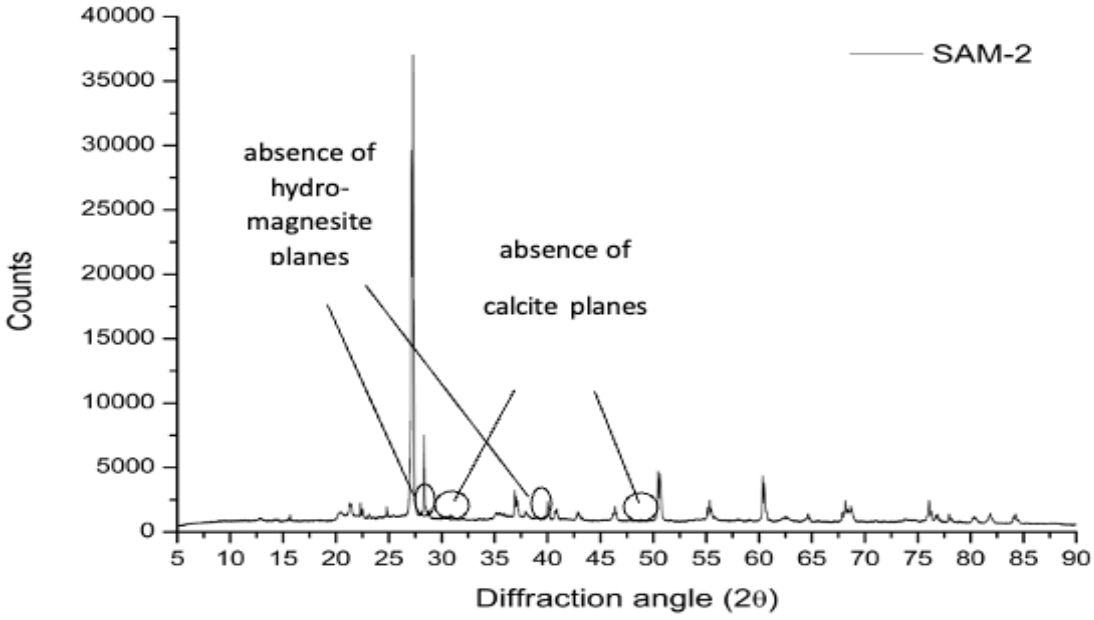

Figure 9: *Absence of calcite and hydromagnesite crystalline phases in diffractogram for SAM-2 group representative sample (S18).*

6. Discussion

Our computational machine learning models trained on two extensive spectral databases: the USDA's KSSL spectral library and the European Union's LUCAS 2015 TopSoil spectral library demonstrated impressive performance metrics (R^2 = 0.87, RPD = 2.14 for MLP) in the prediction set, and (R^2 = 0.68, RPD = 1.47 for CNN) specifically in predicting soil carbonates.

Notably, the MLP exhibits remarkable accuracy, even in predicting extreme experimental values of soil carbonates, below the limit of detection (LOD) of the volumetric method. Its predictions align well with the quantification achieved through X-ray Diffraction and the volumetric method.

Soil carbonates, primarily composed of calcium and magnesium carbonates, manifest distinctive absorption peaks in the NIR region. These peaks stem from the overtone and combination bands of the fundamental bands of CO_3^{2-}, prevalent in the mid-IR region. In the NIR, carbonates exhibit five characteristic bands. Notably, a conspicuous peak around 2340 nm represents an overtone of the asymmetrical stretching v_3 observed at 1415 cm^{-1} in the mid-IR region. Additionally, the peak near 2500-2550 nm corresponds to a combination of symmetrical stretching (v_1) and the first overtone of asymmetrical stretching (v_3), denoted as (v_1 + $2v_3$). Weaker absorptions are evident near 1415 nm due to crystallized water, around 1900 nm (v_1 + $3v_3$), near 2000 nm ($2v_1$ + $2v_3$), and around 2160 nm ($3v_1$ + $2v_4$), where v_4 represents the in-plane bending (v_4, 680 cm-1). It's noteworthy that the positions of these absorption bands vary based on the composition of the carbonates. While few studies have quantified carbonate composition in soil utilizing vis-NIR spectroscopy for estimating carbonate content, a recent study examined soil carbonates content using mid-IR spectroscopy, employing the KSSL library for calibration (44).

In an attempt to determine which wavelength absorbance peaks, possess more weight on the model's performance and due to the fact that it is easier to visualize this through saliency mappings (peaks on the second derivative absorbance spectra) we develop a CNN model as discussed previously. The most favored peaks are in the 1415 nm, in the 1908 nm, in the 2209 nm and in the 2335 nm. The sharp band at 1415 nm that is shown in soil NIR spectra in Figure 6, is due to calcite and hydromagnesite ($Mg_5(CO_3)_4(OH)_2 \cdot 4(H_2O)$) that is a mineral also present in calcareous soils especially in SAM-1 group and absent in SAM-2 group. Hydrous carbonates, like other hydrous minerals, typically exhibit strong bands around 1400 nm due to O–H stretching or a combination of the symmetric H–O–H stretch and H–O–H bend (45). The shape of the absorption peaks can indicate whether this feature is produced by a hydroxyl or water group. The characteristic band near 1415 nm is also due to kaolinite that shows absorption wavelengths near 1400 nm (1395 and 1415 nm) that are overtone vibrations of the O–H stretch near 2778 nm (3600 cm^{-1}), and can to one part be attributed to the first overtone of structural O–H stretching mode in its octahedral layer (46). The 1880 nm band is due to v_1 +$2v_3$, where v_1 is the totally symmetric C-O stretch and v_3 is the doubly degenerate antisymmetric C-O stretching mode occurring near 7000 nm (47)intrinsic spectral features that appear in the form of bands and slopes in the visible and near infrared (.325 to 2.5 µm.

Also, at 1908 nm occurs a combination of H–O–H bending and the asymmetrical stretching fundamentals. This band is possible overlapping with the main band of other minerals and in particular O-H stretch of kaolinite. Also, the peak near 2209 nm is triggered by the presence of calcite. Lastly, around 2235 nm a prominent peak of calcite triggers the saliency map derived from CNN model. Other peaks that are triggered by the content of carbonates by visual inspection of the saliency map, are difficult to assign because of various peak overlaps with hydroxyl and/or water molecules bound to mineral crystallites. As a result, NIR spectral assignment towards elucidation of carbonates peaks is a multiparametric task, especially in complex samples such as soil samples.

In this study, soil samples were collected from two wine fields in Greece: Xatzisavva (SAM-1) in Alexandroupolis and Vourvoukelis (SAM-2) in Avdira, Xanthi. Carbonate content was determined using the volumetric method, recorded as g/100g. Table 1 reveals that at least one soil sample from the SAM-1 group has notably high carbonate content (highest content = 18.14%), while the SAM-2 group exhibits the lowest carbonate content (lowest content = 0.04%). To identify influential wavelength absorbance peaks in the model's performance, saliency mappings were developed through a CNN model. The peaks with the highest significance were observed at 1415 nm, 1880 nm, 1995 nm, and 2209 nm. The sharp band at 1415 nm corresponds to minerals like calcite, monohydrocalcite ($Ca(CO_3) \cdot (H_2O)$), and hydromagnesite ($Mg_5(CO_3)_4(OH)_2 \cdot 4(H_2O)$), prevalent in calcareous soils, particularly in the SAM-1 group and absent in the SAM-2 group.

In addition, the ratio of calcite/hydromagnesite in our soil samples is also calculated by means of X-ray diffraction (XRD). The two farms from which the soil samples were collected, have different farming conditions of operations and handling of soil, with Vourvoukelis farm in-

troducing additional fertilizer in soil while Xatzisavva's operational practice is pure organic. The ratio of calcite/hydromagnesite of soil fertility due to hydrous magnesite complexes that are present in addition to calcite, are important and totally detectable by XRD and saliency maps of 2D-CNN method (Figures 6, 9). The elegant method of 2D-CNN in the analysis of the combined dataset of KSSL and LUCAS-2015 spectral libraries is reported for the first time to our knowledge, exhibiting the major peaks of influence in the regression and in the prediction. The prediction of secondary peaks (hydromagnesite in our prediction set) is in great accordance with the XRD quantification in two samples with different origin (namely SAM-1 and SAM-2).

This research significantly contributes to the field by offering a swift prediction approach for soil carbonates content, particularly in scenarios where a volumetric method is unavailable, and only visible-NIR spectra absorbance data are at hand.

To the best of our knowledge, this study is pioneering, presenting the first prediction model trained on such a comprehensive dataset, showcasing promising outcomes on previously unseen data. These findings robustly affirm the efficacy of deep learning models as potent tools for predicting soil carbonates content and the potency to identify NIR peaks of hydrous minerals by saliency map of 2D-CNN method. The ratio and in particular the quantification of calcite/hydrous compounds (hydromagnesite) is verified by XRD method.

7. Conclusion

Carbonates content of soil is an essential soil chemical property, with a significant impact on growth and production of crops. Soil genesis records and soil classifications as shown in various soil profiles are also mostly affected by the distribution of carbonates content of soils. Here we present a modified way of soil carbonates prediction other than classical volumetric method. A minimal input of a NIR spectra provides the total carbonates content in soil samples, as calibrated with two spectral libraries, namely USDA-NRCS-KSSL and EU-LUCAS-2015-TopSoil with 28,615 NIR spectra, where MLP method is trained in this dataset and applied for prediction. MLP method performed good in a diverse test set ranging from diverse carbonates content as low as 0.07%, to high content (18.14%) in soil samples. CNN method produced less favorable results in terms of prediction with experimentally derived carbonates values and a saliency map showed us the peaks triggered in training and prediction spectral sets. Peak assignment of various carbonates and hydrous carbonates minerals in the NIR region was also established. The presence of hydromagnesite in soil samples with highest carbonates content (SAM-1) was verified by means of XRD Rietveld analysis. Quantification of the total carbonates content in SAM-1 group with XRD, and in representative sample S03, is in good agreement with MLP prediction and volumetric method applied, while the absence of carbonates content is obvious in SAM-2 group with XRD analysis.

8. Acknowledgments

This study was supported by the project "AGRO4+" - Holistic approach to Agriculture 4.0 for new farmers" (MIS 5046239) which is implemented under the Action "Reinforcement of the Research and Innovation Infrastructure", funded by the Operational Programme "Competitiveness, Entrepreneurship and Innovation" (NSRF 2014-2020) and co-financed by Greece and the European Union (European Regional Development Fund).

Authors would like to thank Dr. Nikolaos Kazakis, Dr. Nestor Tsirliganis and Dr. Chairi Kiourt for access to instrumentation and the staff at the USDA-NRCS-KSSL and EU-LUCAS-TopSoil for the data provided in this study.

Code availability section

Carbonates_prediction

Contact: tamvakis.petros@ac.eap.gr, +1-262-960-2449 (USA)

Hardware requirements: CPU/GPU

Program language: Python 3

Software required: https://www.tensorflow.org/ and dependencies therein.

Program size: 110 KB

The source codes are available for downloading at the link: https://github.com/petamva/carbonates_prediction

References

1. Viscarra Rossel RA, Behrens T, Ben-Dor E, Brown DJ, Demattê JAM, Shepherd KD, et al. A global spectral library to characterize the world's soil. Earth-Sci Rev. 2016 Apr;155:198–230.
2. Guerrero C, Wetterlind J, Stenberg B, Mouazen AM, Gabarrón-Galeote MA, Ruiz-Sinoga JD, et al. Do we really need large spectral libraries for local scale SOC assessment with NIR spectroscopy? Soil Tillage Res. 2016 Jan;155:501–9.
3. Bellon-Maurel V, Fernandez-Ahumada E, Palagos B, Roger JM, McBratney A. Critical review of chemometric indicators commonly used for assessing the quality of the prediction of soil attributes by NIR spectroscopy. TrAC Trends Anal Chem. 2010 Oct;29(9):1073–81.
4. Nocita M, Stevens A, van Wesemael B, Aitkenhead M, Bachmann M, Barthès B, et al. Soil Spectroscopy: An Alternative to Wet Chemistry for Soil Monitoring. In: Advances in Agronomy [Internet]. Elsevier; 2015 [cited 2022 Dec 19]. p. 139–59. Available from: https://linkinghub.elsevier.com/retrieve/pii/S0065211315000425
5. Bai Z, Xie M, Hu B, Luo D, Wan C, Peng J, et al. Estimation of Soil Organic Carbon Using Vis-NIR Spectral Data and Spectral Feature Bands Selection in Southern Xinjiang, China. Sensors. 2022 Aug 16;22(16):6124.
6. Morellos A, Pantazi XE, Moshou D, Alexandridis T, Whetton R, Tziotzios G, et al. Machine learning based prediction of soil total nitrogen, organic carbon and moisture content by using VIS-NIR spectroscopy. Biosyst Eng. 2016 Dec;152:104–16.
7. Kooistra L, Wehrens R, Leuven RSEW, Buydens LMC. Possibilities of visible–near-infrared spectroscopy for the assessment of soil contamination in river floodplains. Anal Chim Acta. 2001 Nov;446(1–2):97–105.
8. Askari MS, O'Rourke SM, Holden NM. A comparison of point and imaging visible-near infrared spectroscopy for determining soil organic carbon. J Infrared Spectrosc. 2018 Apr;26(2):133–46.
9. Pribyl DW. A critical review of the conventional SOC to SOM conversion factor. Geoderma. 2010 May;156(3–4):75–83.
10. Conforti M, Matteucci G, Buttafuoco G. Using laboratory Vis-NIR spectroscopy for monitoring some forest soil properties. J Soils Sediments. 2018 Mar;18(3):1009–19.
11. Barthès BG, Kouakoua E, Moulin P, Hmaidi K, Gallali T, Clairotte M, et al. Studying the Physical Protection of Soil Carbon with Quantitative Infrared Spectroscopy. J Infrared Spectrosc. 2016 Jun;24(3):199–214.
12. Jia S, Yang X, Zhang J, Li G. Quantitative Analysis of Soil Nitrogen, Organic Carbon, Available Phosphorous, and Available Potassium Using Near-Infrared Spectroscopy Combined With Variable Selection. Soil Sci. 2014 Apr;179(4):211–9.
13. Reeves JB, Van Kessel JAS. Investigations into near Infrared Analysis as an Alternative to Traditional Procedures in Manure Nitrogen and Carbon Mineralisation Studies. J Infrared Spectrosc. 1999 Jun;7(3):195–212.
14. Cho RK, Lin G, Kwon YK. Nondestructive Analysis for Nitrogens of Soils by near Infrared Reflectance Spectroscopy. J Infrared Spectrosc. 1998 Jan;6(A):A87–91.
15. Reeves JB, McCarty GW, Meisinger JJ. Near Infrared Reflectance Spectroscopy for the Analysis of Agricultural Soils. J Infrared Spectrosc. 1999 Jun;7(3):179–93.
16. Morón A, Cozzolino D. Application of near Infrared Reflectance Spectroscopy for the Analysis of Organic C, Total N and pH in Soils of Uruguay. J Infrared Spectrosc. 2002 Jun;10(3):215–21.
17. Miltz J, Don A. Optimising Sample Preparation and near Infrared Spectra Measurements of Soil Samples to Calibrate Organic Carbon and Total Nitrogen Content. J Infrared Spectrosc. 2012 Dec;20(6):695–706.
18. Genot V, Colinet G, Bock L, Vanvyve D, Reusen Y, Dardenne P. Near Infrared Reflectance Spectroscopy for Estimating Soil Characteristics Valuable in the Diagnosis of Soil Fertility. J Infrared Spectrosc. 2011 Apr;19(2):117–38.
19. Knadel M, Stenberg B, Deng F, Thomsen A, Greve MH. Comparing Predictive Abilities of Three Visible-Near Infrared Spectrophotometers for Soil Organic Carbon and Clay Determination. J Infrared Spectrosc. 2013 Feb;21(1):67–80.
20. Hummel JW, Sudduth KA, Hollinger SE. Soil moisture and organic matter prediction of surface and subsurface soils using an NIR soil sensor. Comput Electron Agric. 2001 Aug;32(2):149–65.
21. Mouazen AM, De Baerdemaeker J, Ramon H. Towards development of on-line soil moisture content sensor using a fibre-type NIR spectrophotometer. Soil Tillage Res. 2005 Jan;80(1–2):171–83.
22. Chodak M, Khanna P, Horvath B, Beese F. Near Infrared Spectroscopy for Determination of Total and Exchangeable Cations in Geologically Heterogeneous Forest Soils. J Infrared Spectrosc. 2004 Oct;12(5):315–24.
23. Liu L, Ji M, Buchroithner M. Transfer Learning for Soil Spectroscopy Based on Convolutional Neural Networks and Its Application in Soil Clay Content Mapping Using Hyperspectral Imagery. Sensors. 2018 Sep 19;18(9):3169.
24. Guo Y, Amundson R, Gong P, Ahrens R. Taxonomic Structure, Distribution, and Abundance of the Soils in the USA.

Soil Sci Soc Am J. 2003 Sep;67(5):1507–16.
25. Orgiazzi A, Ballabio C, Panagos P, Jones A, Fernández‐Ugalde O. LUCAS Soil, the largest expandable soil dataset for Europe: a review. Eur J Soil Sci. 2018 Jan;69(1):140–53.
26. Demattê JAM, Paiva AFDS, Poppiel RR, Rosin NA, Ruiz LFC, Mello FADO, et al. The Brazilian Soil Spectral Service (BraSpecS): A User-Friendly System for Global Soil Spectra Communication. Remote Sens. 2022 Feb 5;14(3):740.
27. Shi Z, Wang Q, Peng J, Ji W, Liu H, Li X, et al. Development of a national VNIR soil-spectral library for soil classification and prediction of organic matter concentrations. Sci China Earth Sci. 2014 Jul;57(7):1671–80.
28. Stevens A, Nocita M, Tóth G, Montanarella L, van Wesemael B. Prediction of Soil Organic Carbon at the European Scale by Visible and Near InfraRed Reflectance Spectroscopy. Chen HYH, editor. PLoS ONE. 2013 Jun 19;8(6):e66409.
29. Lecun Y. Generalization and network design strategies. In: Connectionism in perspective. R. Pfeifer; Z. Schreter; F. Fogelman; L. Steels. Zurich, Switzerland: Elsevier; 1989.
30. Tsakiridis NL, Keramaris KD, Theocharis JB, Zalidis GC. Simultaneous prediction of soil properties from VNIR-SWIR spectra using a localized multi-channel 1-D convolutional neural network. Geoderma. 2020 May;367:114208.
31. Padarian J, Minasny B, McBratney AB. Using deep learning to predict soil properties from regional spectral data. Geoderma Reg. 2019 Mar;16:e00198.
32. Martens H, Næs T. Multivariate calibration. Chichester [England] ; New York: Wiley; 1989. 419 p.
33. Quinlan JR. Learning with Continuous Classes. In: Proceedings of Australian Joint Conference on Artificial Intelligence. Hobart; 1992. p. 343–8.
34. Ng W, Minasny B, Montazerolghaem M, Padarian J, Ferguson R, Bailey S, et al. Convolutional neural network for simultaneous prediction of several soil properties using visible/near-infrared, mid-infrared, and their combined spectra. Geoderma. 2019 Oct;352:251–67.
35. Savitzky Abraham, Golay MJE. Smoothing and Differentiation of Data by Simplified Least Squares Procedures. Anal Chem. 1964 Jul 1;36(8):1627–39.
36. Cuevas J, Cabrera MÁ, Fernández C, Mota-Heredia C, Fernández R, Torres E, et al. Bentonite Powder XRD Quantitative Analysis Using Rietveld Refinement: Revisiting and Updating Bulk Semiquantitative Mineralogical Compositions. Minerals. 2022 Jun 17;12(6):772.
37. Viscarra Rossel RA. ParLeS: Software for chemometric analysis of spectroscopic data. Chemom Intell Lab Syst. 2008 Jan;90(1):72–83.
38. Viscarra Rossel RA, Walvoort DJJ, McBratney AB, Janik LJ, Skjemstad JO. Visible, near infrared, mid infrared or combined diffuse reflectance spectroscopy for simultaneous assessment of various soil properties. Geoderma. 2006 Mar;131(1–2):59–75.
39. de Santana FB, Otani SK, de Souza AM, Poppi RJ. Comparison of PLS and SVM models for soil organic matter and particle size using vis-NIR spectral libraries. Geoderma Reg. 2021 Dec;27:e00436.
40. Suykens JAK, Vandewalle J, De Moor B. Optimal control by least squares support vector machines. Neural Netw. 2001 Jan;14(1):23–35.
41. Kingma DP, Ba J. Adam: A Method for Stochastic Optimization. 2014 [cited 2023 Mar 28]; Available from: https://arxiv.org/abs/1412.6980
42. Goodfellow I, Bengio Y, Courville A. Deep learning. Cambridge, Massachusetts: The MIT Press; 2016. 775 p. (Adaptive computation and machine learning).
43. Chollet F. Deep learning with Python. Second edition. Shelter Island: Manning Publications; 2021. 478 p.
44. Comstock JP, Sherpa SR, Ferguson R, Bailey S, Beem-Miller JP, Lin F, et al. Carbonate determination in soils by mid-IR spectroscopy with regional and continental scale models. Minasny B, editor. PLOS ONE. 2019 Feb 21;14(2):e0210235.
45. Harner PL, Gilmore MS. Visible–near infrared spectra of hydrous carbonates, with implications for the detection of carbonates in hyperspectral data of Mars. Icarus. 2015 Apr;250:204–14.
46. Stenberg B, Viscarra Rossel RA, Mouazen AM, Wetterlind J. Visible and Near Infrared Spectroscopy in Soil Science. In: Advances in Agronomy [Internet]. Elsevier; 2010 [cited 2022 Dec 19]. p. 163–215. Available from: https://linkinghub.elsevier.com/retrieve/pii/S0065211310070057
47. Hunt GR. SPECTRAL SIGNATURES OF PARTICULATE MINERALS IN THE VISIBLE AND NEAR INFRARED. GEOPHYSICS. 1977 Apr;42(3):501–13.
48. Ben Dor E, Ong C, Lau IC. Reflectance measurements of soils in the laboratory: Standards and protocols. Geoder-

ma. 2015 May;245–246:112–24.
49. Pudełko A, Chodak M. Estimation of total nitrogen and organic carbon contents in mine soils with NIR reflectance spectroscopy and various chemometric methods. Geoderma. 2020 Jun;368:114306.
50. Z, Ji W, Viscarra Rossel RA, Chen S, Zhou Y. Prediction of soil organic matter using a spatially constrained local partial least squares regression and the Chinese vis-NIR spectral library: vis-NIR predictions of soil carbon with scL-PLSR. Eur J Soil Sci. 2015 Jul;66(4):679–87.
51. Kühnel A, Bogner C. *In-situ* prediction of soil organic carbon by vis-NIR spectroscopy: an efficient use of limited field data: In-situ prediction of SOC. Eur J Soil Sci. 2017 Sep;68(5):689–702.
52. Gao Y, Cui L, Lei B, Zhai Y, Shi T, Wang J, et al. Estimating Soil Organic Carbon Content with Visible–Near-Infrared (Vis-NIR) Spectroscopy. Appl Spectrosc. 2014 Jul;68(7):712–22.
53. Xu L, Hong Y, Wei Y, Guo L, Shi T, Liu Y, et al. Estimation of Organic Carbon in Anthropogenic Soil by VIS-NIR Spectroscopy: Effect of Variable Selection. Remote Sens. 2020 Oct 16;12(20):3394.
54. Wiesmeier M, Lungu M, Cerbari V, Boincean B, Hübner R, Kögel-Knabner I. Rebuilding soil carbon in degraded steppe soils of Eastern Europe: The importance of windbreaks and improved cropland management. Land Degrad Dev. 2018 Apr;29(4):875–83.
55. Lal R. Restoring Soil Quality to Mitigate Soil Degradation. Sustainability. 2015 May 13;7(5):5875–95.
56. Diacono M, Montemurro F. Long-term effects of organic amendments on soil fertility. A review. Agron Sustain Dev. 2010 Apr;30(2):401–22.
57. Rajan K, Natarajan A, Kumar KSA, Badrinath MS, Gowda RC. Soil organic carbon – the most reliable indicator for monitoring land degradation by soil erosion. Curr Sci. 2010;99(6):823–7.
58. Manlay RJ, Feller C, Swift MJ. Historical evolution of soil organic matter concepts and their relationships with the fertility and sustainability of cropping systems. Agric Ecosyst Environ. 2007 Mar;119(3–4):217–33.
59. Krupenikov IA, Boincean BP, Dent D. Humus – Guardian of Fertility and Global Carbon Sink. In: The Black Earth [Internet]. Dordrecht: Springer Netherlands; 2011 [cited 2022 Dec 19]. p. 39–50. Available from: http://link.springer.com/10.1007/978-94-007-0159-5_7
60. Lal R. Soil Carbon Sequestration Impacts on Global Climate Change and Food Security. Science. 2004 Jun 11;304(5677):1623–7.
61. Houghton RA. Balancing the Global Carbon Budget. Annu Rev Earth Planet Sci. 2007 May 1;35(1):313–47.
62. Chen S, Xu D, Li S, Ji W, Yang M, Zhou Y, et al. Monitoring soil organic carbon in alpine soils using in situ vis□NIR spectroscopy and a multilayer perceptron. Land Degrad Dev. 2020 May 15;31(8):1026–38.
63. Ramírez PB, Calderón FJ, Haddix M, Lugato E, Cotrufo MF. Using Diffuse Reflectance Spectroscopy as a High Throughput Method for Quantifying Soil C and N and Their Distribution in Particulate and Mineral-Associated Organic Matter Fractions. Front Environ Sci. 2021 May 17;9:634472.
64. Seema, Ghosh AK, Das BS, Reddy N. Application of VIS-NIR spectroscopy for estimation of soil organic carbon using different spectral preprocessing techniques and multivariate methods in the middle Indo-Gangetic plains of India. Geoderma Reg. 2020 Dec;23:e00349.
65 Li H, Jia S, Le Z. Prediction of Soil Organic Carbon in a New Target Area by Near-Infrared Spectroscopy: Comparison of the Effects of Spiking in Different Scale Soil Spectral Libraries. Sensors. 2020 Aug 5;20(16):4357.
66. Amin I, Fikrat F, Mammadov E, Babayev M. Soil Organic Carbon Prediction by Vis-NIR Spectroscopy: Case Study the Kur-Aras Plain, Azerbaijan. Commun Soil Sci Plant Anal. 2020 Mar 25;51(6):726–34.
67. Gruszczyński S. Prediction of soil properties with machine learning models based on the spectral response of soil samples in the near infrared range. Soil Sci Annu. 2019 Dec 1;70(4):298–313.
68. Goodfellow I, Bengio Y, Courville A. Deep learning. Cambridge, Massachusetts: The MIT Press; 2016. 775 p. (Adaptive computation and machine learning).
69. Chollet F. Deep learning with Python. Second edition. Shelter Island: Manning Publications; 2021. 478 p.
70. Goodfellow I, Bengio Y, Courville A. Deep learning. Cambridge, Massachusetts: The MIT Press; 2016. 775 p. (Adaptive computation and machine learning).
71. Zhou, Chellappa. Computation of optical flow using a neural network. In: IEEE International Conference on Neural Networks [Internet]. San Diego, CA, USA: IEEE; 1988 [cited 2023 Apr 3]. p. 71–8 vol.2. Available from: http://ieeexplore.ieee.org/document/23914/
72. Kingma DP, Ba J. Adam: A Method for Stochastic Optimization. 2014 [cited 2023 Apr 3]; Available from: https://arxiv.org/abs/1412.6980

73. Fukushima K. Cognitron: A self-organizing multilayered neural network. Biol Cybern. 1975;20(3–4):121–36.
74. Rietveld HM. A profile refinement method for nuclear and magnetic structures. J Appl Crystallogr. 1969 Jun 2;2(2):65–71.
75. Doebelin N, Kleeberg R. *Profex* : a graphical user interface for the Rietveld refinement program *BGMN*. J Appl Crystallogr. 2015 Oct 1;48(5):1573–80.
76. Bergmann, J., Friedel, P., Kleeberg, R. BGMN - a new fundamental parameters based Rietveld program for laboratory X-ray sources, it's use in quantitative analysis and structure investigations. Comm Powder Diffr IUCr. 1998;20:5–8.
77. Barthès BG, Kouakoua E, Moulin P, Hmaidi K, Gallali T, Clairotte M, et al. Studying the Physical Protection of Soil Carbon with Quantitative Infrared Spectroscopy. J Infrared Spectrosc. 2016 Jun;24(3):199–214.
78. Viscarra Rossel RA, Hicks WS. Soil organic carbon and its fractions estimated by visible-near infrared transfer functions: Vis-NIR estimates of organic carbon and its fractions. Eur J Soil Sci. 2015 May;66(3):438–50.
79. Morellos A, Pantazi XE, Moshou D, Alexandridis T, Whetton R, Tziotzios G, et al. Machine learning based prediction of soil total nitrogen, organic carbon and moisture content by using VIS-NIR spectroscopy. Biosyst Eng. 2016 Dec;152:104–16.
80. Cortes C, Vapnik V. [No title found]. Mach Learn. 1995;20(3):273–97.
81. Morellos A, Pantazi XE, Moshou D, Alexandridis T, Whetton R, Tziotzios G, et al. Machine learning based prediction of soil total nitrogen, organic carbon and moisture content by using VIS-NIR spectroscopy. Biosyst Eng. 2016 Dec;152:104–16.
82. Zamanian K, Zhou J, Kuzyakov Y. Soil carbonates: The unaccounted, irrecoverable carbon source. Geoderma. 2021 Feb;384:114817.
83. Barthès BG, Kouakoua E, Moulin P, Hmaidi K, Gallali T, Clairotte M, et al. Studying the Physical Protection of Soil Carbon with Quantitative Infrared Spectroscopy. J Infrared Spectrosc. 2016 Jun;24(3):199–214.
84. Wang C, Pan X. Improving the Prediction of Soil Organic Matter Using Visible and near Infrared Spectroscopy of Moist Samples. J Infrared Spectrosc. 2016 Jun;24(3):231–41.
85. Aichi H, Fouad Y, Lili Chabaane Z, Sanaa M, Walter C. Prediction accuracy of local and regional soil total carbon models, calibrated based on visible-near infrared spectra, in the Djerid arid region. J Infrared Spectrosc. 2018 Oct;26(5):322–34.
86. Fontán JM, López-Bellido L, García-Olmo J, López-Bellido RJ. Soil Carbon Determination in a Mediterranean Vertisol by Visible and near Infrared Reflectance Spectroscopy. J Infrared Spectrosc. 2011 Aug;19(4):253–63.
87. Morón A, Cozzolino D. Application of near Infrared Reflectance Spectroscopy for the Analysis of Organic C, Total N and pH in Soils of Uruguay. J Infrared Spectrosc. 2002 Jun;10(3):215–21.
88. Reeves JB, Van Kessel JAS. Investigations into near Infrared Analysis as an Alternative to Traditional Procedures in Manure Nitrogen and Carbon Mineralisation Studies. J Infrared Spectrosc. 1999 Jun;7(3):195–212.
89. Reeves JB, McCarty GW, Meisinger JJ. Near Infrared Reflectance Spectroscopy for the Analysis of Agricultural Soils. J Infrared Spectrosc. 1999 Jun;7(3):179–93.
90. Peng Y, Knadel M, Gislum R, Deng F, Norgaard T, de Jonge LW, et al. Predicting Soil Organic Carbon at Field Scale Using a National Soil Spectral Library. J Infrared Spectrosc. 2013 Jun;21(3):213–22.

Investigation and recording of livestock waste for the creation of biogas plant

Christos P. Triantafyllou[2,3], Athanasios Sotirios Dounavis[1,2,3,4,5] and Christina G. Tassopoulou[2]
[1]*Department of Agriculture, University of Western Macedonia, Florina, GR-53100*
[2]*Department of Electrical and Computer Engineering, University of Western Macedonia, Kozani, GR-50100*
[3]*Department of Mechanical Engineering, University of Western Macedonia, Kozani, GR-50100*
[4]*Department of Chemical Engineering, University of Western Macedonia, Kozani, GR-50100*
[5]*MSc Program "Environmental Design", Laboratory of Technology and Policy of Energy and Environment, School of Applied Arts and Sustainable Design, Hellenic Open University, Parodos Aristotelous 18, GR-26335 Patras, Greece*
Email: adounavis@uowm.gr
x.triantafyllou@hotmail.com

DOI: 10.62579/JAGC0002

Abstract
In this paper, the research focuses on the recording of livestock waste and the investigation of the views of cattle, sheep and goat farmers of the Municipality of Amyntaio (Region of Western Macedonia in Greece) regarding renewable energy sources and more specifically biogas plants which can contribute to waste management. In order to achieve the research goal, a quantitative survey was carried out on a sample of 38 livestock farmers, which showed that the farmers are not negative towards the prospect of creating a biogas plant in their area, but they do not have sufficient knowledge about it, thus requiring training in the area.
Keywords: livestock waste, biogas, renewable energy sources

Introduction

Biogas is a renewable source of energy, which is becoming more and more popular today, at a time when the shift towards Renewable Energy Sources is more intense than ever, due to the energy and environmental crisis that shape modern reality **([1], [2], [3]).** The research which is going to be presented below is a quantitative, descriptive research, which aims to investigate the positions and opinions of the farmers of the Municipality of Amyntaio (Region of Western Macedonia in Greece) regarding waste management through biogas production. For this reason, the bibliographic review was used as well as the method of quantitative research with a questionnaire and descriptive, statistical analysis.

Energy consumption is one of the primary pillars supporting today's global economic development model. Undoubtedly, modern societies use large amounts of energy to transport people and goods, to light and heat homes, and to operate industrial plants. The increase in energy demand is directly linked to the continuous rise in living standards **([4], [5]).**

Biomass production from livestock in the Municipality of Amyntaio

The Animal husbandry (Livestock) in the Municipality of Amyntaio is an important factor in the local economy and for this reason it is proved to be particularly strong. Cattle and a significant number of sheep and goats are raised in the Municipality **[6].** The aim is to create awareness and formulate policy on sustainable development that concerns the treatment of wastes such as animal waste, crop residues.

Recording potential of livestock biomass

As far as the recording potential of livestock biomass in the Municipality of Amyntaio is concerned, the data on the quantities of goats, sheep and cattle were obtained after a request to the Ministry of Rural Development and Food (Table 1).

Methodology

The research is developed with the method of quantitative research using a questionnaire and carrying out a statistical analysis. To conduct the research, an original questionnaire was used, which was distributed to a sample of 38 livestock farmers in the Municipality of Amyntaio. The majority of livestock farmers were aged from 40 until 60 and secondary school graduates. Research results extracted from participant responses were analyzed by descriptive statistical analysis and visualized through the use of bar charts and pie charts.

Table 1. Total recording livestock potential in the Municipality of Amyntaio

Goats and sheep	Cattle	Average organic load (for goats and sheep)	Average organic load (for cattle)	Dry material from Goats and sheep	Dry material from Cattle
Number	Number	kg/d	kg/d	kg/d	kg/d
58,065	2,588	174,195.00	90,580.00	69,678.00	9,058.00
Annual organic load (for goats and sheep) 63,581.18 tn/y				63,581,175.00	kg/y
Annual organic load (for cattle) 33,061.70 tn/y				33,061,700.00	kg/y
Biogas Production from **goats and sheep x60 m³/tn FRM (fresh raw material)**				3,814,870.80	/y
Biogas Production from cattle x20 /tn FRM (fresh raw material)				661,234.00	/y
Biogas Production (Total)				4.476.104,80	/y

Results

Most survey participants, in terms of age, were between 40 and 60 years old, as shown in the following Figure 1:

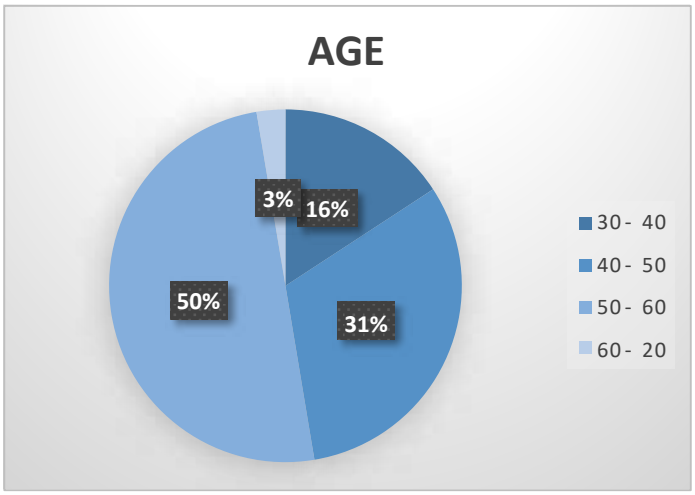

***Figure 1**: Age*

In terms of educational level, most participants have completed the secondary education, while several have completed only the primary education and a few have completed the high education, as shown in the Figure 2. Moreover, 37 of the 38 participants were residents of the survey area.

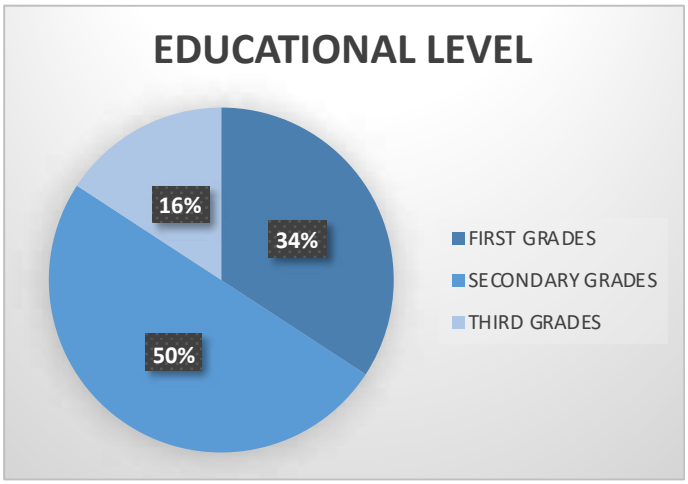

***Figure 2:** Educational Level*

After completing their biographical information, participants were asked to respond to targeted questions, which were answered on a Likert scale. The scale was five-point, allowing responses from **1 (Nothing), 2 (Little bit), 3 (Moderately), 4 (Well), 5 (Very Well).**

There were 12 questions to the participants and their answers are presented in the below diagrams such as:

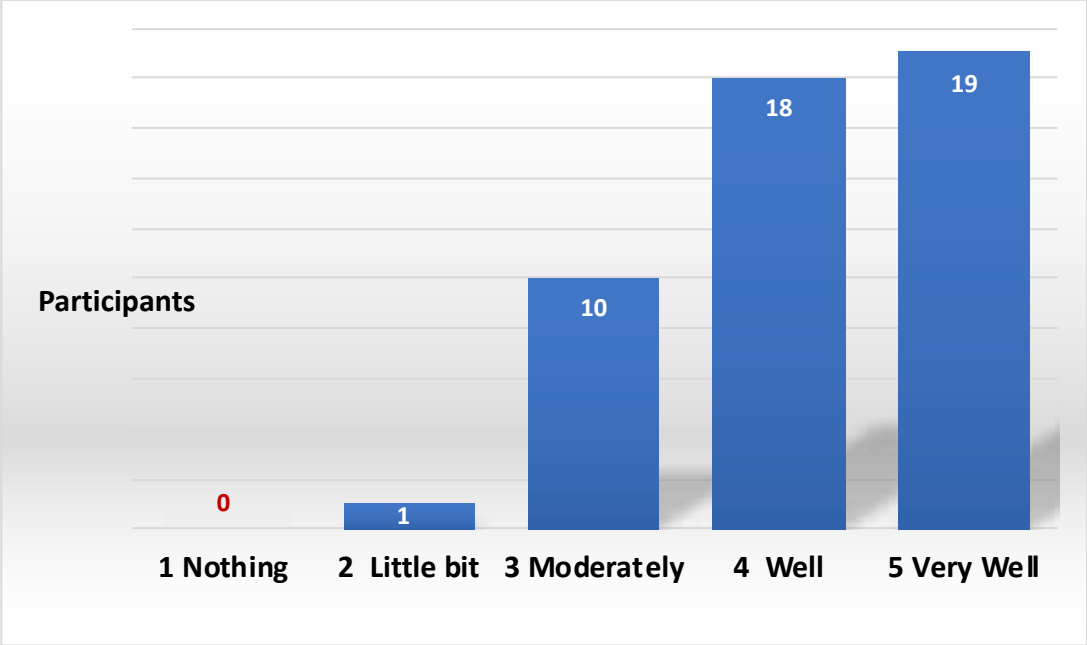

***Diagram 1**: Unit power cost*

a) Is the cost of electricity a large financial expense for the operation of your unit? (Diagram 1)
b) In the livestock unit you operate, do you use any form of Renewable Energy Sources (RES) for the production of electricity (wind turbines, photovoltaics, etc.) to meet the needs of electricity? (Diagram 2).
c) Do you know the financial benefits of using Renewable Energy Sources? (Diagram 3)
d) Do you have any problems with waste management? (Diagram 4)
e) Have you attended any informational activity on livestock waste management? (Diagram 5)
f) Would you participate in a waste management training program? (Diagram 6)
g) Do you know the economic benefits of a biogas plant? (Diagram 7)
h) Do you think that a biogas plant would be efficient? (Diagram 8)
i) Would you invest in a biogas plant? (Diagram 9)
j) Have you considered installing a biogas plant in order to treat the plant's waste? (Diagram 10)
k) Do you know how a biogas plant works? (Diagram 11)
l) Could you work with other livestock farmers or a livestock cooperative to set up a biogas plant in your area? (Diagram 12)

As it is seen from the Diagram 1, the majority of respondents consider the cost of electricity extremely important for their unit, having great concern for the reason that it causes an increase in the costs of the manufactured product they have. And quite a large percentage is afraid of a domino stoppage of payments which can be caused by the inability to repay electricity bills.

As it can be shown from the Diagram 2, the strong majority of the sample did not use any form of RES in the activity unit, the four have installed Photovoltaics, the given answers (not at all - a little) show that there is a lack of information about RES, but also a large scope for development and entrepreneurship in green energy in livestock units.

In the Diagram 3, the answers were mixed, however, none of the participants chose option 5 (Very Well). This shows the lack of knowledge, maybe misinformation, but also the absence of information from the state on RES issues.

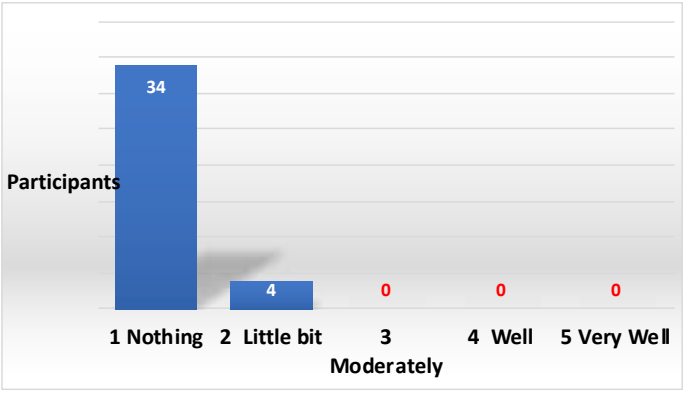

***Diagram 2**: Use of RES*

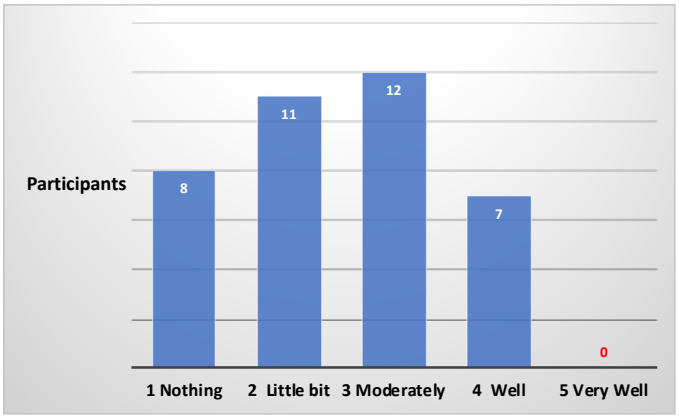

***Diagram 3**: Ability of knowledge for the benefits of using RES*

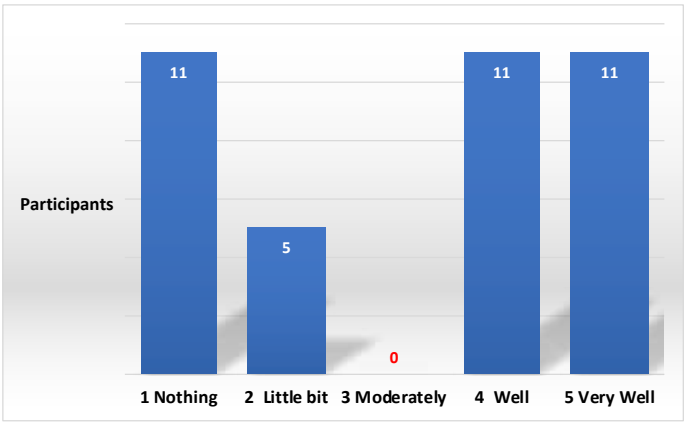

***Diagram 4**: Problems with the waste management*

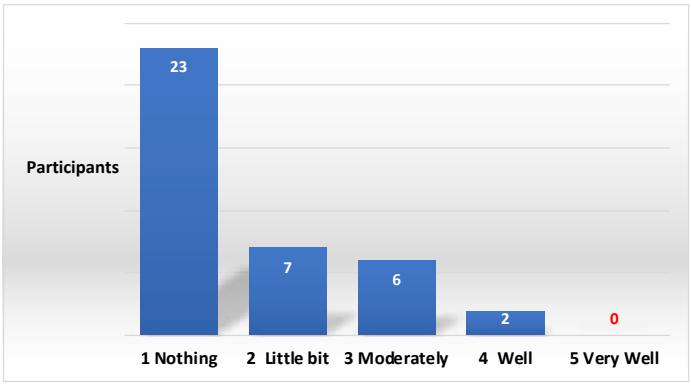

***Diagram 5**: Monitoring of informational action for waste management*

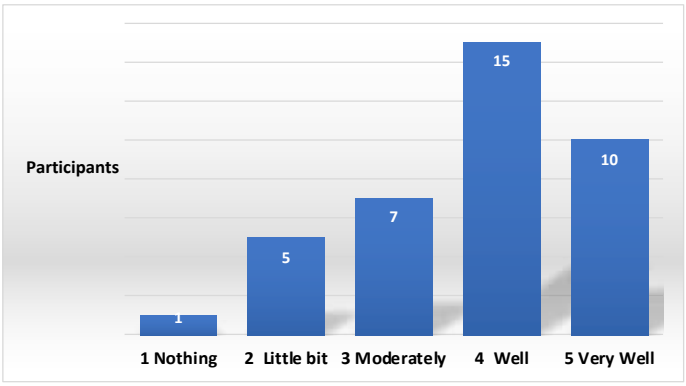

***Diagram 6**: Willingness to participate in the future*

In the Diagram 4, the results showed a particular polarization between responses, with half of the sample stating that the participants face problems not at all to a little, with the other half reporting that they face problems a lot to very much, these responses are due to the fact that some farmers are also farmers i.e. cultivate the fields to produce their own food for their animals, with the result that livestock waste is used as fertilizer. The respondents, who answered that livestock waste is a problem for them, are the livestock farmers who do not cultivate fields in order to produce the food of their lives.

The option "Nothing" received more responses, as shown in the Diagram 5. The question, however, recorded a big problem, that of insufficient information on the livestock waste management. In this way, there is a lot of scope for informational actions, seminars, workshops and other kinds of actions to inform livestock farmers about this issue.

In the Diagram 6, only one of the participants was negative, while the largest group were those who supported the choice "Well", this result shows that the impressive will of livestock farmers and willingness to participate in informative events and entrepreneurship actions with the aim of developing the profession who are active.

In the Diagram 7, the participants ignore important information which would help them in order to reduce the costs of their businesses and grow them. Therefore, in this topic, an update could be made on the benefits, mainly the financial ones for the creation of a biogas unit.

In the Diagram 8, most likely, the research participants consider that a biogas plant would be effective because it will manage their livestock waste. In addition, the biogas which will result from waste management will help the businesses to reduce some basic costs (eg energy costs).

In the Diagram 9, the results confirm the positive attitude of the livestock farmers in the area of the Municipality of Amyntaio towards both the waste management of their units and the reduction of the energy footprint of their businesses. In this way, breeders realize the financial benefit they will have even if this is done in the long term.

In the Diagram 10, the thought of installing a gas plant to process their livestock waste is almost non-existent (only 8 out of 38 answered positively). In essence, no experts in biogas units, waste management and financial tools have approached the farmers in the area to guide them in such an investment.

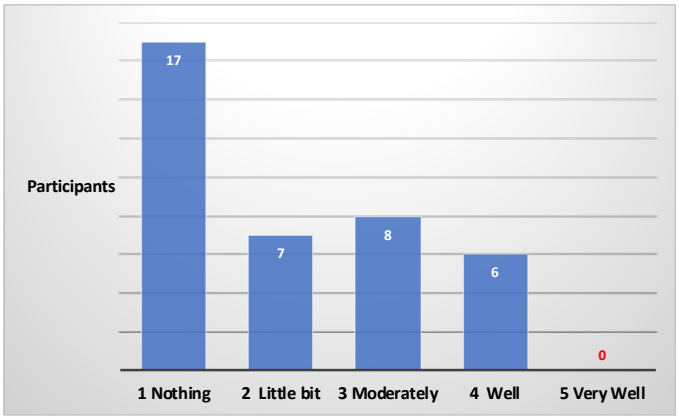

***Diagram 7**: Knowledge about the economic benefits of a biogas plant*

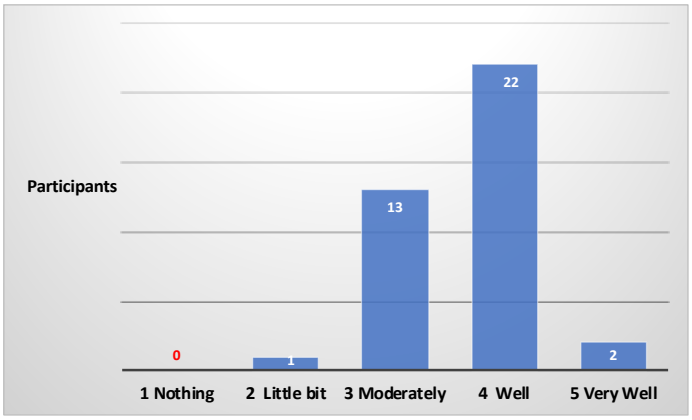

***Diagram 8**: Biogas plant efficiency*

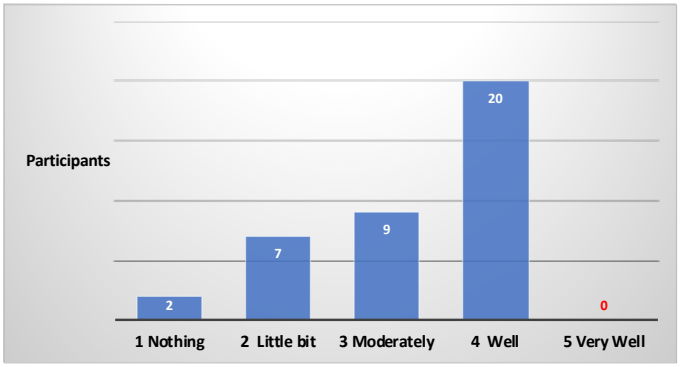

***Diagram 9**: Investment in a biogas plant*

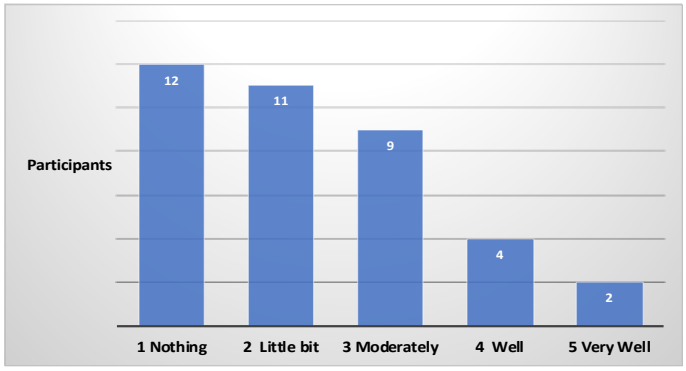

***Diagram 10**: Possibility of installing a biogas plant in the employment unit*

In the Diagram 11, the responses of the participants were expected. This happens because the educational level of the area's livestock farmers is low and also there is no thought of installing a biogas plant which will properly manage their livestock waste.

As it can be observed from the answers to all the previous questions, the livestock farmers of the area are positive about the prospect of installing a biogas plant and there is the need for the creation of a breeders' cooperative emerges, as shown in the Diagram 12. This cooperative will manage the waste of livestock units on behalf of its members. Of course, in the past the cooperatives which were created, mainly among farmers, did not have the best results. Therefore, taking into account the example of agricultural cooperatives, perhaps the reason can be identified why the majority of the participating farmers answered positively (Well) but not definitely (Very Well).

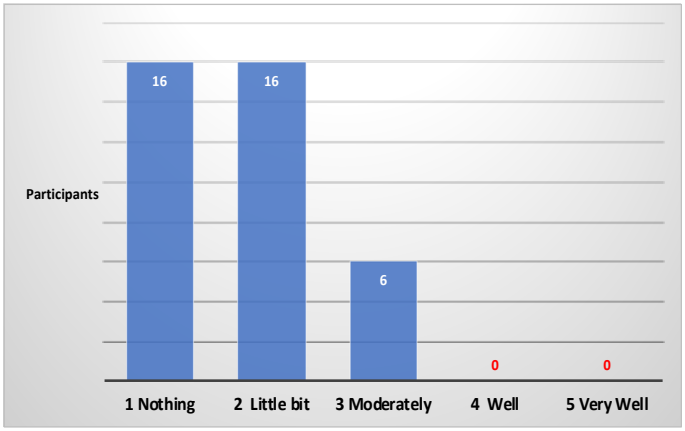

***Diagram 11**: Ability of knowledge of biogas plant operation*

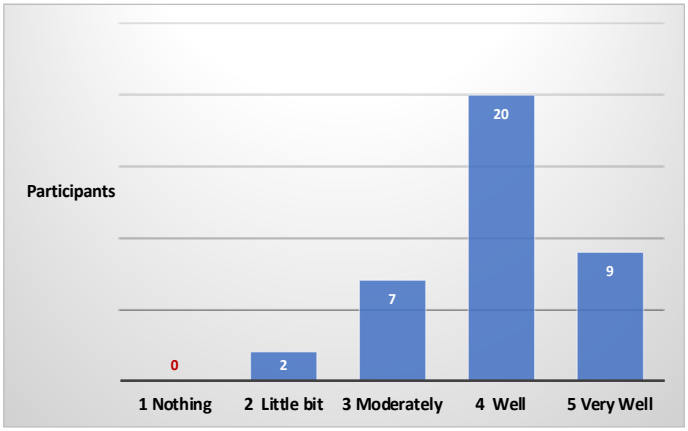

***Diagram 12:** Collaboration to create a biogas* plant

Conclusions

To summarize, the investigation and recording of livestock waste was studied with the aim of creating a biogas unit. Initially, from the registration of the animals in the area of the Municipality of Amyntaio, it appears that there are the required livestock units with the animal potential to support the project of operating a biogas unit in the area from their waste. Moreover, from the calculations made, it is found that there will be a significant economic benefit since the quantities of livestock waste are very high.

Additionally, through the installation of the biogas unit, for which the majority of the participating breeders is agreed, the proper livestock waste management will be achieved. The result of proper waste management will be the reduction of the environmental footprint of the livestock units in the area. In this way, the main goal will be achieved, which based on the findings of the research is also the goal of the breeders, which is the care of the environment in the area of the Municipality of Amyntaio.

Finally, from the answers given by the breeders, it was found that they have not been informed about the installation and operation of a biogas plant and about the waste management of their livestock units. In addition, while the majority of livestock farmers are positive about the prospect of operating a biogas plant, on an individual or cooperative level, they are unaware of important tools (e.g. funding from European Union programs), strategies and policies which facilitate such ventures.

A typical example is that they ignore the policy of the European Union for the circular economy, which includes the reuse of waste for the production of new products. In this particular case, the reuse of livestock waste in the production of biogas is ignored, which will significantly help both in terms of energy sufficiency and saving resources.

Solutions for these problems can be found very easily and efficiently. The design and implementation of training seminars on the subject of biogas units as well as waste management could cover the information gap of the livestock farmers in the area. In the context of the specific programs, modules could be included which would refer to the available financial tools for an investment in a biogas plant and to give good practices for the use tools.

For example, a presentation of existing biogas units could show the progress of the unit from the beginning (eg business plan) to the operation of the unit and mentioning all the tools used at each stage. In this way, the breeders of the area, will be informed about the issues previously mentioned, and will also understand, through the examples of the existing biogas units, that there is a good investment which can be carried out and help on many levels both their own the livestock units and as well as the Municipality of Amyntaio.

References

[1] Athanasios Sotirios Dounavis, Ioanna Ntaikou and Gerasimos Lyberatos, "Production of biohydrogen from crude glycerol in an upflow column bioreactor", *Bioresource Technology* Volume 198, (December 2015): Pages 701-708. http://dx.doi.org/10.1016/j.biortech.2015.09.072

[2] Athanasios Sotirios Dounavis, Ioanna Ntaikou, Maria Kamilari and Gerasimos. Lyberatos, "Production of advanced biobased hydrogen enriched methane from waste glycerol in a two stage continuous system", *Waste and Biomass Valorization* Volume 7, (March 2016): Pages 677-689. https://doi.org/10.1007/s12649-016-9538-9

[3] Athanasios Sotirios Dounavis and Anastasios Tasionas, "Techno-economic Analysis of the Olive Oil Mills Waste Valorisation for Energy Production: A Case Study of Corfu", *Environmental Research, Engineering and Management Journal* Volume 75, No 4 (December 2019): Pages 18-29. https://doi.org/10.5755/j01.erem.75.4.23072

[4] Charles Shaaba Saba, Charles Raoul Tchuinkam Djemo, Joel Hinaunye Eita and Nicholas Ngepah, "Towards environmental sustainability path in Africa: The critical role of ICT, renewable energy sources, agriculturalization, industrialization and institutional quality", *Energy Reports* Volume 10, (November 2023): Pages 4025-4050. https://doi.org/10.1016/j.egyr.2023.10.039

[5] Spiru Paraschiv, "Analysis of the variability of low-carbon energy sources, nuclear technology and renewable energy sources, in meeting electricity demand", *Energy Reports* Volume 9, Supplement 11 (October 2023): Pages 276-283. https://doi.org/10.1016/j.egyr.2023.09.008

[6] Municipality of Amyntaio (2022). https://www.amyntaio.gr/oikonomia/2-kthnotrofia

The impact of restriction measures implementation due to covid-19 ov particulate atmospheric pollution in greek urban areas

Kofinas Periklis[1], Kelessis Apostolos[1,2], Kassomenos Pavlos[1,3]

[1] Hellenic Open University, School of Sciences and Technology/WM, Aristotelous 18, Patras 26335, Greece. E-mail: periskofinas@gmail.com / std122888@ac.eap.gr

[2] Environmental Department, Municipality of Thessaloniki, Kleanthous 18, Thessaloniki GR-54642.

[3] University of Ioannina, Department of Physics, Lab. of Meteorology, Ioannina 45110, Greece.

DOI: 10.62579/JAGC0003

Abstract

In this work, the variation on the levels of suspended particulates, in Greek urban areas, was examined, for the period of the restrictive measures implementation (period 1: March to May 2020 and period 2: November 2020 to January 2021) due to the pandemic caused by the COVID-19 virus. The PM_{10} and $PM_{2.5}$ concentrations are measured by the National Air Pollution Monitoring Network of Greece monitored by the Energy/Environment Ministry. In particular, a comparison of the PM_{10} and $PM_{2.5}$ concentration levels was made, concerning the above time periods, with the corresponding atmospheric pollution levels during the periods 2001-2009 (period before the Greek economic crisis), 2010-2019 (period during the Greek economic crisis), as well as with the entire time period 2001-2019. The assessment showed a significant reduction in the levels of both PM_{10} concentrations, which ranged from 8% to 45%, and $PM_{2.5}$ concentrations, which ranged from 13% to 48%, thus demonstrating the effectiveness of the control measures in improving air quality in Greek urban areas. The above findings show that with appropriate emission control strategies, vital improvements in the air environment of urban areas can be achieved.

Keywords

Atmospheric pollution, Particle pollution, COVID-19 pandemic, restrictive measures.

Introduction and background

Airborne particulate matter, particularly PM_{10} (particles with an aerodynamic diameter equal to or less than 10μm) and $PM_{2.5}$ (particles with an aerodynamic diameter equal to or less than 2.5μm), are frequently investigated in urban areas due to their adverse health effects such as respiratory problems, cardiovascular diseases and neurodevelopmental effects [1-2]. Particularly, PM_{10} and $PM_{2.5}$ include inhalable particles that are small enough to penetrate the thoracic region of the respiratory system, which cause health effects that include respiratory and cardiovascular morbidity, such as aggravation of asthma, respiratory symptoms, an increase in hospital admissions and mortality from cardiovascular and respiratory diseases as well as from lung cancer [3]. In 2020, exposure to concentrations of fine particulate matter above the 2021 WHO guideline level resulted in 238,000 premature deaths in the 27 EU Member States (EU-27), although in 2020, the number of premature deaths attributable to exposure to fine particulate matter above the WHO guideline level fell by 45% in the EU-27, compared to 2005 [4]. Besides premature deaths, in 2019, exposure to $PM_{2.5}$ led to 175,702 years lived with disability (YLDs) due to chronic obstructive pulmonary disease in 30 European countries [4]. For these reasons, over the last two decades, several time-series and cohort epidemiological studies have been conducted to investigate the health significance of ambient particulate matter [5-6] and established the association between human exposure and the risk of increased mortality and morbidity.

The largest metropolitan urban areas in Greece suffer from poor air quality due to variety of emission sources, topography and climatic conditions favoring the accumulation of pollution. Nevertheless, over the last two decades, a significant reduction in PM concentration levels was observed in the largest Greek urban areas due to evolution of the environmental legislation, with more stringent air quality standards coming into effect, the replacement of old polluting vehicles, the improvement of fuel quality, the establishment of various measures and traffic interventions and the new socio-economic conditions that come up, after 2010, due to the Greek economic crisis (cutback in private car use, fuel price increase, etc.) and especially in the 2010-2019 decade the constantly increasing use of natural gas as an energy source in various industrial production processes and for building heating [7-17]. The de-

creasing trend of the PM_{10} and $PM_{2.5}$ concentrations, due to the above-mentioned changes in emissions sources, is particularly encouraging for the air quality in Greek cities. Nevertheless, the exceedances of the annual PM_{10} EU limit remain frequently, in Athens and Thessaloniki [7, 17].

The COVID-19 pandemic caused an unprecedented and multi-layered global crisis, and the implementation by the state of a set of restrictive measures to limit the spread of Covid-19, in addition to the health and economic consequences, brought about a change in the emission of air pollutants.

The question of the effects of restriction measures on the variation of the particulate matter concentrations in urban cities has been addressed in several studies internationally [18-21]. These studies agree that there has been a significant reduction in particulate matter concentrations during the periods of implementation of traffic control measures, due to the COVID-19 pandemic. As a result, over four Italian cities (Milan, Turin, Bologna, and Florence), concentrations of PM_{10} and $PM_{2.5}$ decreased, up to 23% and 21%, respectively [18]. Also, in Milan-Italy a decrease of PM_{10} and $PM_{2.5}$ was found up to 48.0% and 47.2%, respectively [22]. Additionally, in the five largest cities of Poland (Warsaw, Wroclaw, Lodz, Krakow and Gdansk) a decrease of the PM_{10} and $PM_{2.5}$ concentrations, up to 33.9% and 26.4%, respectively, was found [23]. Moreover, in Chandigarh-India a significant decrease of PM_{10} and $PM_{2.5}$ concentrations was found, up to 36.8% and 28.8%, respectively [24] while in Canada's four largest cities (Toronto, Montreal, Vancouver, and Calgary) a decrease up to 17% in $PM_{2.5}$ was found [25]. Kumari and Toshniwal [26] reviewed data from 162 monitoring stations from 12 cities across the world and concluded that the lockdown restrictions led to, PM_{10} and $PM_{2.5}$ concentrations decreases by, 24–47% and 20–34%, respectively. As far as the Greek region, the studies for the PM_{10} and $PM_{2.5}$ levels showed a decrease of $PM_{2.5}$ concentrations, up to 18%, in the Greater Area of Athens [27], while in the city of Volos, a reduction of 37.4% in mean daily $PM_{2.5}$ concentration was found, according to Kotsiou et al. [28] and also, a decrease, up to 24%, for the PM_{10} concentrations in the city center of Athens [29]. Furthermore, on the air of Western Macedonia, according to Begou et al. [30], a decrease in average $PM_{2.5}$ concentrations was found, ranging from −1% to −36% and a higher decrease in average PM_{10} concentrations ranging from −13% to −40% was found.

In this work, the variation of the suspended particulate levels, in major Greek cities, were examined, for the two periods of the implementation of the government restrictive measures (period 1: March to May 2020 and period 2: November 2020 to January 2021), due to the pandemic, caused by the COVID-19 virus, in comparison to the corresponding months of three specific periods. These periods were 2001-2009 (the period before the Greek economic crisis), 2010-2019 (period during the Greek economic crisis), as well as with the entire time period 2001-2019. The study was conducted to investigate the changes in the PM_{10} and $PM_{2.5}$ concentration levels, during the above mentioned two periods when the restrictive measures were implemented by the state in Greek urban and suburban areas in order to examine the impact of these control measures on air pollution levels.

The present study was extended to all the major cities in Greece, for which there were available PM concentration data. Therefore, PM_{10} and $PM_{2.5}$ concentration measurements for Athens, Thessaloniki, Patra, Larisa and Volos, were examined during an extended time period, from 2001 to 2019. Thus, the comparison of the PM_{10} and $PM_{2.5}$ concentration levels, during the two periods of the restrictive measures implementation due to the pandemic caused by the COVID-19 virus, were studied in the largest Greek cities not only during this entire 19-years period, but also, during the time interval 2001-2009 that is a period before the Greek economic recession and the 2010-2019 time interval that is a period during the Greek economic crisis (during this period the prevailing economic conditions may affect air pollution concentrations levels). This quantitative assessment in the measured PM concentration levels can be proved essential in order to show the effectiveness of the control measures in improving air quality in Greek urban areas.

Materials and Methods

Air quality data, and in particular, the PM_{10} and $PM_{2.5}$ hourly concentrations measurements, from ground-based monitoring stations, located in the greater area of Athens, Thessaloniki, Patra and Volos, were provided by the National Air Pollution Monitoring Network (NAPMN), of the Department of Atmospheric Quality, of the Ministry of Environment and Energy of Greece [31]. From these monitoring stations, the hourly concentration measurements of PM_{10} and $PM_{2.5}$ (μgm^{-3}), during 2001 to 2019, were used in the analysis [7]. The PM_{10} and $PM_{2.5}$ analyzers are using the beta-gauge principle, according the EU standards [32], while the calibrations of the analyzers were based on standard sample of known particulate concentration and performed according to the technical standards of the instruments [31]. For the study of the variations of PM_{10} and $PM_{2.5}$ levels, representative monitoring stations (see Fig.1 and Table 1) from NAPNM [31] were selected, in deferent sites of major Greek cities.

Table 1. The representative monitoring stations of the National Air Pollution Monitoring Network (NAPMN), of the Department of Atmospheric Quality, of the Ministry of Environment and Energy of Greece in greater area of Athens, Thessaloniki, Patra, Larisa and Volos [31].

Station name and code	WGS84		GGRS 87		Altitude (m –asl)	type of monitoring station
	Geographical longitude	Geographical latitude	X (m)	Y(m)		
Aristotelous (ARI)	23,7276178492125	37,9880660501340	475932	4204238	75	urban traffic
Lykovrysi (LYK)	23,7889866802124	38,0677931723947	481341	4213070	234	suburban background
Marousi (MAR)	23,7873721482217	38,0308379318551	481190	4208970	170	urban background
Peiraias I (PIR)	23,6452301569805	37,9446567667974	468679	4199446	4	urban traffic
Agia Paraskevi (AGP)	23,8194215757818	37,9951106089158	483995	4205000	290	suburban background
Thracomacedones (THR)	23,7581958361834	38,1435214274982	478662	4221479	550	suburban background
Koropi (KOR)	23,8790262856793	37,9013083393701	489215	4194584	140	suburban background
Agia Sophia (AGS)	22,9450997512424	40,6337247192803	410641	4498347	12	urban traffic
Panorama (PAO)	23,0316894494349	40,5889178187916	417909	4493289	363	suburban background
Kordelio (KOD)	22,8932185580361	40,6734529005153	406309	4502811	30	Industrial
Sindos (SIN)	22,8021687222328	40,6578424569135	398590	4501179	14	Industrial
Patras -2 (PAII)	21,7345123031810	38,2464695337774	301601	4235301	8	urban traffic
Volos -1 (VOL)	22,9429220469889	39,3667116624368	408789	4357718	31	urban background
Larisa (LAR)	22,4145498503763	39,6355309133568	363796	4388220	85	urban background

Thus, the monitoring stations were located in the city center (urban traffic monitoring station), in the peripheral areas of the city (urban background monitoring station), in the greater area of the city (suburban background monitoring station) and in the industrial area of the city (industrial monitoring station). The measurements of the suspended particulates were used only if they met the following criteria:

- They were recorded for at least 10 years between 2001 and 2019.
- They were recorded during the months when the government imposed restrictive measures due to the COVID-19 pandemic.

Therefore, PM_{10} and $PM_{2.5}$ mean monthly values, during these two periods [March-May 2020 (for the 1st period of the restrictive measures) and November 2020-January 2021 (for the 2nd period of the restrictive measures], were compared with the PM_{10} and $PM_{2.5}$ mean monthly values of the corresponding months, during three specific periods. As mentioned before these periods were 2001-2009 (the period before the Greek economic crisis), 2010-2019 (the period during the Greek economic crisis - during this period the prevailing economic conditions may affect air pollution concentrations levels), as well as with the entire time period 2001-2019.

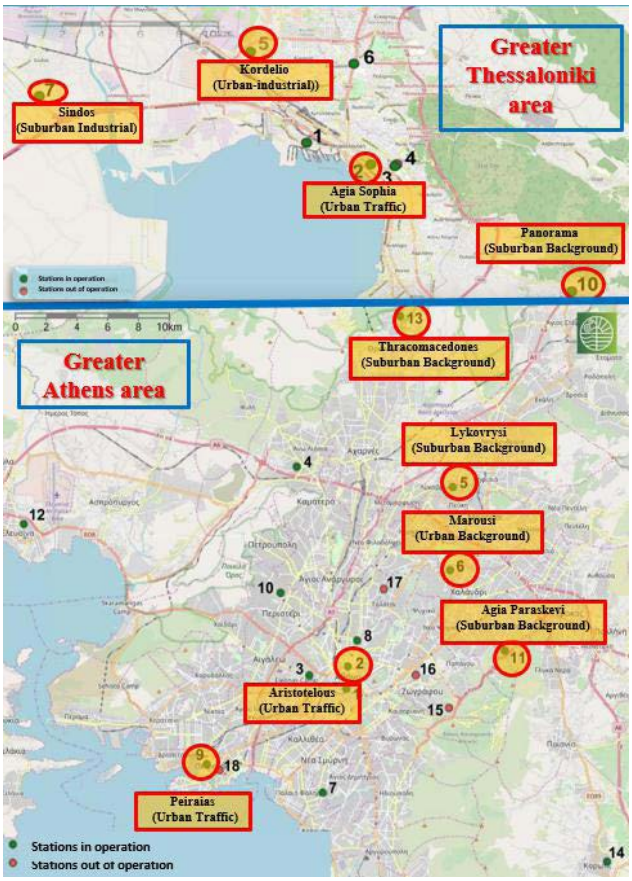

Figure. 1. *The representative monitoring stations (marked with a red circle/frame) of the National Air Pollution Monitoring Network (NAPMN), in the greater area of Thessaloniki (upper part) and in the greater area of Athens (lower part) [31].*

Results, Discussion

PM_{10} and $PM_{2.5}$ mean monthly concentrations (μgm^{-3}), of the two periods of the restrictive measures (1st period March-May 2020 and 2nd period November 2020-January 2021), were calculated and compared with the PM_{10} and $PM_{2.5}$ mean monthly values and the standard deviation ($\pm 1\sigma$), during the corresponding months, through the three specific time intervals (2001-2009 - period before the Greek economic crisis, 2010-2019 - period during the Greek economic crisis and with the entire time period 2001-2019), at representative monitoring stations, in major Greek cities. Also, the linear regression trend of the PM_{10} and $PM_{2.5}$ mean yearly concentrations, was calculated through the entire period (2001-2019).

From the figures and tables below (Fig. 2-5(a) and Tables 2-5) we found a clear decrease in the concentrations of both PM_{10} and $PM_{2.5}$ levels, for the months under review (1st period March-May 2020 and 2nd period November 2020-January 2021), when the restrictive measures were in force due to the COVID-19 pandemic, in all major Greek cities (Athens, Thessaloniki, Patra, Volos and Larisa). This decrease was found, almost similarly, at the urban traffic sites (Fig. 2(a) and Table 2), which are located in the centers of the cities, at urban background sites (Fig. 3(a) and Table 3), which are located in the peripheral areas of the cities, at the suburban background sites (Fig. 4(a) and Table 4), which are located in the greater areas of the cities and also at the industrial areas of the cities (Fig. 5(a) and Table 5). Moreover, this significant decrease, in almost all cases, exceeds the range of values of the standard deviation (+/-σ), of both PM_{10} and $PM_{2.5}$ mean monthly concentrations, of the corresponding months, throughout the three specific periods (2001-2009, 2010-2019 and 2001-2019).

The assessment showed that this significant percentage reduction in the concentration levels (Tables 2-5), over the two periods of the restrictive measures (1st period March-May 2020 and 2nd period November 2020-January 2021), when the restrictive measures were in force, due to the COVID-19 pandemic, for PM_{10} levels ranged, from 19% to 45%, at the urban traffic sites (Fig. 2(a) and Table 2), from 10% to 41%, at urban background sites (Fig. 3(a) and Table 3), from 24% to 41%, at the suburban background sites (Fig. 4(a) and Table 4), and from 8% to 43%, at the industrial areas of the cities (Fig. 5(a) and Table 5). Accordingly, for $PM_{2.5}$ levels the reduction ranged, from 33% to 48%, at the urban traffic sites (Fig. 2(a) and Table 2), and from 13% to 44%, at suburban background sites (Fig. 4(a) and Table 4).

We also note, that the reduction in the concentrations of both PM_{10} and $PM_{2.5}$ levels during the months of the two periods of the restrictive measures, was, almost in all cases, higher in the period 2001-2009, compared to the period 2010-2019 and the entire period 2001-2019 (Fig. 2-5(a) and Tables 2-5). This was mainly due to the significant reduction in the levels of air pollutants resulting from the new socio-economic conditions that arose, after 2010, because of the Greek economic crisis [7, 10-12, 14-15] and the ever-increasing use of natural gas as an energy source in various industrial production processes and for building heating, especially in the 2010-2019 decade [7, 11-13], while the continuously changing environmental legislation imposed ever more stringent systems of air pollution control and control of industrially emitted pollutants [11, 14-16].

In addition, it was found that the reduction in PM_{10} and $PM_{2.5}$ concentrations was roughly of the same order of magnitude over the two periods of the restrictive measures (Tables 2-5), which was calculated in comparison, respectively, with the PM_{10} and $PM_{2.5}$ mean monthly values, for the corresponding months, during the three periods (2001-2009, 2010-2019 and 2001-2019), in major Greek cities. This founding was found, even though in the first period of the restrictive measures (March-May 2020) a complete reduction in vehicle traffic (and thus emissions) was imposed. One possible explanation of this result may be the meteorological conditions and the dispersion processes that prevail, at each measurement site, as well as the local characteristics of each site, which determine decisively the degree of accumulation of the particulate pollutants. It must also be noted that both PM_{10} and $PM_{2.5}$ levels show significant seasonal variation, resulting in increased PM levels during the winter period of the year, mainly due to the increased vehicle traffic emissions and the emissions from building heating, especially in densely populated urban areas [7, 9-12, 14-17]. It should be pointed out, that the second period of the restrictive measures, when the PM levels increase, was implemented during winter period November 2020-January 2021. Also, the PM_{10} and $PM_{2.5}$ levels, during these two periods, were below the European Union annual limit of $40\mu g/m^3$ for PM_{10} and the corresponding annual limit of $25\mu g/m^3$ for $PM_{2.5}$.

PM_{10} Urban Traffic Stations

Greater Athens area

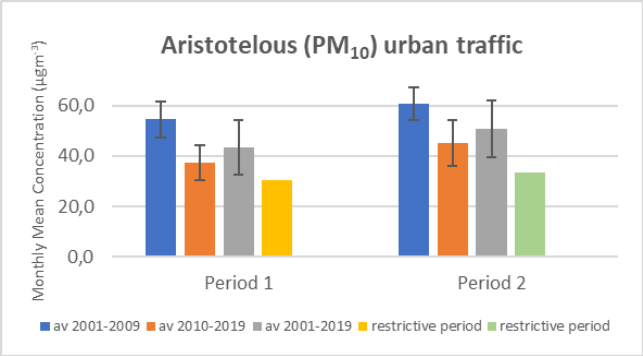

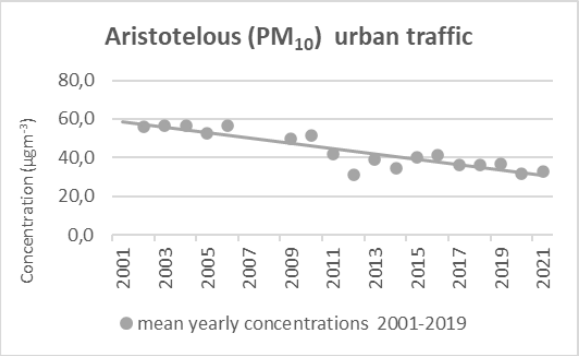

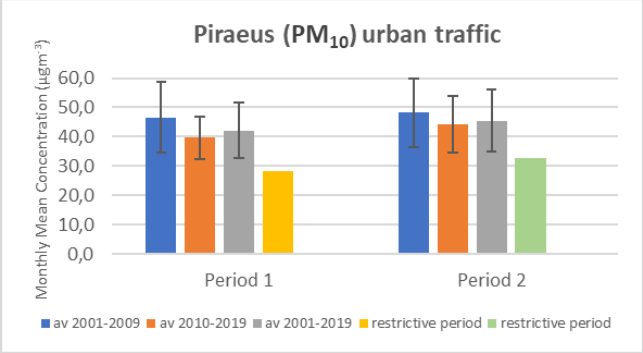

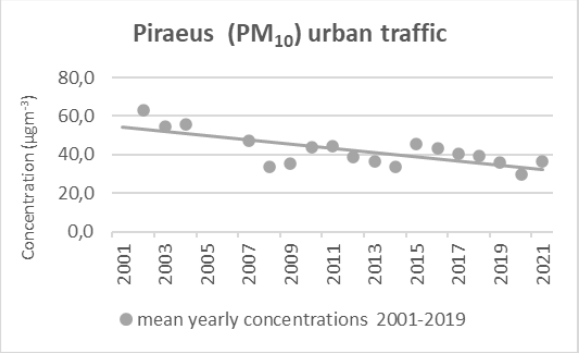

Greater Thessaloniki area

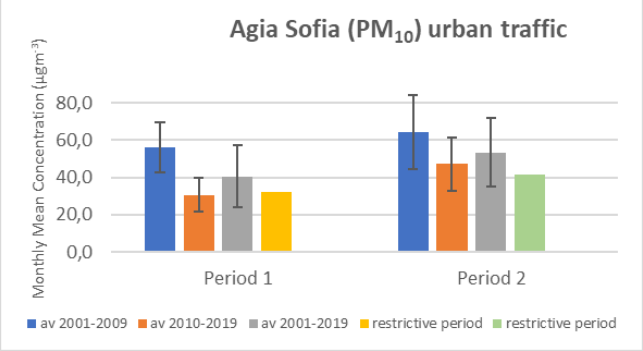

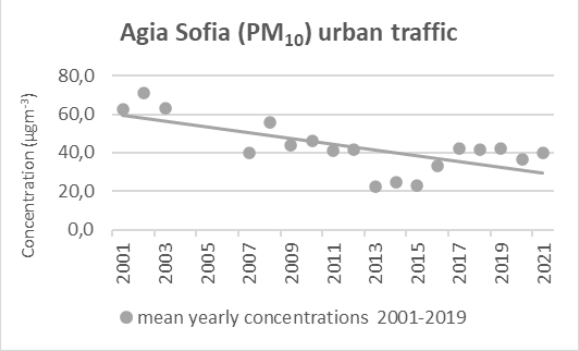

Patra

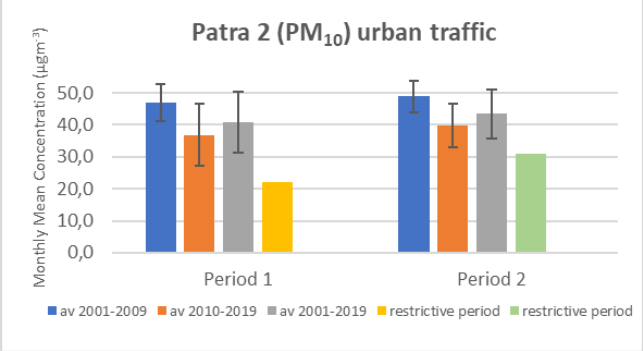

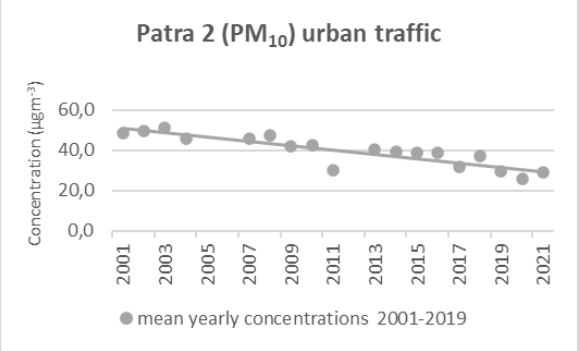

$PM_{2.5}$ Urban Traffic Stations
Greater Athens area

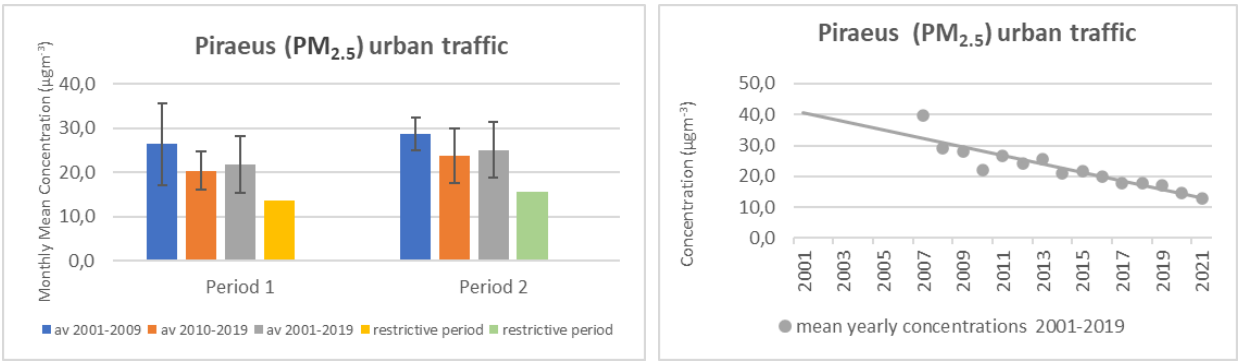

Figure. 2. *(a) PM10 and PM2.5 mean monthly concentrations (μgm-3), during the two periods of the restrictive measures (1st period March-May 2020 and 2nd period November 2020-January 2021), in comparison, respectively, with the PM10 and PM2.5 mean monthly values and standard deviation (+/-σ), of the corresponding months, through the three specific periods (2001-2009, 2010-2019 and 2001-2019), at urban traffic sites, in major Greek cities. (b) The linear regression trend of the PM10 and PM2.5 mean yearly values (μgm-3), through the entire period (2001-2019), at urban traffic sites, in major Greek cities.*

Table 2. The percent (%) differences of PM_{10} and $PM_{2.5}$ mean monthly concentrations, during the two periods of the restrictive measures (1st period March-May 2020 and 2nd period November 2020-January 2021), which were calculated, respectively, in comparison with the PM_{10} and $PM_{2.5}$ mean monthly values, for the corresponding months, during the three time intervals (2001-2009, 2010-2019 and 2001-2019), at urban traffic sites, in major Greek cities.

PM_{10} Urban Traffic Sites		
Time interval	1st period	2nd period
2001-2009	-45%	-37%
2010-2019	-19%	-21%
2001-2019	-32%	-28%

$PM_{2.5}$ Urban Traffic Sites		
Time interval	1st period	2nd period
2001-2009	-48%	-45%
2010-2019	-33%	-34%
2001-2019	-38%	-37%

PM_{10} Urban Background Stations
Athens area

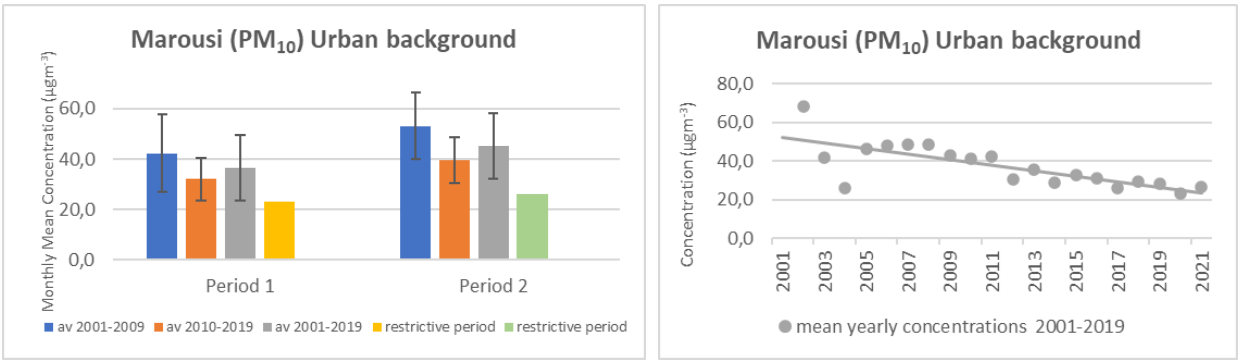

Volos

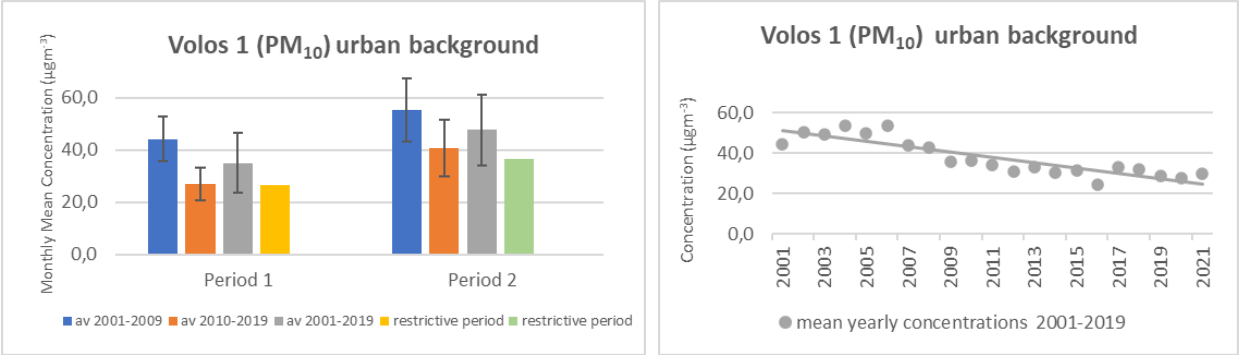

Larisa

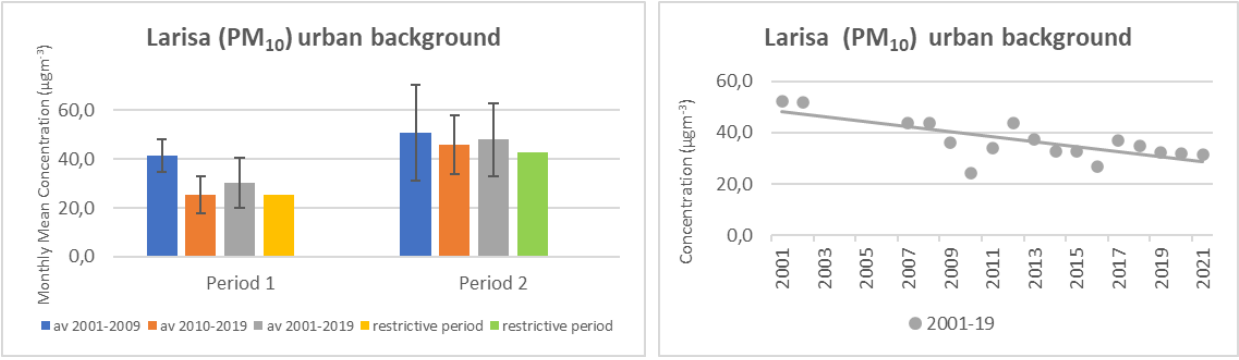

Figure. 3. *(a) PM10 mean monthly concentrations (μgm-3), during the two periods of the restrictive measures (1st period March-May 2020 and 2nd period November 2020-January 2021), in comparison, respectively, with the PM10 mean monthly values and standard deviation (+/-σ), of the corresponding months, through the three specific periods (2001-2009, 2010-2019 and 2001-2019), at urban traffic sites, in major Greek cities. (b) The linear regression trend of the PM10 mean yearly values (μgm-3), through the entire period (2001-2019), at urban background sites, in major Greek cities.*

Table 3. The percent (%) differences of PM_{10} mean monthly concentrations, during the two periods of the restrictive measures (1st period March-May 2020 and 2nd period November 2020-January 2021), which were calculated in comparison, respectively, with the PM_{10} mean monthly values, for the corresponding months, during the three time intervals (2001-2009, 2010-2019 and 2001-2019), at urban background sites, in major Greek cities.

PM_{10} Urban Background Sites		
Time interval	1st period	2nd period
2001-2009	-41%	-33%
2010-2019	-10%	-16%
2001-2019	-26%	-25%

PM_{10} Suburban Background Stations
Greater Athens area

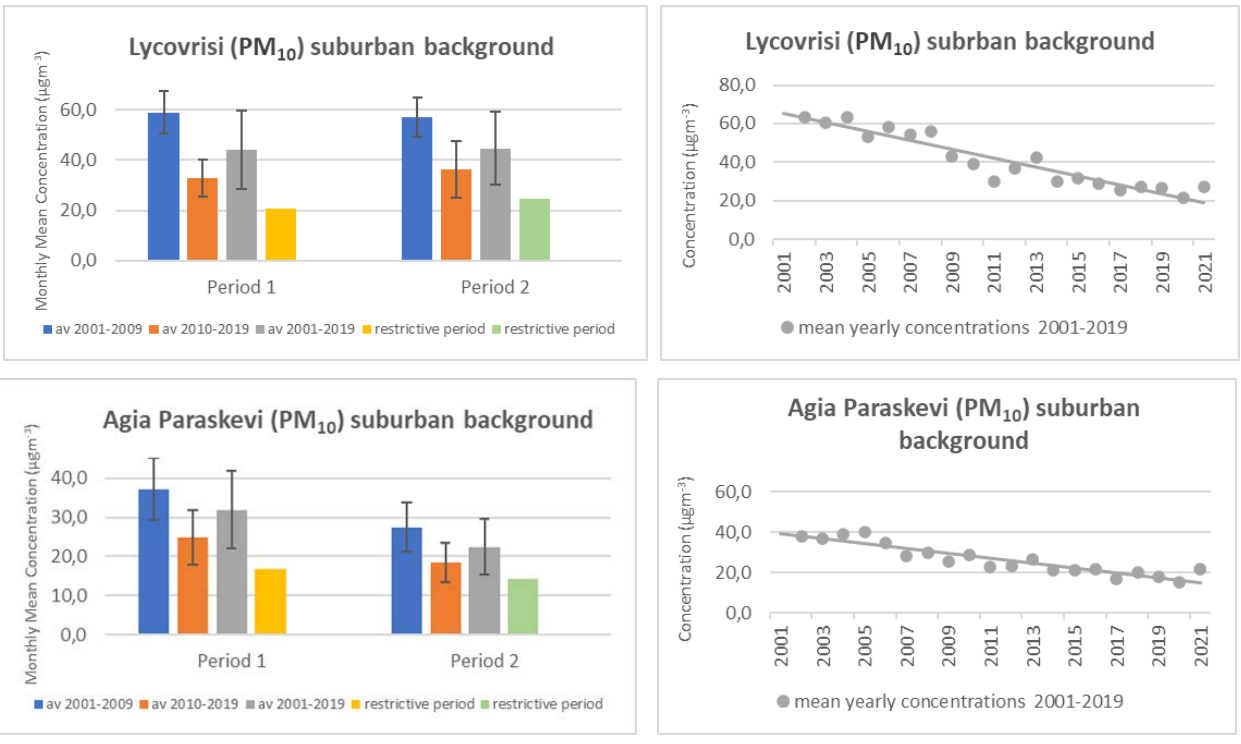

Figure. 4. *(a) PM_{10} and $PM_{2.5}$ mean monthly concentrations (μgm^{-3}), during the two periods of the restrictive measures (1st period March-May 2020 and 2nd period November 2020-January 2021), in comparison, respectively, with the PM_{10} and $PM_{2.5}$ mean monthly values and the standard deviation (+/-σ), of the corresponding months, through the three specific periods (2001-2009, 2010-2019 and 2001-2019), at urban traffic sites, in major Greek cities. (b) The linear regression trend of the PM_{10} and $PM_{2.5}$ mean yearly values (μgm^{-3}), through the entire period (2001-2019), at suburban background sites, in major Greek cities*

Table 4. The percent (%) differences of PM_{10} and $PM_{2.5}$ mean monthly concentrations, during the two periods of the restrictive measures (1st period March-May 2020 and 2nd period November 2020-January 2021), which were calculated, respectively, in comparison with the PM_{10} and $PM_{2.5}$ mean monthly values, for the corresponding months, during the three periods time intervals (2001-2009, 2010-2019 and 2001-2019), at suburban background sites, in major Greek cities.

$PM_{2.5}$ Suburban Background Sites		
Time interval	1st period	2nd period
2001-2009	-44%	-30%
2010-2019	-13%	-13%
2001-2019	-22%	-18%

PM_{10} Suburban Background Sites		
Time interval	1st period	2nd period
2001-2009	-41%	-39%
2010-2019	-24%	-27%
2001-2019	-31%	-32%

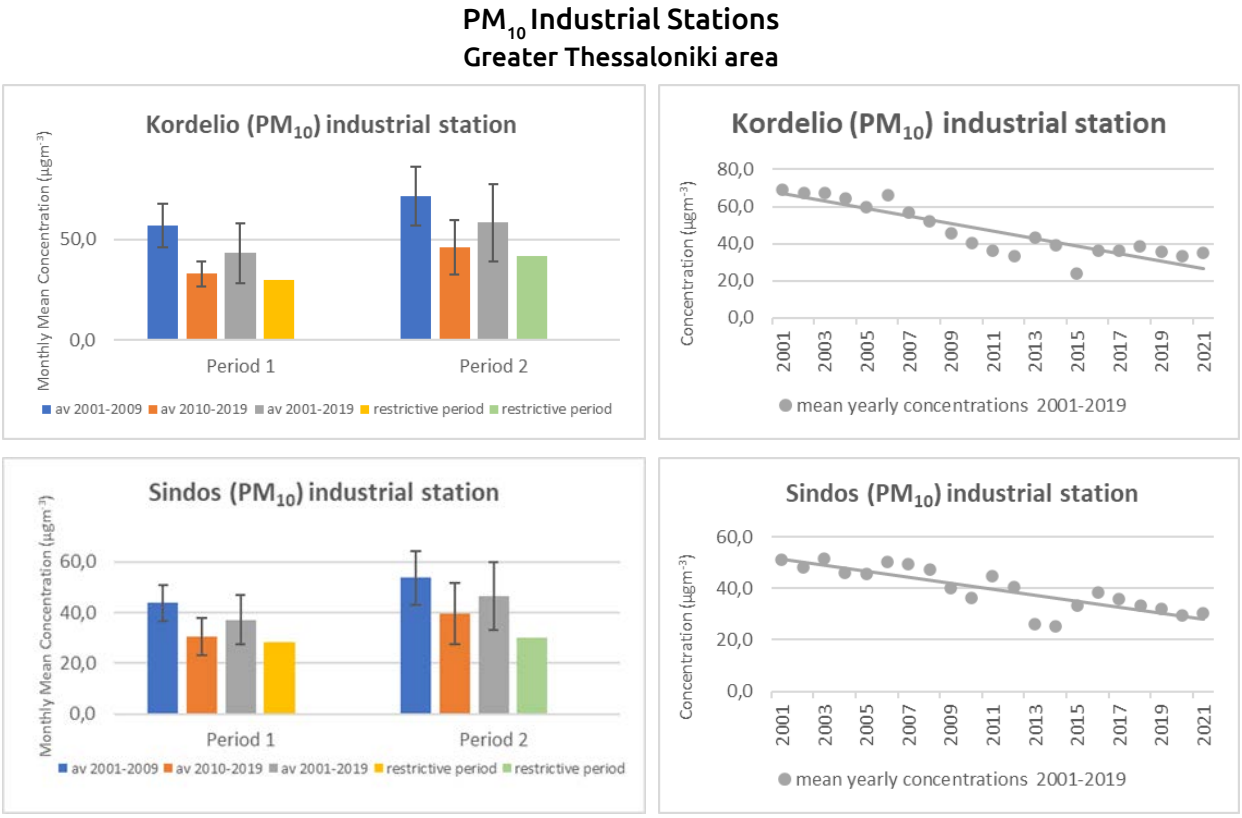

Figure. 5. *(a) PM_{10} mean monthly concentrations (μgm^{-3}), during the two periods of the restrictive measures (1st period March-May 2020 and 2nd period November 2020-January 2021), in comparison, respectively, with the PM_{10} mean monthly values and the standard deviation (+/-σ), of the corresponding months, through the three specific periods (2001-2009, 2010-2019 and 2001-2019), at urban traffic sites, in major Greek cities. (b) The linear regression trend of the PM_{10} mean yearly values (μgm^{-3}), through the entire period (2001-2019), at industrial sites, in major Greek cities.*

Table 5. The percent (%) differences of PM_{10} mean monthly concentrations, during the two periods of the restrictive measures (1st period March-May 2020 and 2nd period November 2020-January 2021), which were calculated, respectively, in comparison with the PM_{10} mean monthly values, for the corresponding months, during the three periods time intervals (2001-2009, 2010-2019 and 2001-2019), at industrial sites, in major Greek cities.

PM_{10} Industrial Sites		
Time interval	1st period	2nd period
2001-2009	-42%	-43%
2010-2019	-8%	-17%
2001-2019	-28%	-32%

From the above assessment (Fig. 2-5(b)) we have also found that over the last two decades there has been a significant downward trend in both PM_{10} and $PM_{2.5}$ concentration levels in the atmosphere of major Greek cities, which is due to various mitigation measures taken in Greece, such as the replacement of old polluting vehicles, the improvement of fuel quality and the various traffic interventions (such as ring roads, metro and tram in Athens, bus lanes, unleveled intersections, etc.) Also, the important downward trend in both PM_{10} and $PM_{2.5}$ concentration levels can be attributed to the evolution of the environmental legislation, with more stringent air quality standards coming into effect and the new socio-economic conditions that come up, after 2010, due to the Greek economic crisis (decrease in private car use, fuel price increase, etc.) and especially in the 2010-2019 decade the constantly increasing use of natural gas as an energy source in various industrial production processes and for building heating [7, 11-12, 14-17].

Moreover, the PM_{10} and $PM_{2.5}$ percentage reductions, almost in all cases examined, were higher in the period 2001-2009, compared to the period 2010-2019 and the entire period 2001-2019. Finally, these decreases in the concentrations of both PM_{10} and $PM_{2.5}$ levels, during the months of the restrictive measures due to the COVID-19 pandemic, in all major Greek cities were similar to the results of other researchers in Greek urban areas [19-20, 27-30].

Conclusions

In summary, the analysis of the data showed that there was a significant reduction in the PM_{10} and $PM_{2.5}$ concentrations levels in all sites (urban, suburban and industrial areas) of major Greek cities that were examined in the present study, during the two periods of the traffic restriction measures taken due to the COVID-19 pandemic. The assessment showed a reduction in the PM_{10} concentration levels which ranged from 8% to 45%, and in the $PM_{2.5}$ concentration levels which ranged from 13% to 48%.

Pollution control strategies are based in law, policy, regulation, and technology, are science-driven, and focus on the protection of public health. The strategies include targeted reductions in emissions of pollutants, transitions to non-polluting, renewable sources of energy, the adoption of non-polluting technologies for production and transportation, and the development of efficient, accessible, and affordable public transportation systems [1-3, 6]. The above assessment show that the emissions control measures adopted during the last two decades in Greek urban areas [7-8, 11-17, 33] if they are in line with proposed mitigation strategies [34] can be crucial in order improve the air quality in large Greek cities.

In conclusion, the present study found that the mandatory traffic restriction and the resulting reduction of human activities, improved the atmospheric conditions, in terms of particulate pollutants, in urban, suburban areas and industrial areas of Greek cities, during the two periods of implementation of the restrictive measures in Greece, due to the pandemic caused by the COVID-19 virus. Therefore, it is concluded that with appropriate emission control strategies, a significant improvement in air quality can be achieved.

Acknowledgements

The Authors would like to thank the National Air Pollution Monitoring Network (NAPMN), of the Department of Atmospheric Quality, of the Ministry of Environment and Energy of Greece for the provision of the air pollution data.

References

[1] WHO, "Overview of methods to assess population exposure to ambient air pollution". WHO Air Quality and Health Unit, Geneva 27, (2023), Switzerland. ISBN 978-92-4-007349-4 (electronic version), ISBN 978-92-4-007350-0 (print version), https://www.who.int/teams/environment-climate-change-and-health/ air-quality-and-health.

[2] WHO, UN (UNDP, UN environment, UNICEF), "Compendium of WHO and other UN guidance on health and environment: version with International Classification of Health Intervention (ICHI) codes", WHO Department of Environment, Climate Change and Health, Geneva 27, (2023), Switzerland. ISBN 978-92-4-008806-1 (electronic version), ISBN 978-92-4-008807-8 (print version), http://www.who.int/teams/environment-climate-change-and-health

[3] World Health Organization (WHO), "Health Effects of Particulate Matter. Policy Implications for Countries in Eastern Europe, Caucasus and Central Asia", WHO Regional Office for Europe, Copenhagen Ø (2013), Denmark. ISBN 978-92-890-0001-7, https://iris.who.int/handle/10665/344854.

[4] European Environment Agency (EEA), "Air quality in Europe - Report 2022", WEB Report, Published 24 Nov 2022. https://www.eea.europa.eu/publications/air-quality-in-europe-2022/

[5] Pope, C Arden III and Dockery W Douglas, "Health effects of fine particulate air pollution: Lines that connect", Journal of the Air & Waste Management Association 56, no. 6 (2006): 709–42, https://doi.org/10.1080/10473289.2006.10464485.

[6] Landrigan, Philip J., Richard Fuller, Nereus J R Acosta, Olusoji Adeyi, Robert G. Arnold, Niladri Basu, Abdoulaye Bibi

Baldé, Roberto Bertollini, Stephan Bose-O'Reilly, Jo Ivey Boufford et al. "The Lancet Commission on Pollution and Health." The Lancet 391, no. 10119 (2018): 462–512. https://doi.org/10.1016/s0140-6736(17)32345-0.

[7] Greek Ministry of the Environment and Energy, Department of Atmospheric Quality, National Air Pollution Monitoring Network (NARMN), "Annual reports on air pollution 2002 - 2023". https://ypen.gov.gr/perivallon/poiotita-tis-atmosfairas/ektheseis/.

[8] Progiou, Athena, and Ioannis Ziomas, "Road Traffic Emissions Impact on Air Quality of the Greater Athens Area Based on a 20-year Emissions Inventory". Science of the Total Environment 410–411 (2011): 1–7. https://doi.org/10.1016/j.scitotenv.2011.09.050.

[9] Eleftheriadis, Konstantinos, Ochsenkuhn, Klaus M., Lymperopoulou, Theopisti, Karanasiou, Angeliki, Razos, P., and Ochsenkuhn-Petropoulou, Maria, "Influence of local and regional sources on the observed spatial and temporal variability of size resolved atmospheric aerosol mass concentrations and water-soluble species in the Athens metropolitan area". Atmospheric Environment, 97, 252-261 (2014) doi:10.1016/j.atmosenv.2014.08.013

[10] Samara, Constantini, Dimitra Voutsa, Athanasios Kouras, Maximos Petrakakis, Apostolos Kelessis, and Paraskevi Tzoumaka, "$PM_{2.5}$ and carbonaceous species in Thessaloniki, Greece during the economic recession period." Proceedings of 9th International Conference on Air Quality Science and Application, Garmisch-Partenkirchen, pp. 266, 24-28 March 2014, Thessaloniki.

[11] Petrakakis, Maximos, Papagiannopoulos, Nikolaos, Kelessis, Apostolos, Tzoumaka, Paraskevi, Tzourelis, Georgios, Kanellopoulou, Zafeiro, Tsaknia, Anna, Koutsari, Elisavet, and Zoumakis, Nikolaos, "Evaluation of the long-term evolution of air pollutants in the area of Thessaloniki." Proceedings, 3nd Environmental Conference of Macedonia, 14-17 March 2008, Thessaloniki.

[12] Kanellopoulou, Zafeiro, Apostolos Kelessis, Paraskevi Malea, Maximos Petrakakis, Pavlos Kassomenos, and Paraskevi Tzoumaka, "Evaluation of the atmospheric quality of Thessaloniki before and during the economic crisis in Greece." Proceedings, 22nd National Conference of Chemistry «Chemistry: Research and Education for Sustainable Development» (CD), 2-4 December 2016, Thessaloniki.

[13] Kelessis, Apostolos, Vasiliki Kostea, Pavlos Kassomenos, Emmanuela Remoundaki and Maximos Petrakakis, "The evolution of photochemical pollution in Greek cities during the last decade." Proceedings, 6th Environmental Conference of Macedonia, 5-7 May 2017, Thessaloniki.

[14] Haina, Evagelia, Apostolos Kelessis, Maximos Petrakakis, Pavlos Kassomenos, and Anastasia Parascha, "Air pollution from particulate matter PM_{10} in major Greek urban cities before and after the economic crisis." Proceedings, 12th International Conference on Chemistry Greece-Cyprus entitled «Chemistry, Pillar of Development in the Post-Crisis Era » (CD), 8-10 May 2015, Thessaloniki.

[15] Petrakakis, Maximos, Apostolos Kelessis, Paraskevi Tzoumaka, Konstantini Samara and Pavlos Kassomenos, "The impact of the economic crisis on particulate matter levels in the atmosphere of Thessaloniki." Proceedings of the 5th, International Environmental Conference of Macedonia, pp. 51 (CD), 14-16 March 2014, Thessaloniki.

[16] Evagelopoulos, Vasilios, Maximos Petrakakis, Stamatis Zoras, Apostolos Kelessis and Dimitrios Sotiropoulos, "Concentrations of suspended particles in polluted areas of Northern Greece." Proceedings of 4th International Conference on Environmental Management, Engineering, Planning and Economics (CEMEPE 13), pp. 171, 24-28 June 2013, Mykonos, Greece.

[17] Stogiannis, Kleonikos, Apostolos Kelessis and Pavlos Kassomenos, "Spatial and time distribution of particulate air pollution in Greek urban areas." Proceedings of the 7th Environmental Conference of Macedonia, p. 159, 30 October - 1 November 2020, Thessaloniki, Greece. ISBN: 978-618-81196-2-8, ISSN: 1791-4280.

[18] Gualtieri, Giovanni, Lorenzo Brilli, Federico Carotenuto, Carolina Vagnoli, Alessandro Zaldei and Beniamino Gioli, "Long-Term COVID-19 Restrictions in Italy to Assess the Role of Seasonal Meteorological Conditions and Pollutant Emissions on Urban Air Quality." Atmosphere 13, no. 7 (2022): 1156. https://doi.org/10.3390/atmos13071156.

[19] Progiou, Athena, Ioannis Sebos, Aikaterini-Maria Zarogianni, Eirini Tsilibari, Anastasios Adamopoulos, and Petros Varelidis, "Impact of covid-19 pandemic on air pollution: the case of Athens, Greece," Environmental Engineering and Management Journal, no 21 issue 5 (2022): 879-889. https://eemj.eu/index.php/EEMJ/article/view/4525.

[20] Avdoulou, Maria, Aristidis Golfinopoulos and Ioannis Kalavrouziotis, "Monitoring Air Pollution in Greek Urban Areas during the Lockdowns, as a Response Measure of SARS-COV-2 (COVID-19)." Water, Air, & Soil Pollution 234, no. 1 (2022). https://doi.org/10.1007/s11270-022-06024-7.

[21] Liu, Feng, Meichang Wang, and Meina Zheng, "Effects of COVID-19 Lockdown on Global Air Quality and Health." Science of the Total Environment 755 (2021): 142533. https://doi.org/10.1016/j.scitotenv.2020.142533.

[22] Collivignarelli, Maria Cristina, Alessandro Abbà, Roberta Pedrazzani, Paola Ricciardi, and Marco Carnevale Miino, "Lockdown for CoViD-2019 in Milan: What Are the Effects on Air Quality?" Science of the Total Environment 732, (2020): 139280. https://doi.org/10.1016/j.scitotenv.2020.139280.

[23] Filonchyk, Mikalai, Volha Hurynovich, and Haowen Yan. "Impact of Covid-19 Lockdown on Air Quality in the Poland, Eastern Europe." Environmental Research 198 (2021): 110454. https://doi.org/10.1016/j.envres.2020.110454.

[24] Mor, Suman, S. Ananth Kumar, Tanbir Singh, Sushil Dogra, Vivek Pandey, and Khaiwal Ravindra, "Impact of COVID-19 Lockdown on Air Quality in Chandigarh, India: Understanding the Emission Sources during Controlled Anthropogenic Activities." Chemosphere 263 (2021): 127978. https://doi.org/10.1016/j.chemosphere.2020.127978.

[25] Mashayekhi, Rabab, Radenko Pavlovic, Jacinthe Racine, Michael D. Moran, Patrick M. Manseau, Annie Duhamel, Ali Katal, Jessica Miville, David Niemi, Si Jun Peng, et al, "Isolating the Impact of COVID-19 Lockdown Measures on Urban Air Quality in Canada." Air Quality, Atmosphere & Health 14, no. 10 (2021): 1549–70. https://doi.org/10.1007/s11869-021-01039-1.

[26] Kumari, Pratima, and Durga Toshniwal, "Impact of Lockdown on Air Quality over Major Cities across the Globe during COVID-19 Pandemic." Urban Climate 34 (2020): 100719. https://doi.org/10.1016/j.uclim.2020.100719.

[27] Grivas, Georgios, Eleni Athanasopoulou, Anastasia Kakouri, Jennifer Bailey, Eleni Liakakou, Iasonas Stavroulas, Panayiotis Kalkavouras, Aikaterini Bougiatioti, Dimitris Kaskaoutis, Michel Ramonet, et al, "Integrating in Situ Measurements and City Scale Modelling to Assess the COVID–19 Lockdown Effects on Emissions and Air Quality in Athens, Greece." Atmosphere 11, no. 11 (2020): 1174. https://doi.org/10.3390/atmos11111174.

[28] Kotsiou, Ourania S., Georgios K. D. Saharidis, George Kalantzis, Evangelos C. Fradelos, and Konstantinos Gourgoulianis, "The Impact of the Lockdown Caused by the COVID-19 Pandemic on the Fine Particulate Matter (PM2.5) Air Pollution: The Greek Paradigm." International Journal of Environmental Research and Public Health 18, no. 13 (2021): 6748. https://doi.org/10.3390/ijerph18136748.

[29] Barmparesos, Nikolaos, Chrysanthi Efthymiou, Panagiotis Tasios, Dimosthenis Asimakopoulos, and Margarita Niki Assimakopoulos, "Preliminary results of COVID-19 restriction measures on the air pollution levels in the city center of Athens, Greece," AIP Conf. Proc. Vol. 2437, Issue 1, 020198, 17 August 2022. https://doi.org/10.1063/5.0092493.

[30] Begou, Paraskevi, Vasilios Evagelopoulos, and Nikolaos D. Charisiou, "Variability of Air Pollutant Concentrations and Their Relationships with Meteorological Parameters during COVID-19 Lockdown in Western Macedonia." Atmosphere 14, no. 9 (2023): 1398. https://doi.org/10.3390/atmos14091398.

[31] Greek Ministry of the Environment and Energy, Department of Atmospheric Quality, National Air Pollution Monitoring Network (NARMN), "Air pollution measurement data", accessed September 4, 2023. https://ypen.gov.gr/perivallon/poiotita-tis-atmosfairas/dedomena-metriseon-atmosfairikis-rypansis/.

[32] "Directive 2008/50 - Ambient Air Quality and Cleaner Air for Europe", EU Monitor. https://www.eumonitor.eu/9353000/1/j4nvk6yhcbpeywk_j9vvik7m1c3gyxp/vitgbgioeuzt.

[33] Kanakidou, Maria, Nikolaos Mihalopoulos, Tayfun Kindap, Ulas Im, Mihalis Vrekoussis, Evangelos Gerasopoulos, Eirini Dermitzaki, Alper Unal, Mustafa Koçak, Kostas Markakis, Melas Dimitrios Kouvarakis Georgios, et al, "Megacities as hot spots of air pollution in the East Mediterranean", Atmospheric Environment, Volume 45, Issue 6, (2011): 1223-1235. doi:10.1016/j.atmosenv.2010.11.048.

[34] Aleksandropoulou, Vasiliki, Konstantinos Eleftheriadis, Evangelia Diapouli, Kjetil Torseth and Michalis Lazaridis, "Assessing PM_{10} source reduction in urban agglomerations for air quality compliance", Journal of Environmental Monitoring, 14, Issue 1, (2012): 266–278. doi:10.1039/C1EM10673B.

Utilization of renewable biogas and ladfill gas sources for ethanol and methanol synthesis

Savvas Vasileiadis[1], Artemis Vasileiadou[2], Zoe Ziaka[1*], Elias Fatmelis[1] and Christina Spourtoudi[1]
[1]Department of Catalysis and Environmental Protection, School of Technology and Physical Sciences, Hellenic Open University, Greece.
[2]Department of Physics, Aristotle University of Thessaloniki, Greece.

*corresponding author, bookeng@hotmail.com
DOI: 10.62579/JAGC0004

ABSTRACT
An improved efficient catalytic method of ethanol synthesis is discussed from synthesis gas based on waste biogas and landfill gas resources. Wise utilization of waste biogas and landfill gases can be essential in the renewable area of energy and chemicals production. Improved practices for ethanol and methanol production that contribute to enhanced utilization of renewable resources are investigated in this article. Ethanol can be produced via a direct catalytic one-step process from synthesis gas coming out from a conventional reactor or from a membrane type reformer.
Moreover, methanol synthesis from synthesis gas based on waste biogas and landfill gas resources is also discussed showing a significant potential.
The detailed flowsheet of the corresponding processes is presented to show the reactors pathway.

Keywords: ethanol/methanol production, biogas and landfill-gas conversion, catalytic membrane reformer, hydrogen and syn-gas utilization.

INTRODUCTION
It is important to be addressed that the production of biogas and landfill gas resources has been growing steadily for the last 25 years. There is a number of different sources today that produce these gases at global scale, especially as the earth population increases.
Today, most of the developed places in the world are looking for a relief from the increasing demand of energy and the large cost of oil and natural gas. This fact has heightened the focus in utilizing alternative and renewable energy sources. It is predicted that after 2050's, more than 50% of world energy demand will be produced from renewable energy resources. Energy security, economic development and protection of the today's world resources are the priorities of the national energy policy for many countries in the modern world. Utilization of waste-gases can be a partial solution to the requirements and expectations of the proposed renewable energy sources development.
In this paper, we report a new design and process for the capability of ethanol and methanol synthesis /production from renewable feedstocks such as biogas and landfill gas type sources.
Ethanol is a very important chemical component in the chemical industry. It can be used as antiseptic, antidote, anesthetic, medical solvent, for making several drugs in the pharmacology area, as an engine and rocket fuel, in a DEFC (direct ethanol fuel cell), in household heating and cooking, as a feedstock and chemical solvent, and in other uses as well.
Methanol is also a valuable chemical that can be used in several applications including its direct use as automobile fuel. Methanol, among others uses, can be converted into gasoline with the use of the Mobil zeolite process. Also, it can be used directly in a methanol fuel cell for direct electricity generation (DMFC).
Table 1 reports the composition of several related waste feedstocks for ethanol or methanol synthesis relating them with the composition of natural gas.

Table 1. Chemical Composition of Various Waste Gases [10]:

Components	Natural gas	Biowaste	Industrial waste	Landfill gas
CH_4	91 %	67 %	77 %	50 %
CO_2	0.5 %	33 %	23 %	43 %
N_2	0.6 %	0.2 %	Traces	5%
O_2	Traces	Traces	Traces	2 %
H_2	Traces	Traces	Traces	Traces
H_2S	Traces	<10 ppm	<10 ppm	300 ppm
CnHm	7.8 %	<10 ppm	<10 ppm	50 ppm

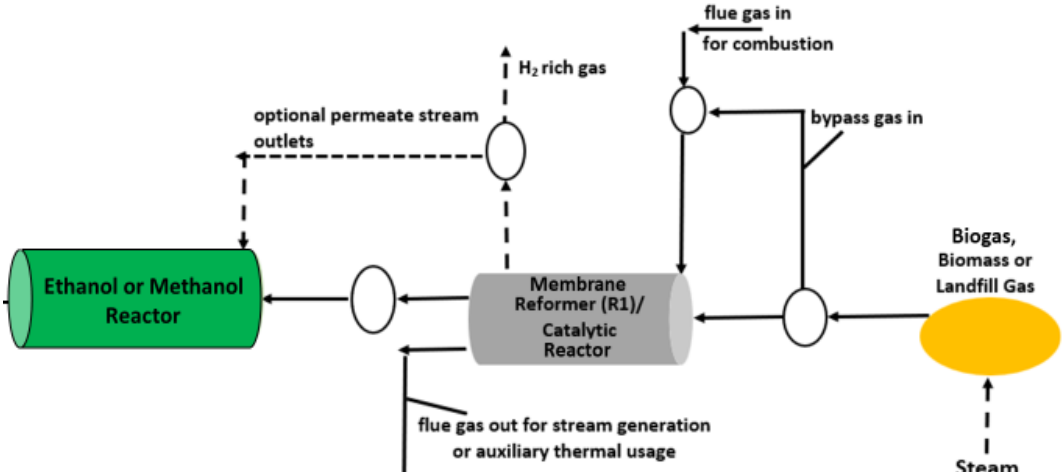

Figure 1. *Flowsheet of the processes.*

CO_2 is one of the main reactants for the methanol synthesis as it is described in the results section. Moreover, CH_4 and CO_2 are the reactants for the steam and CO_2 reforming reactions as well. H_2 is needed for both ethanol and methanol synthesis as well.

Further, H_2 can be optionally added in small quantities in the reformer inlet to prevent catalyst deactivation from carbon deposition. Table 1 reports the percentage composition of inlet waste/renewable gases for comparison purposes.

Thus, the chemical compositions of typical waste gases, coming from various sources, are shown in detail in the following Table 1 [10].

RESULTS AND DISCUSSION

Renewable sources of interest to this paper are the biogas and landfill gases. Two reaction methods are reported: Ethanol and methanol synthesis.

Syngas coming from the reforming of renewable sources such as biogas and landfill gases can be converted directly into ethanol or methanol in a catalytic synthesis reactor with significant yield and selectivity [3,4].

The syngas production outcome at various temperatures is presented in the Table 2 below [10]. It shows results from plant biomass such as wood ships. Biogas is coming from the treatment of biomass.

Reforming of the above gases can take place catalytically usually in a fixed bed catalytic reactor or in a catalytic membrane reactor [1-4, 9, 11]. Mostly Ni, Cr, Rh, and Ru catalysts and their mixtures, are used in the reforming of biogas and landfill gases after their initial purification. Pd, Pt, Co and Fe catalysts have been also used but with lower yields in synthesis gas.

STEAM AND CO_2 REFORMING REACTIONS

$$CH_4 + H_2O \rightleftharpoons CO + 3H \qquad \Delta H^0_{298} = 206.1\ kJ/mol \qquad (1)$$

$$CH_4 + CO_2 \rightleftharpoons 2CO + 2H_2 \qquad \Delta H^0_{298} = 247.3 kJ/mol \qquad (2)$$

$$H_2 + CO_2 \rightleftharpoons CO + H_2O \qquad \Delta H^0_{298} = 41.15\ kJ/mol \qquad (3)$$

CO and hydrogen are the direct products from the reforming reactions of such renewable gases as described in previous communications [1-4, 8-11].

The optional use of the membrane in the reforming reactor (membrane reformer or permreactor) provides more hydrogen at the exit streams so that the stoichiometry of the reactants in equations (1) and (2) is more easily satisfied.

A detailed flowsheet of the described processes is shown in Fig 1.

The flowsheet of the process consists of the inlet gas system, of the catalytic reactor (conventional reformer or membrane type reformer) and of the ethanol or methanol synthesis reactor where the corresponding discussed reactions take place.

Figures 2 and 3 include both experimental and modeling

Table 2. Syngas production (kmol/ton of biomass) at various Temperatures (K) and Pressure of 24 atmospheres [10].

Temperature (K)	CH_4	H_2	CO_2	CO	H_2O
1000	8	12	20	12.5	12.5
1200	1	24	12	27.5	13
1400	0	24	9	31	14

results. The modeling results are produced based on the following mathematical model.

MATHEMATICAL MODEL

A theoretical model presented in the Figures 2 and 3 is described below:

The corresponding mathematical modeling of the methane-steam reformer for a steady-state fixed-bed catalytic reactor, including the species reaction terms in the mass balance equation, is as it is presented:

$$\frac{dX^A}{dz} = \left(\frac{\pi d_T^2}{4n_{A_o}}\right)\rho_B R_A \qquad \text{(a)}$$

Species can be any of the reactants and products of the reactions (1), (2) and (3).

With:

$$R_{CH_4} = -R_1 - R_2,$$
$$R_{CO_2} = -R_2 - R_3,\ R_{CO} = R_1 + 2R_2 + R_3,$$
$$R_{H_2} = 3R_1 + 2R_2 - R_3,\ R_{H_2O} = -R_1 + R_3, \qquad \text{(b)}$$

where R_1, R_2 and R_3 are the heterogeneous reaction rates of the corresponding reactions given above.

In addition, the thermal balance in a nonisothermal reformer is given as follows:

$$\frac{dT_T}{dz} = \left(\frac{\pi d_T^2}{4}\right)\left(\frac{1}{m'c_p}\right) + \{\rho_B[(-\Delta H_r^1)R_1 + (-\Delta H_r^2)R_2 + (-\Delta H_r^3)R_3] - 4\left(\frac{U}{d_T}\right)(T_T - T_S)\} \qquad \text{(c)}$$

Moreover, the reformer pressure balance which describes the pressure drop along the fixed bed of catalyst is given as follows:

$$\frac{-dP_T}{dz} = \frac{2f\rho_g u_s^2}{g_c d_p} \qquad \text{(d)}$$

and the above equations are complemented by initial conditions as shown: at (reactor/reformer inlet),

$$X^A = 0,\ T_T = T_o,\ P_T = P_{T_o} \qquad \text{(e)}$$

A more specific analysis of the model, its parameters, and their variation is discussed in earlier communications [1,2,3].

The above system of governing equations (a) to (d) is integrated numerically as an initial value problem to provide the reactant conversions, product yields, reactor temperature, and pressure along the axial length and to obtain the axial profiles of these variables and their values at the reactor exit.

With the use of an inorganic permreactor/membrane reactor as the main catalytic processing unit to convert biogas/landfill gas feedstocks into synthesis gas, the above design equations are modified accordingly to include the permeation effects via the membrane of the different components.

Moreover, the following mathematical part has to be added at the right hand side of equation (a) to account for the permeation effects within the mass balance equation:

$$-\left(\frac{2\pi}{n_{A_o}^T}\right)P_{A,e}\left[\frac{p_A^T - p_A^S}{\ln(r_1/r_2)}\right] \qquad \text{(f)}$$

wherein is the effective permeability coefficient of species via the catalytic or noncatalytic (blank) membrane. Superscript T stands for the tubeside or reaction side of the membrane reactor, while S for the permeate side of it.

It is worthy to declare that in our experimental reaction studies we utilized mesoporous aluminum oxide membranes having a thin permselective layer (3-5 thickness, porosity) with pore diameter . The membrane is a multilayer structure supported on an a-alumina support thickness, porosity, and pore diameter).

When a permreactor/membrane reactor is used, the corresponding mass, temperature, and pressure variation equations are written as well for the gas which permeates via the membrane wall material and flows in the permeate side of the membrane reactor.

It is assumed that there are no reactions occurring in the permeate membrane side. An analysis of the model for the permreactor has been described as well in earlier communications [3].

By employing equations (a) to (f) within the modeling procedure, a complete reactor analysis is obtained for the two different reformer configurations. Solution of the equations is obtained numerically by using an initial value integration technique for ordinary differential equations with variable stepsize to ensure higher accuracy (implicit Adams-Moulton method) .

In our previous papers, we have described and analyzed the reaction, separation (i.e., permeation), and process (conversion, yield) characteristics of membrane based catalytic reactors and related processes for methane steam reforming, water-gas shift, and methane carbon dioxide reforming reactions including catalysis and membrane materials characteristics.

The main categories of reactors described were membrane reformers which were utilized as single permreactor [1,3], permreactor-separator in series or reactor-separator in series and permeactor-permeactor in series .

COMPARISON OF EXPERIMENTAL AND MODELING STUDIES

In Fig. 2 there are experimental and simulation/modeling results for the methane conversion from the catalytic plug flow reactor (PFR) of the reforming reactions (1) and (3) taking place together [3].

The conversion is increased as the reaction temperature increases as it is expected since it is an overall endothermic reaction. It also increases as the space time of the reactor increases.

The significance of this work, is also the fact that there is a satisfactory agreement between the modeling and experimental data [1-3].

Moreover, methane conversions for the plug flow and membrane reactors at various rea tubeside reaction pressures of the reactors are shown in Fig. 3 for the same reactions as in Fig.2. The reaction temperature is fixed at 550 °C. Results from the modeling studies together with the corresponding calculated thermodynamic equilibrium conversions are included in the figure [3]. As it is expected, the conversion is decreased as the tubeside pressure increases because we have an overall volume expansion reaction.

The membrane reactor performs better than the conventional plug flow catalytic reactor and overcomes the equilibrium limited conversions. At all cases, the model agrees well with the experimental data [1-3].

Methane conversion is measured as follows:

(moles of methane in - moles of methane out) / moles of methane in (%).

The specific CH_4:H_2O:H_2 = 1:4:0.20 feed ratio, in the two figures, is defined as the ratio of the reactants in the reformer inlet, and used as an optimized one for best results.

H_2 is needed in the reformer inlet to avoid catalyst deactivation, and steam used as a main reactant in excess. The detailed description of the theoretical simulation model used in Figures 2 and 3 was presented above.

ETHANOL SYNTHESIS REACTION

The direct ethanol process from the CO and H_2 gas constituents is projected more economic and efficient than other competent methods of ethanol synthesis [3,5-7,12].

The direct exothermic synthesis reaction is given below in equation (4):

$$2CO + 4H_2 \rightleftharpoons C_2H_5OH + H_2O \qquad \Delta H^0_{500} = -28.4\ kJ/mol \qquad (4)$$

Ethanol synthesis and selectivity are shown at various temperatures at the Table 3 for catalytic reaction using catalyst of K^+–ZnO–ZrO_2 | H-MOR–DA–12MR | Pt–Sn/SiC system and are consistent with the literature [12].

Various catalysts and their mixtures can be used for ethanol synthesis such as Cu, Co, and Rh, Ru, Pd, Pt and Fe based metals as described in previous pertinent communications [3-7,12]. Depending on the catalyst used and the other details of the reaction, the conversion, yield, and selectivity to ethanol varies at different levels. The corresponding analysis is a subject of future study as well.

Ethanol selectivity is defined as follows:

(moles of ethanol produced / moles of all products) %.

During the ethanol synthesis reaction olefins and CO_2 are produced as byproducts as well.

Methane reforming reactions are favorable at higher temperatures since there are endothermic reactions. Howev-

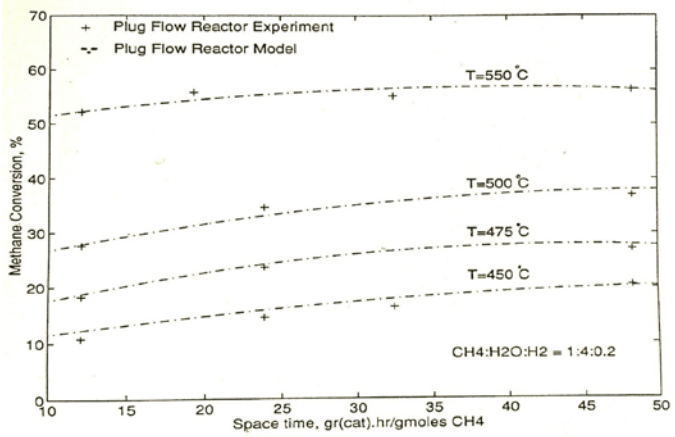

***Figure 2**. Methane Conversions vs Space times at various reaction Temperatures from both experimental and simulation/modeling data of a Plug Flow Catalytic Reactor.*

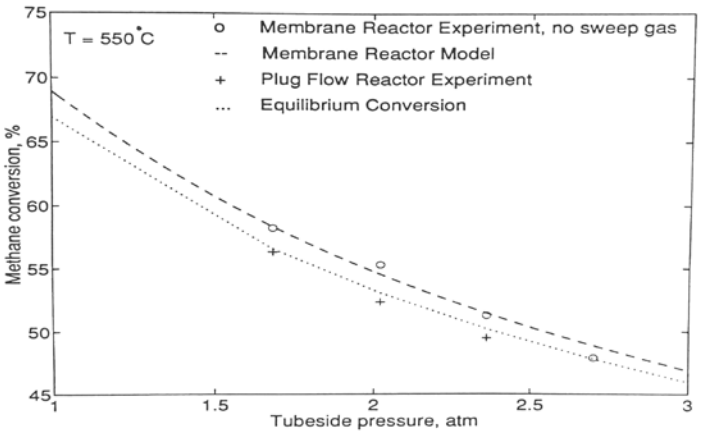

***Figure 3**. Methane Conversions vs various tubeside reaction pressures from both experimental and simulation/modeling data of a Plug Flow Catalytic Reactor and a Plug Flow Catalytic Membrane Reactor.*

Table 3. Conversion and Selectivity to Ethanol at various temperatures [12].

Temperature (°C)	500	550	590	630	640
Conversion to Ethanol %	9.2	8.1	7.3	5.2	3.7
Ethanol Selectivity %	90	81	70	50	33

er, ethanol synthesis reaction is favorable at lower temperatures since it is an exothermic reaction. Therefore, operation at lower temperatures gives the best achievable results for ethanol synthesis with better energy consumption.

Beyond ethanol synthesis the valuable synthesis gas coming out of the reformer can be used in other usages such as a feed in high temperature solid oxide and molten carbonate fuel cells for electricity generation [1-4, 8, 9]. Work in this area is continuing within our research group.

Syngas from the reformers can be also utilized to produce methanol as we have discussed at previous communications [3,4,8].

METHANOL SYNTHESIS REACTIONS

$$CO + 2H_2 \rightleftharpoons CH_3OH \qquad \Delta H^0_{298} = -128.2 \text{ kJ/mol} \qquad (5)$$

$$CO_2 + 3H_2 \rightleftharpoons CH_3OH + H_2O \qquad \Delta H^0_{298} = -49.5 \text{ kJ/mol} \qquad (6)$$

The achieved conversions to methanol have been investigated and reported under different catalyst operating conditions and are presented in Table 4 below [13].

Moreover, there is a potential study for ethanol synthesis from CO_2 and H_2 which can be of further research interest after a proper catalyst is found. The investigation of the proper catalyst is a demanding task and opens a complete new section for further study. This is an important reaction because it utilizes the waste CO_2 as the main reactant. Research in this area is continuing within our group. The reaction is as follows:

$$2CO_2 + 6H_2 \rightleftharpoons C_2H_5OH + 3H_2O \qquad (7)$$

CONCLUSIONS

In this communication, the direct production of ethanol and methanol from synthesis gas has been discussed using biogas and/or landfill gas sources.

A catalytic reformer and membrane reformer for syngas production are presented including experimental and modeling results that show satisfactory fitting at various temperatures, pressures and space times. Moreover, the membrane reformer seems to perform better than the conventional catalytic reformer.

The conversion to ethanol and selectivity are shown to indicate operation at lower temperatures with the highest outcome.

Methanol synthesis under different catalysts and temperatures has been also addressed. The discussed processes are shown in a detailed flowsheet.

Energy security, economic improvement, and environmental protection of the various resources have to be the priorities for every country in the modern society.

In conclusion, turning waste renewable gases into chemicals (such as ethanol and/or methanol) is not only a viable solution with important potential to reduce the dependence on fossil fuels, but also a wise and efficient way to produce valuable decentralized energy with a smaller carbon footprint.

Table 4. Conversion to Methanol for various temperatures and catalysts [13].

Temperature at various catalysts	Commercial catalyst at 220 °C	Nanocatalyst at 220 °C	Mixed oxide catalyst at 240 °C
Conversions to Methanol	18.9%	22.6%	36.3%

REFERENCES

1) S. Vasileiadis and Z. Ziaka-Vasileiadou "***Biomass reforming process for integrated solid oxide-fuel cell power generation"*** Chemical Engineering Science, Elsevier, 59, 4853-4869, 2004.
2) S. Vasileiadis and Z. Ziaka-Vasileiadou ***"Efficient Catalytic Reactors-Processors for Fuel Cells and Synthesis Applications"*** Separation and Purification Technology Journal, Vol.34, pp.213-225, 2004.
3) Z. Ziaka and S. Vasileiadis; ***"Membrane Reactors for Fuel Cells and Environmental Energy Systems"***, Book, Xlibris Publishing., 2009.

4) S. Vasileiadis and Z. Ziaka, *"**Permreactor and separator type fuel processors for production of hydrogen and hydrogen, carbon oxides mixtures**"*, US Patent No 6,919,062 B1, 2005.

5) L. Lopez, J. Velasco, V. Montes, A. Marinas, S. Cabrera, M. Boutonnet, S. Järås, ***"Synthesis of Ethanol from Syngas over Rh/MCM-41 Catalyst: Effect of Water on Product Selectivity."*** Catalysts, *5*, 1737-1755, 2015.

6) Y.M. Choi and P. Liu, ***"Mechanism of Ethanol Synthesis from Syngas on Rh(111)"***, J. Am. Chem. Soc., 131, 36, 13054–13061, 2009.

7) Z.J. Zuo, F. Peng, and W. Huang, ***"Efficient Synthesis of Ethanol from CH_4 and Syngas on a Cu-Co/TiO_2 Catalyst Using a Stepwise Reactor"*** Sci. Rep. 6, 34670, 2016.

8) S. Vasileiadis, Z. Ziaka, A. Vasileiadou, M. Dova, ***"Utilization of Renewable Biogas and Landfill gases as chemical Production and Power Sources"***, J Biosens & Renew. Sci. 1(5)- 2022. JBRS.MS.ID.000122. **DOI:** 10.32474/JBRS.2022.01.000122.

9) A. A. Panteloglou, Z. D. Ziaka and S. P. Vasileiadis, ***"An Alternative to Flare Gas Processing: A Feasibility Study of Natural Gas to Liquid Processes",*** Journal of Materials Science and Engineering A 11 (1-3), 2021, 11-25 doi: 10.17265/2161-6213/2021.1-3.002.

10) C. Spourtoudi, ***"Production of Methanol from Biomass: Problems & Prospects"***, MSc thesis, Hellenic Open University, Greece, 2012.

11) J. Xu and G.F. Froment, ***" Methane Steam Reforming, Methanation and Water-Gas Shift. Intrinsic Kinetics"***, AIChE Journal (35): 88-96, 1989.

12) I. Kang, S. He, W. Zhou, Z. Shen, Y. Li, M. Chen, Q. Zhang, Y. Wang***, "Single-pass transformation of syngas into ethanol with high selectivity by triple tandem catalysis"***, Nature Communications 11, 827, 2020.

13) V. Burnett, S. Iyer, S. Krim, M. McCutcheon and G. Singh "***Optimization of Synthesis Gas to Methanol Conversion",*** Case study, Chemical and Molecular Engineering Program, Materials Science and Engineering Department, Stony Brook, NY, USA, 2020.

Biogenic Copper Nanoparticles from Rosemary Leaf Extract of Antibacterial Impact

Michail T. Poravos[a], Andria Constantinou[a], Christina N. Banti[a,*], Sotiris K. Hadjikakou[a,b,*]

[a] *Biological Inorganic Chemistry Laboratory, Department of Chemistry, University of Ioannina, 45110 Ioannina, Greece.*
[b] *University Research Centre of Ioannina (URCI), Institute of Materials Science and Computing, Ioannina, Greece*

*All correspondence should be addressed to:
Dr. C.N. Banti (Adjunct Lecturer); email: cbanti@uoi.gr
Dr S.K. Hadjikakou (Professor); e-mail: shadjika@uoi.gr; tel. xx30-26510-08374
DOI: 10.62579/JAGC0005

ABSTRACT

Rosemary leaf extract (**RMLE**) was employed for the eco-friendly biogenic synthesis of copper nanoparticles (**CuNPs@RMLE**). The copper nanoparticles **CuNPs@RMLE** were characterized by X-ray fluorescence (XRF) and Attenuated Total Reflection Fourier Transform Infrared (ATR-FTIR) spectroscopy in solid state. The antibacterial effectiveness of **CuNPs@RMLE** was assessed against Gram-negative strains, *Pseudomonas aeruginosa* (*P. aeruginosa*) and *Escherichia coli* (*E. coli*), as well as Gram-positive strains as *Staphylococcus epidermidis* (*S. epidermidis*) and *Staphylococcus aureus* (*S. aureus*). It is compared with the corresponding effectiveness exhibited by **RMLE** and copper(II).

KEYWORDS:

Biological Inorganic Chemistry; Copper Nanoparticles; Rosemary Extract Leaves; Antimicrobial Activity

INTRODUCTION

Bacterial infections are projected to remain a leading cause of mortality in the coming decades [1]. This is due to the bacteria resistance to antibiotics as a significant challenge impacting global health since the early 21st century [2]. The drug resistance has reached epidemic levels, particularly in developing countries [2]. One strategy suggested to tackle antibiotic resistance involves utilizing metal and metal oxide nanoparticles (MetNP's, MetONP's).

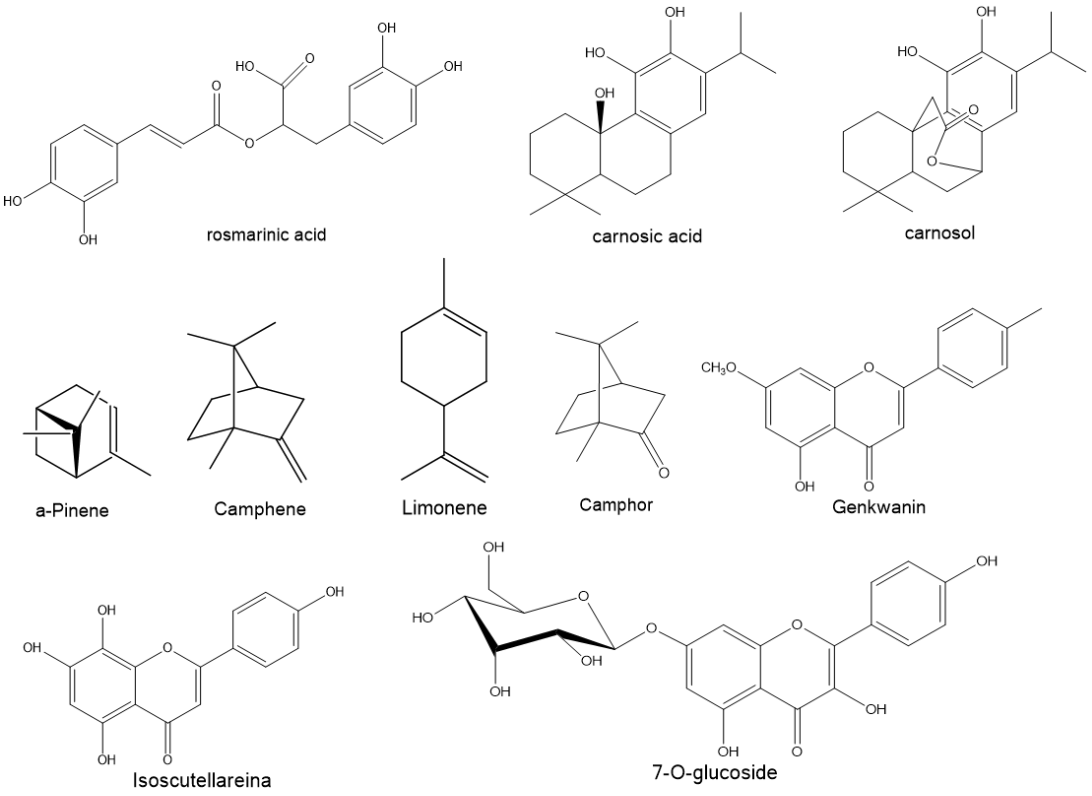

Scheme 1. *Rosemary main ingredients*

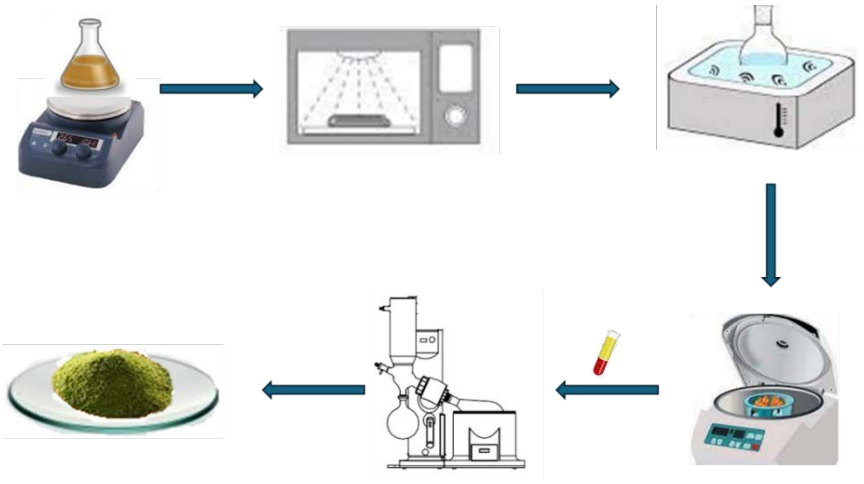

Scheme 2. *The synthetic route for* ***CuNPs@RMLE*** *preparation*

Among the transition elements, copper is being considered as the preferred element for creating these nanoparticles (MetNP's and MetONP's) [2]. Copper plays a role in various essential biological functions within the body [3] and demonstrates antibacterial properties against both Gram-positive or negative bacteria [4].

Biogenic synthesis, on the other hand, is valuable due to its lower environmental impact in contrast to certain physicochemical production methods [5-6], but also because it enables the production of substantial quantities of nanoparticles [7]. Different synthesis methods involve the use of different types of biological agents to yield nanoparticles of different sizes and shape [8].

Rosemary, known as *Rosmarinus officinalis L.*, is a evergreen shrub naturally found across most Mediterranean countries. Belonging to the Lamiaceae family, this plant extract, as per traditional medicine, is believed to aid in various health aspects. Rosemary contains several substances that hold promise for biological activity [9]. In addition to double distilled water and other solvents such as ethanol are used for the rosemary's active components extracting [9]. Rosemary leaves extracts bioactive components include caffeolyl derivatives (rosmarinic acid), diterpenes (carnosic acid, carnosol), phenolic mono-terpenes (Scheme 1) [9]. Rosemary has shown inhibitory effects against various bacteria, such as *S. aureus*, *L. monocytogenes* and *E. coli* [10-11]. By disrupting and reducing the impermeability of these bacteria's membranes, rosemary exhibits the potential to combat drug resistance in specific bacterial strains [11].

In the course of our research towards the development of new efficient multi targeted antimicrobial agent which therefore prevent the bacterial resistance [12-13] we report here the biogenic synthesis of copper nanoparticles **CuNPs@RMLE** using rosemary (*Rosmarinus officinalis L.*) plant extract.

Results and Discussion

General Aspects: The rosemary leaf extract (RMLE) was employed for the biogenic synthesis of copper nanoparticles (**CuNPs@RMLE**). RMLE extract serves as capping agent in the chemical synthesis process of nanomaterials. The synthetic route of nanoparticles involves diluting copper nitrate in the water extract of rosemary under stirring,

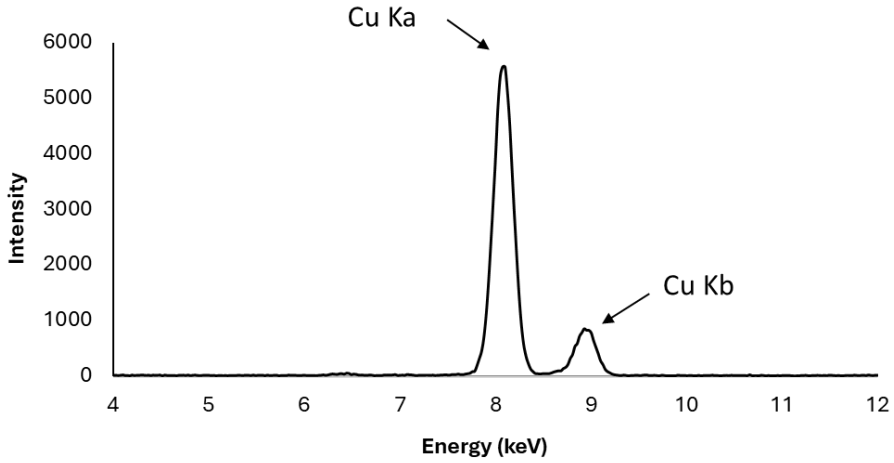

Figure 1. *XRF spectrum of C****uNPs@RMLE***

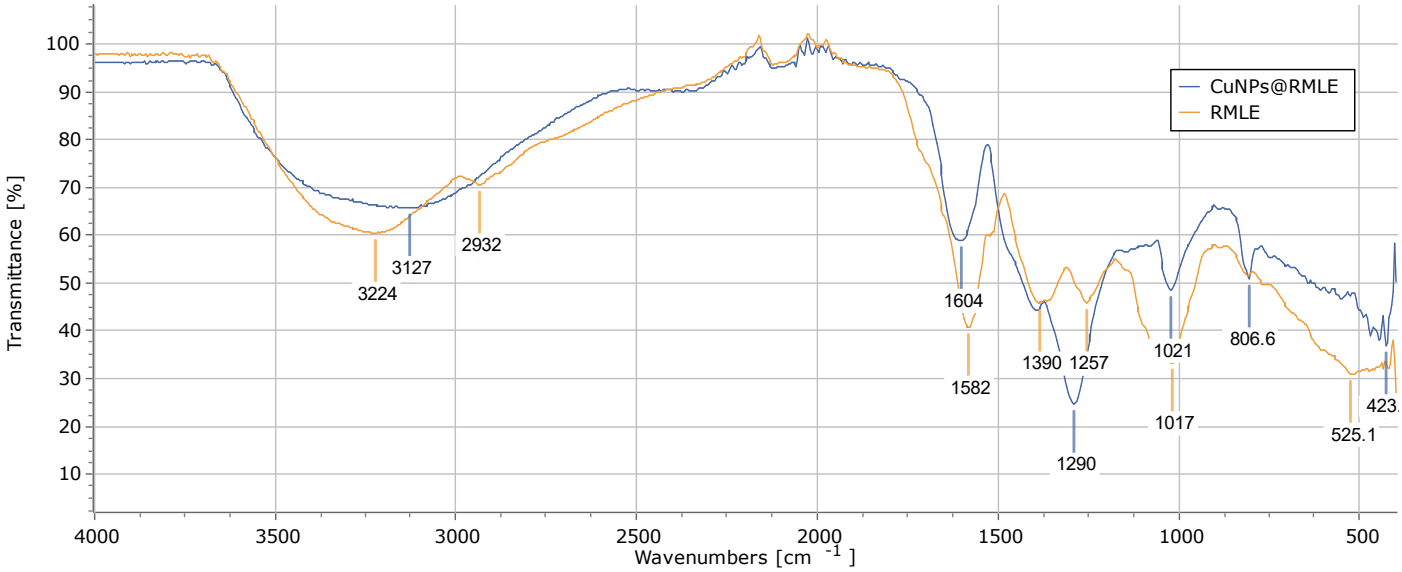

Figure 2. *ATR-FTIR of RMLE and* ***CuNPs@RMLE****.*

followed by microwave irradiation of the nanoparticles, sonication, and centrifugation. After removal of the supernatant to dryness, using a rotary evaporator, the **CuNPs@RMLE** obtained and subsequently dried in oven at 50 °C for 24 h (Scheme 2).

X-ray Fluorescence Spectroscopy: Dry solid **CuNPs@RMLE** was ground to powder. The XRF spectrum of **CuNPs@RMLE** confirmed the presence of copper in the samples (Figure 1). Thus, the presence of the photon energies, of principal K-, L-, and M-shell emission lines for copper CuKα and CuKβ at 8.05 and 8.91 KeV in the XRF spectrum of the **CuNPs@RMLE** (Figure 1) confirms the presence of copper [14]. X-ray emission spectroscopies, particularly Kβ mainlines, have been demonstrated to diagnose the metal oxidation state and spin state in 3d transition metals. However, since the Kβ mainlines of copper show very similar K$\beta_{1,3}$ energies (8904.6–8904.7 eV) with no significant shifts between the various copper oxidation states, it is impossible to determine the oxidation state of the metal ion [14].
The content of copper in **CuNPs@RMLE** was determined to (41.62±0.07)% w/w.

Vibrational Spectroscopy: In order to confirm the formation of **CuNPs@RMLE** nanoparticles, FTIR spectra were obtained for both RMLE and **CuNPs@RMLE** (Figure 2). The FTIR spectrum of rosemary displays distinctive absorption bands. These include a broad vibrational band at 3224 cm^{-1}, which corresponds to ν(O-H) stretching bands of alcoholic groups. The band at 2932 cm^{-1} is consistent with the vibration of the $\nu(C_{conjugate}\text{-H})$ bonds. Furthermore, bands observed in the spectrum at 1586, 1386, 1360, 1254, 1067, 1020 and 807 cm^{-1}, are consistent with the ν_{as}(COO) and ν_{s}(COO) of the carboxylic acid groups, ν(C=O), ν(C-O), ν(C-C) of phenyl groups, and ν(C-O) vibrations, respectively (Scheme 1, Figure 2). These bands emerge at 3127, 1604, 1390, 1290, 1021, and 806 cm^{-1} with the formation of **CuNPs@RMLE** nanoparticles (Figure 2). The most notable alteration is observed in the ν_{s}(COO) band at 1290 cm^{-1} in **CuNPs@RMLE**, which is initially appeared at 1254 cm^{-1} in RMLE. This is consistent with the interaction between copper ions and the carboxylic groups of RMLE ingredients.

Antibacterial activity of **CuNPs@RMLE**
Determination of the Inhibition Zone (IZ) through agar disk-diffusion method: The agar disk-diffusion technique was utilized to assess the microorganism's sensitivity to the antibacterial agent [15]. Figure 3 shows the diameter of the inhibition zones formed when *P. aeruginosa, E. coli, S. epidermidis*, and S. *aureus* are treated with **CuNPs@RMLE** after incubation for 20 hours. The biological experiments evaluating the antimicrobial activity of the material were performed using a consistent amount of material administered to the microbes (100 mg/mL), which corresponds to a copper contented of 41.6% w/w. Each experiment was repeated at least three times to ensure statistical significance in the results. The inhibition zones caused by **CuNPs@RMLE** are 18.3±1.7 mm, 23.5±1.0 mm, 31.0±2.0 mm, and 21.5±1.0 mm against *P. aeruginosa, E. coli, S. epidermidis,* and *S. aureus*, respectively (Figure 3). Copper nanoparticles inhibit both Gram negative (*P. aeruginosa, E. coli)* and positive bacteria (*S. epidermidis* and *S. aureus)* effectively (Figure 3). However, more pronounced activity is noted against Gram-positive bacteria.

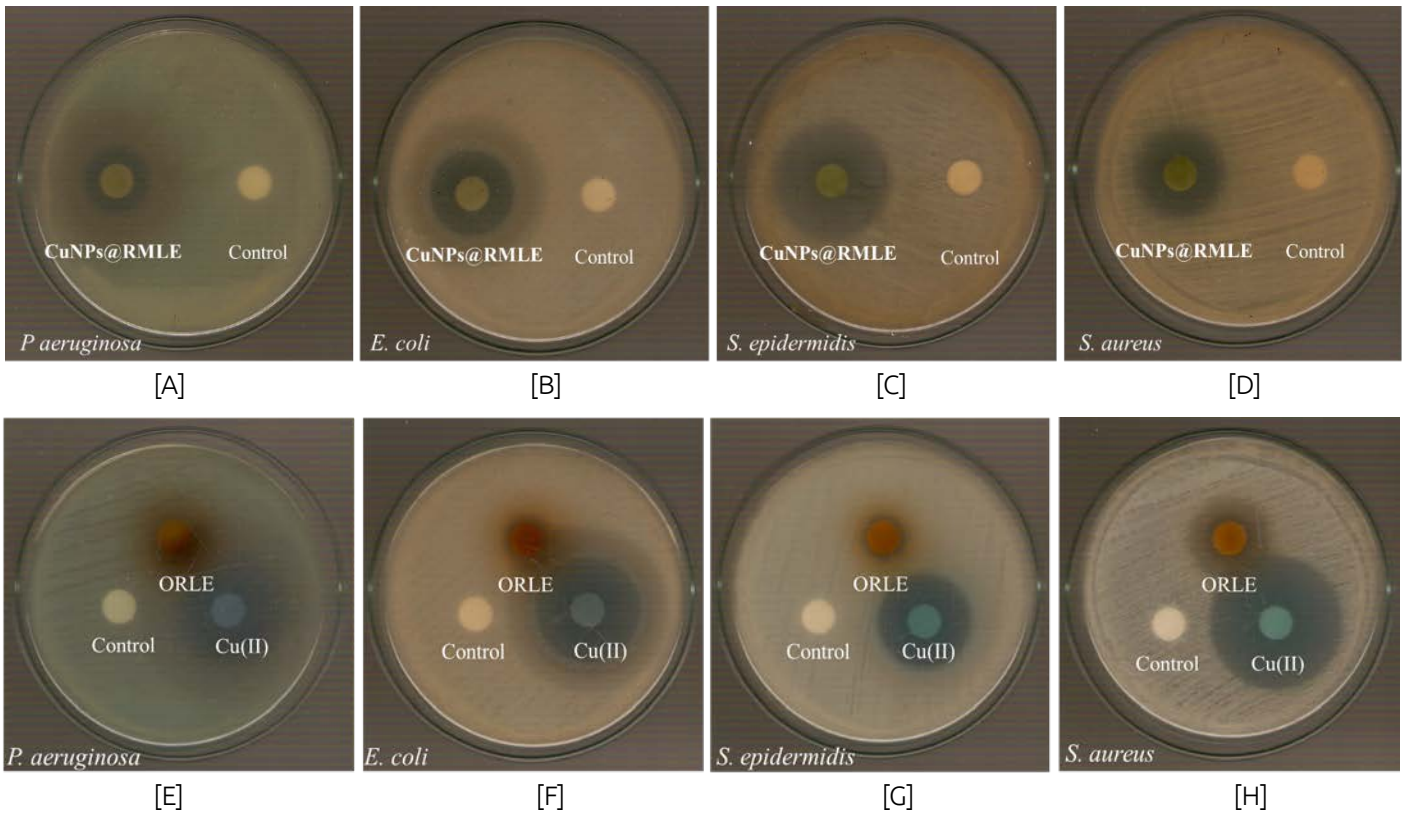

***Figure 3**. Inhibition zones of microbial strains treated with CuNPs@RMLE ([A] P. aeruginosa (18.3±1.7 mm); [B] E. coli (23.5±1.0 mm); [C] S. epidermidis (32.0±2.0 mm); and [D] S. aureus (21±1.0 mm)); RMLE ([E] P aeruginosa (9.0±0.0 mm); [F] E. coli (11.5±0.9 mm) [G]; S. epidermidis (13.8±0.5 mm) and [H] S. aureus (11.0±0.0 mm); Cu(II) ([E] P aeruginosa (26.7±1.7 mm); [F] E. coli (26.3±0.7 mm) [G]; S. epidermidis (32.7±2.8 mm) and [H] S. aureus (27.8±2.6 mm).*

Copper nanoparticles exhibited the strongest activity against *S. epidermidis*,, being twice as effective as against *P. aeruginosa* or *S. aureus*.

Additionally, the antibacterial activity of **RMLE** at 100 mg/mL and a Cu(II) solution (in the form of $Cu(NO_3)_2{\cdot}3H_2O$) at 41.6% w/w were also assessed (Figure 3). The inhibition zones (IZ) created by **RLME** against *P. aeruginosa, E. coli, S. epidermidis,* and *S. aureus*, were measured at 9.0±0.0, 11.5±0.9, 13.8±0.5, and 11.0±0.0 mm, respectively. In comparison, the IZ of the Cu(II) solution were 26.7±1.7, 26.3±0.7, 32.7±2.8, and 27.8±2.6 mm, respectively. Therefore the antibacterial activity of **CuNPs@RMLE** is comparable to that of Cu(II) ions but superior to that exhibited by **RMLE** alone.

Usually, microbial strains are classified into three groups based on the size of the inhibition zone (IZ) produced by a specific amount of an antimicrobial agent in their agar dilution culture: (i) strains showing an IZ ≥17 mm are labeled as susceptible, (ii) those with an IZ between 13 to 16 mm (13 ≤ IZ ≤ 16 mm) are classified as intermediate, and (iii) strains with an IZ ≤ 12 mm are deemed resistant [16]. The classification of the activity of the **CuNPs@RMLE** towards the microbe strains studied here was based on the criterion mentioned above rather the comparison of the inhibition zones developed by microbe cultures that exposed to a specific amount of the agent **CuNPs@RMLE** and its precursors, (copper salt and solidified extract of rosemary). Therefore, the antibacterial activity of **CuNPs@RMLE** is superior to that exhibited by **RMLE** alone. In comparison to CuNPs, **CuNPs@RMLE** demonstrates similar antimicrobial activity against *P. aeruginosa, E. coli, S. epidermidis*, and slightly superioractivity against *S. aureus*.

This suggests that additive benefits or synergies may be realized with **CuNPs@RMLE** although this appears to be bacteria specific. Further work is underway to identify cases where such enhanced antimicrobial activity by **CuNPs@RMLE** is achieved.

Conclusion

Biogenic nanoparticles are essential due to their unique properties and environmentally friendly production techniques. Their biocompatibility makes them promising candidates for treating various diseases. As part of our ongoing investigations in this domain, we conducted research into the development of copper nanoparticles (**CuNPs@RMLE**) employing leaf extract (RMLE) and explored their antimicrobial efficacy.

The antibacterial activity of copper nanoparticles synthesized with rosemary leaf extract, has been demonstrated to be highly effective against bacterial strains including *P. aeruginosa, E. coli, S. epidermidis,* and *S. aureus*. With a substantial copper content of 40% in **CuNPs@RMLE** and its notable solubility in water, this material demonstrates exceptional efficacy against both Gram-negative and Gram-positive strains. The antibacterial effectiveness of **CuNPs@RMLE** surpasses that of **RMLE** alone. When compared to **Cu(II), CuNPs@RMLE** shows comparable antimicrobial activity *against P. aeruginosa, E. coli, S. epidermidis*, and slightly enhanced activity against *S. aureus*. This implies that there may be additional benefits or synergies with **CuNPs@RMLE**, although this seems to vary depending on the bacteria. However, further research into the mechanisms underlying the antibacterial activity of copper nanoparticles, as well as their safety and efficacy in various applications, is warranted to fully harness their therapeutic potential in combating bacterial infections.

Experimental

Materials and instruments: Double distilled water was obtained using the BIDY WATER BI-DISTILLER B.E. 115 apparatus manufactured by BICASA, MILANO, ITALY. Copper nitrate trihydrate ($Cu(NO_3)_2$ $3H_2O$) was purchased from Merk. Tryptone tryptophan medium, beef extract powder, peptone bacteriological, soy peptone was purchased from Biolife. Agar and yeast extract were purchased from Fluka Analytical. D(+)-glucose, di-potassium hydrogen phosphate trihydrate were purchased from Merck. Melting points were measured in open tubes with a Stuart Scientific apparatus and are uncorrected. ATR-FT-IR spectra in the region of 4000-370cm^{-1} were obtained with a Cary 670 FTIR spectrometer, Agilent Tech-nologies. XRF measurements were carried out with a Rigaku NEX QC EDXRF analyzer (Austin, TX, USA).

*Preparation of **RMLE** and **CuNPs@RMLE**:* To prepare the rosemary extract, 2 g of commercially dried rosemary leaves were ground until a fine powder and it placed in a Soxhlet extraction apparatus. A spherical flask containing 40 ml of distilled water was assembled into the apparatus. After 12 hours under reflux, a brownish-clear solution of rosemary extract was obtained.

0.241 g (1 mmol) of copper nitrate trihydrate ($Cu(NO_3)_2$ $3H_2O$) was added into 10 ml of the extract and stirred for 3 h. Then, the suspension, was irradiated under microwave radiation (700 W microwave oven) for 1 minute, followed by ultrasonic treatment for 10 minutes. The solution is centrifugated at 4000 rpm for 20 minute afterwards. The supernatant was isolated and concentrated to dryness using a rotary evaporator. Green powder, highly soluble in water, was collected and stored in darkness.

CuNPs@RMLE: yield 150 mg, green powder; melting point >250 °C, ATR-FTIR (cm^{-1}): 3127br, 2372m, 1289vs, 1020s, 806s, 423m

Biological tests:

Bacterial Strains: The bacterial strains of *P. aeruginosa*, *E. coli*, *S. epidermidis* (ATCC® 14990™) and *S. aureus* (ATCC® 25923™) were used in the experiments [12-13]. The bacterial strains *P. aeruginosa and E. coli* were kindly offered from Medical School of the University of Ioannina [12-13]. The biological experiments were performed in triplicates. The statistical analysis software package included in the MS Office excel was used for the data processing.

Determination of the inhibition zone (IZ),: The procedure was performed as previously reported [12-13]. A standardized inoculum (10^8 cfu/mL) of the microorganisms was incubated in agar plates. A cotton swab is dipped in the inoculum (10^8 cfu/mL) of the microorganisms. The excess fluid is removed by turning the swab against the inside of the tube. The inoculum is spread evenly over the entire of the agar petri dishes in three directions. Disks with 10 mm diameter were soaked in solutions of **CuNPs@RMLE** at the concentration of 100 mg/mL and placed on the agar surface and the Petri plates were incubated for 20 h at 37°C.

References

[1] L. Wang, C. Hu, L. Shoa, The antimicrobial activity of nanoparticles: Present situation and prospects for the future, Int. J. Nanomed, 2017, 12, 1227–1249

[2] E. Hassan, A.A. Gahlan, G.A. Gouda, Biosynthesis approach of copper nanoparticles, physicochemical characterization, cefixime wastewater treatment, and antibacterial activities, BMC Chemistry, 2023, 17, 71

[3] H.M. Al-Saidi, G.A. Gouda, O.A. Farghaly, Potentiometric Study of a New Schiff Base and its Metal Ion Complexes: Preparation, Characterization and Biological Activity, Int. J. Electrochem. Sci., 2020,15 10785-10801

[4] S.K. Chaerun, B.A. Prabowo, R. Winarko, Bionanotechnology: The formation of copper nanoparticles assisted by biological agents and their applications as antimicrobial and antiviral agents, Environ. Nanotechnol. Monit. Manag., 2022, 18, 100703

[5] J.A. Dahl, B..LS. Maddux, J.E. Hutchison, Toward greener nanosynthesis. Chem Rev, 2007, 107, 2228–2269

[6] S.S. Shankar, A. Rai, A. Ahmad, M. Sastry, Rapid synthesis of Au, Ag, and bimetallic Au core–Ag shell nanoparticles

using Neem (Azadirachta indica) leaf broth, J Colloid Interface Sci, 2004, 275, 496–502
[7] S. Das, D.K. Tiwari, Biogenic Synthesis of Nanomaterials Toward Environment-Friendly Approach. In: Arora, P.K. (eds) Microbial Products for Health, Environment and Agriculture . Microorganisms for Sustainability, 2021, 31, Springer, Singapore.
[8] M. Rai, A. Gade, A. Yadav, Biogenic Nanoparticles: An Introduction to What They Are, How They Are Synthesized and Their Applications. In: Rai, M., Duran, N. (eds) Metal Nanoparticles in Microbiology, 2011, Springer, Berlin, Heidelberg.
[9] E. Aziz, R. Batool, W. Akhtar, T. Shahzad, A. Malik, M.A. Shah, S. Iqbal, A. Rauf, G. Zengin, A. Bouyahya, M. Rebezov, N. Dutta, M.U. Khan, M. Khayrullin, M. Babaeva, A. Goncharov, M.A. Shariati, M. Thiruvengadam, Rosemary species: a review of phytochemicals, bioactivities and industrial applications, S. Afr. J. Bot, 2022, 151, 3-189
[10] L. Gachkar, D. Yadegari, B. Rezaei, M. Taghizadeh, S.A. Astaneh, I. Rasooli, Chemical and biological characteristics of Cuminum cyminum and Rosmarinus officinalis essential oils, Food Chemistry, 2007, 102, 898-904,
[11] M. Oluwatuyi, G.W. Kaatz, S. Gibbons, Antibacterial and resistance modifying activity of Rosmarinus officinalis, Phytochemistry, 2004, 65, 3249-3254
[12] A. Meretoudi, C.N. Banti, P.K. Raptis, C. Papachristodoulou, N. Kourkoumelis, A.A. Ikiades, P. Zoumpoulakis, T. Mavromoustakos, S.K. Hadjikakou, Silver Nanoparticles from Oregano Leaves' Extracts as Antimicrobial Components for Non-Infected Hydrogel Contact Lenses, Int. J. Mol. Sci. 2021, 22, 3539
[13] A.K. Rossos, C.N. Banti, P.K. Raptis, C. Papachristodoulou, I. Sainis, P. Zoumpoulakis, T. Mavromoustakos, S.K. Hadjikakou, Silver Nanoparticles Using Eucalyptus orWillow Extracts (AgNPs) as Contact Lens Hydrogel Components to Reduce the Risk of Microbial Infection, Molecules 2021, 26, 5022
[14] B.L. Geoghegan, Y. Liu, S. Peredkov, S. Dechert, F. Meyer, S. DeBeer, G.E. Cutsail III, Combining Valence-to-Core X-ray Emission and Cu K-edge X-ray Absorption Spectroscopies to Experimentally Assess Oxidation State in Organometallic Cu(I)/(II)/(III) Complexes, J. Am. Chem. Soc. 2022, 144, 6, 2520–2534
[15] Clinical and Laboratory Standards Institute (CLSI). Performance Standards for Antimicrobial Susceptibility Testing; Approved Standard, 25th Informational Supplement, CLSI document M100–S25; Clinical and Laboratory Standards Institute: Wayne, PA, USA, 2015.
[16] N. Doroshenko, S. Rimmer, R. Hoskins, P. Garg, T. Swift, H.L.M. Spencer, R.M. Lord, M. Katsikogianni, D. Pownall, S. MacNeil, C.W.I, Douglas, J. Shepherd, Antibiotic functionalised polymers reduce bacterial biofilm and bioburden in a simulated infection of the cornea, Biomater. Sci., 2018, 6, 2101–2109

The learning effects of a teaching learning sequence (tls) about building the concept of density of pure substances and solutions in primary school students

Maria Gaitanidi [1*], Panagiotis Giannakoudakis [2]
[1] PhD Candidate, Department of Chemistry, Aristotle University of Thessaloniki, Greece
[2] Professor, Department of Chemistry, Aristotle University of Thessaloniki, Greece
*Corresponding author's email: mgaitanidi@chem.auth.gr
DOI: 10.62579/JAGC0006

ABSTRACT
This paper (which is a part of a doctoral research) studies the learning outcomes of an integrated Teaching Learning Sequence (TLS), which, by first approaching the necessary background knowledge of the concepts of mass and volume, aims to build the concept of density of both pure substances and solutions. This TLS was developed based on students' already known alternative ideas from the existing literature about the difficulties of understanding density and its intensive character. The analysis of the results showed quite satisfactory learning outcomes of the TLS, with the exception of some difficulties and failures expected to some extent based on the literature, for both primary grades' students, with a predominance of the 6th grade students, which showed higher percentages of better understanding of density and its intensive character.

Keywords: density, 5th - 6th grade students, Teaching Learning Sequence (TLS)

INTRODUCTION

The importance of 'alternative ideas' in Science teaching

In recent years, it has been scientifically accepted within constructivism, both in the international and Greek literature, that a very important factor influencing learning is the ideas that students have formed, from a very young age, depending on the environment in which they live and their respective experiences **[1] [2]**. These pre-existing ideas are often referred to as 'alternative ideas' as they contradict or do not fit into a scientifically accepted framework **[2] [3]** and there is growing evidence for the existence of alternative conceptions in children's understanding of natural phenomena **[4]**. Indeed, some of these are so strong that they are not easily changed, bringing about what is known as cognitive conflict in the learner. Teaching science encounters more obstacles than teaching other subjects, as most scientific concepts are abstract and difficult for students to understand **[5]**. Indeed, according to Borreguero et al. **[6]**, the scientific knowledge acquired by students during traditional textbook-based instruction does not allow for the conceptual change of alternative ideas presented by students, which implies that concepts are not learned in a meaningful way and end up being forgotten over time. Teachers' knowledge of students' alternative ideas about different subjects in science, helps teachers to choose the appropriate teaching approach or even to write more targeted school textbooks and curricula.

The concept of density to be studied

The density of an object is defined as the mass per unit volume of the object. Density is an abstract concept **[7], [8], [9], [10]** and a deep understanding of density is based on an understanding of the concepts of mass and volume and the relationship of density to each **[11]**. In Greece, density is a concept that is introduced in Science course in the 5th grade, according to the curriculum of the Greek Ministry of Education. Density is a concept in Science that is difficult to understand for children aged 10-12 years old, which is confirmed in the literature **[11], [7], [12], [13]**, etc. The difficulty of understanding lies in the fact that children of this age have many misconceptions about matter and thus cannot differentiate the concepts of weight and density **[14], [15], [16]**. Another difficulty is the fact that density is an intensive quantity, which, in order to be calculated, requires the simultaneous consideration of the mass and volume of a material body and according to Rowell & Dawson **[17]** and Seah et al. **[18]** students of this age have difficulty understanding the concept of the ratio of two quantities. Although students successfully calculate density by dividing mass and volume when given physical numbers (building on their mathematical knowledge of fractions) **[18]**, they still struggle to understand what this ratio means **[2], [19]**. It is no coincidence that four out of ten Greek school students, who have the scientific idea of density, also have some

18) I have two cubes of the same volume. One is made of stone and the other of Styrofoam. Which cube do you think has a lower density of material? Put an X in the correct answer and briefly justify your answer.

A) The stone cube has a lower density	
B) Styrofoam cube has lower density	
C) Both cubes have the same density	

α) Justify your answer: You can use some of the words (mass, volume, smaller, larger, same):

The cube made of_____ has a lower density because _____

_____

Figure 1*: A closed-ended question from the questionnaire with the corresponding open-ended question that serves as a justification for the first*

good or relatively good opinion about the defining quantities of density **[20]**. As an extension of the concerns about students' problems with the concept of density in pure substances **[21]**, another thing that children have difficulty with is the density of solutions, since in order to decide whether a solution is dense or dilute, they must consider both the mass of the solute and the volume of the solvent. In order to improve children's understanding, the concept of density is approached qualitatively (e.g. the experimental setup of the study of the density of sugar water) and from this, through the discovery model of teaching, its quantitative expression is derived.

The Teaching Learning Sequence (TLS)

Many studies, that attempt to identify students' perceptions around different concepts, are based on Teaching Learning Sequences (TLS), that attempt to develop improved ways of teaching the underlying topics **[22], [23]**. In the European science education community, this trend is being implemented through the design, development, implementation and evaluation of Teaching Learning Sequences (TLS), which are a mid-scale curriculum product covering a scientific topic **[23]**. According to Fassoulopoulos et al. **[24]** and Zongo et al. **[15]**, students' approach to the concept of density is best done with the help of liquids, because they have advantages over solids and gases. That is why this experimental teaching intervention contains experiments mainly using liquids, thus making experimental use of the so-called "density column". The difficulties, that students usually face in understanding the concept of density, usually identified after traditional teaching, as well as their alternative ideas known to the research community, were taken into account in the design of the relevant activities of this Teaching Learning Sequence (TLS) **[25], [26]**.

METHODOLOGY

The population for the present study consists of students aged 11-12 years old, attending the 5th and 6th grade of primary school. 90 students in 5th grade and another 90 students in 6th grade were selected from primary schools throughout Greece. More specifically, the 5th grade students were taught the units on mass, volume and density from the textbook 4 to 7 months before the main research was conducted, while the 6th grade students were taught the corresponding units 16-19 months before. An attempt was also made to distribute between boys and girls, such that it was consistent with the distribution in the general population. Consequently, 72 boys (40%) and 108 girls (60%) participated in the research. An effort was also made to ensure that all students were at a similar socio-economic level, in order to limit the influence of other factors as much as possible.

More detailed, as to the process and timing of the main research: First, the initial questionnaire (Pre-test) was given to the students, in order to record and study their initial ideas - "alternative ideas" as before understanding the concepts of mass, volume, density of pure substances and density of solutions. After one week, the three experimental teaching interventions of the Teaching Learning Sequence (TLS) were implemented in the classroom over a maximum of two weeks with the corresponding worksheets. At the end of the experimental teaching and after 7-10 days from the first experimental teaching intervention, the students were given the final questionnaire (Post-test) to evaluate the learning outcomes of the experimental teaching interventions.

The questionnaire, that was distributed, consists of 21 questions and both the Pre-test and the Post-test are the same questionnaire, precisely to better assess the room for improvement of students' learning outcomes. The coding of the answers differs from case to case. Furthermore, all questions are closed-ended, but there are some open-ended sub-questions, where students are usually asked to justify their answer to the main close- ended question [Figure 1, 2]. In addition, it is worth noting that the questions deal with both mass and volume and density of both pure substances and solutions. Furthermore,

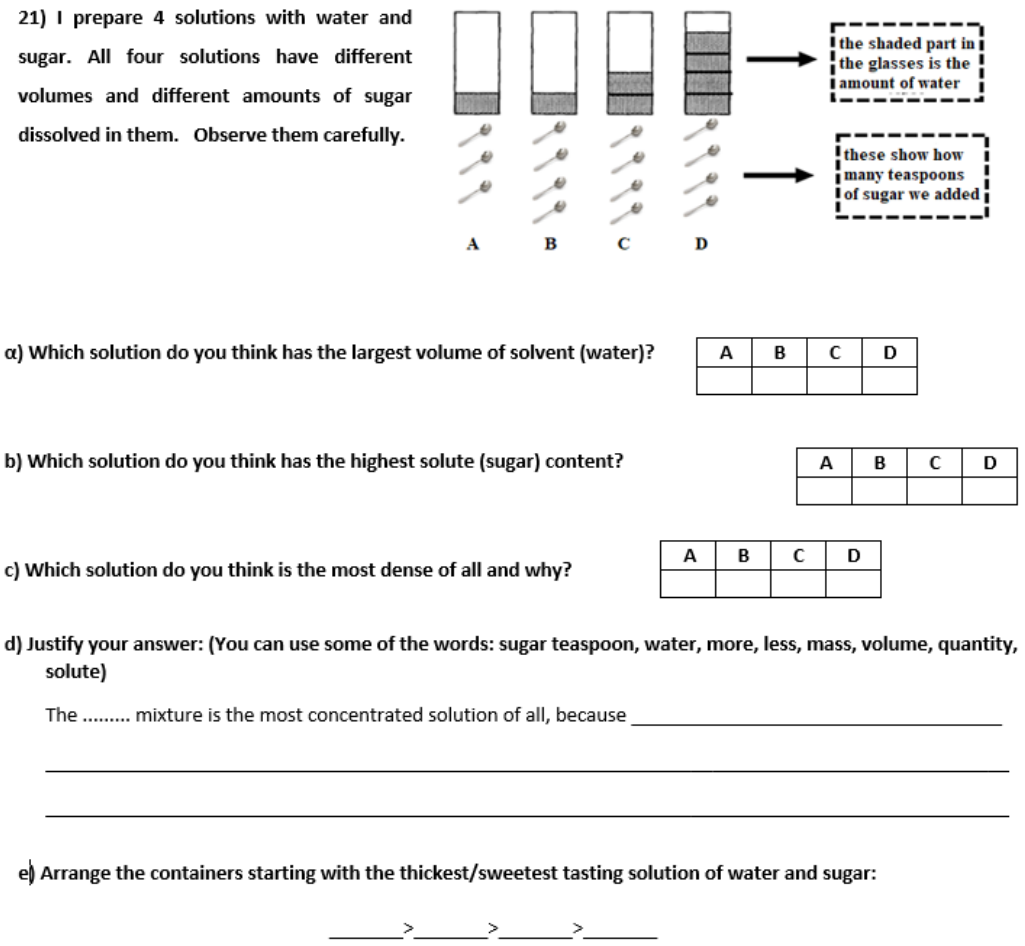

***Figure 2**: A question from the questionnaire with closed or open-ended sub-questions to be answered by observing the figure with four solutions of different solvent volumes and different solute masses*

groups of questions were created, which will be used later, targeting different aspects of the topic under study.

RESULTS

Statistical analysis and processing of the results was carried out using SPSS 23 statistical software and application of the non-parametric Mann-Whitney test to determine whether there was a significant difference between the two groups of students in terms of their total score on each factor of the research.

As Table 1 shows, during Phase 1 of the research (Pre -test Phase), students in the two classes had approximately the same scores on the factors being studied. The only exception was the total score on understanding the density of solutions with different solvent volumes and different solute masses (U=3378.000, p=0.020). In this case, the students in 6th grade showed a significantly higher score (M.=0.81, S.D.=1.13) than the students in 5th grade (M.=0.41, S.D.=0.81). On the other hand, it appears that after the implementation of the teaching intervention, there was a significant difference between the 5th and 6th grade students in their scores on each of the two major factors studied, concerning the knowledge of the density of pure substances (U=2844,000, p=0.001) and solutions (U=3308,500, p=0.033). In fact, in both factors, a higher score is noted among the 6th grade students (M.=17.23, S.D.=2.43; M.=10.93, S.D.=2.58 respectively) compared to the 5th grade students (M.=15.84, S.D.=2.62; M.=10.18, S.D.=2.37).

Furthermore, students in the two classes also appear to differ significantly in the remaining scores of the smaller factors, that were formed and studied in relation to density. Specifically, students in the two classes scored significantly differently on understanding density as an intensive quantity that depends solely on the type of material (U=3338,500, p=0.037), on understanding the concept of mass (U=2918,500, p<0.001), and on intuitive understanding of density through floating and sinking theory (U=3287,500, p=0.025). In each of these factors, a higher score was obtained by the 6th grade students (M.=3.46, S.D.=1.26; M.=3.39, S.D.=0.75; M.=6.16, S.D.=1.23 respectively) compared to the 5th grade (M.=3.02, S.D.=1.41;

M.=3,01, S.D.=0,79; M.=5.69, S.D.=1.37 respectively). Finally, the two groups of students also seem to differ significantly in their understanding of the density of solutions with different volumes of solvent and different masses of solute (U=3128.000, p=0.005). Once again, there was a significant superiority of the students of the 6th grade (M.=1.60, S.D.=1.28) over the rest of the 5th grade students (M.=1.09, S.D.=1.26). However, as the averages show, the teaching intervention was successful for both classes in all factors, sometimes a little and sometimes a lot.

Table 1: Results of the difference tests on the total score obtained by students in the 2 phases (where M.=Average and where S.D.=Standard Deviation)

Factors	1st Phase (Pre-test Phase)			2nd Phase (Post-test Phase)		
	M. ± S.D. (5th grade)	M. ± S.D. (6th grade)	U (p)	M. ± S.D. (5th grade)	M. ± S.D. (6th grade)	U (p)
Knowledge of the mass, volume and density of pure substances (0 – 22)	9,17 ± 2,89	9,29 ± 2,20	3974,500 (0,827)	15,84 ± 2,62	17,23 ± 2,43	2844,000 (**0,001**)
Knowledge of mass, volume and density of solutions (0 – 15)	5,87 ± 2,35	6,31 ± 2,53	3738,000 (0,368)	10,18 ± 2,37	10,93 ± 2,58	3308,500 (**0,033**)
Understanding density as an intensive quantity that depends solely on the type of material (0 – 5)	1,12 ± 1,22	1,33 ± 1,13	3498,500 (0,099)	3,02 ± 1,41	3,46 ± 1,26	3338,500 (**0,037**)
Understanding of volume concept (0 – 3)	1,92 ± 0,81	1,77 ± 0,81	3742,500 (0,340)	2,52 ± 0,57	2,34 ± 0,69	3542,000 (0,103)
Understanding the concept of mass (0 – 4)	1,96 ± 1,02	2,09 ±0,88	3799,000 (0,448)	3,01 ± 0,79	3,39 ± 0,75	2918,500 (**<0,001**)
Understanding mass/density differentiation (0 – 7)	1,64 ± 1,26	1,49 ± 1,07	3783,000 (0,428)	4,06 ± 1,39	4,41 ± 1,38	3482,500 (0,097)
Intuitive understanding of material density through floating/sinking theory (0 – 8)	3,36 ± 1,28	3,13 ± 1,07	3591,000 (0,174)	5,69 ± 1,37	6,16 ± 1,23	3287,500 (**0,025**)
Understanding material density based on particle structure (0 – 1)	0,31 ± 0,47	0,36 ± 0,48	3870,000 (0,528)	0,83 ± 0,38	0,74 ±0,44	3690,000 (0,145)
Understanding the parts of the density fraction (0 – 3)	1,19 ± 0,78	1,27 ± 0,83	3790,000 (0,426)	2,02 ± 0,79	2,10 ± 0,82	3806,500 (0,451)
Understanding the density of different materials with the same volume and different mass (0 – 3)	1,44 ± 0,72	1,46 ± 0,64	4032,000 (0,954)	2,18 ± 0,76	2,23 ± 0,65	3962,500 (0,783)
Understanding the solvent/solute ratio for solution characterization (0 – 9)	2,54 ± 1,60	2,86 ± 1,90	3725,500 (0,344)	5,62 ±1,80	6,04 ± 2,17	3564,000 (0,159)
Same volumes of solvent and different mass of solute (0 – 3)	1,26 ± 0,82	1,14 ± 0,74	3640,000 (0,204)	2,50 ± 0,68	2,54 ± 0,71	3828,000 (0,458)
Different volumes of solvent and different mass of solute (0 – 3)	0,41 ± 0,81	0,81 ±1,13	3378,000 (**0,020**)	1,09 ± 1,26	1,60 ± 1,28	3128,000 (**0,005**)

CONCLUSIONS

The statistical analysis of the responses revealed that both 5th grade and 6th grade students showed very positive learning outcomes after the implementation of the Teaching Learning Sequence (TLS) on all factors of the survey, either on a small scale or on a large scale. It should be noted that students in both grades, during the first phase of the research, i.e. before the implementation of the TLS, had generally the same success rate on the questions, which is reasonable, since they had been taught the same items from the textbook, while after the implementation of the TLS, the superiority of the 6th grade students over the students in 5th grade was evident, in most of the factors of the research. It should be noted that the scores of the students in Phase 1 of the survey were quite low on most of the survey factors, i.e. below 50%, with the exception of their responses related to their intuitive understanding of material density through floating/sinking theory, which is normal, given that children of this age already have enough knowledge through systematic observation from their daily life. Of particular interest is the fact that after the experimental teaching intervention they scored quite satisfactory (almost three times as high) in terms of understanding the concept of density as an intensive quantity, which depends exclusively on the type of material and not so much on the deep understanding of the concept of the ratio of two quantities (mass/volume in the case of density). Besides, regarding the density of different materials with the same volume and different mass, a slight improvement was observed with a relative difficulty in interpreting and justifying it, due to the difficulty at this age of simultaneously considering both parts of the density fraction (d= m/V).

Difficulty and partial failure, even after implementation of the experimental intervention, was observed in the students of both grades in understanding the density in solutions with different solvent volume and different solute mass, while on the contrary, all students understood the density of solutions with the same solvent volume and different solute mass to a very good level. Besides, and according to the literature **[2], [17], [18], [19]**, students of this age find it difficult to manage the simultaneous consideration of the mass and volume of a material body, let alone a solution.

In general, on the whole, the TLS was successful in terms of learning to understand the difficult for this age concept of density of both pure substances and solutions. It would be best, of course, if density were to be included in the 6th grade Science Curriculum and introduced for the first time as a concept in the 6th grade science class rather than in the 5th grade science class, in order to be understood to a greater extent by the pupils in the last grade of primary school and to achieve a smooth transition to high school. It is also proposed to use this TLS as a teaching material for the concept of density, as the textbook, according to phase 1 of the research, showed low learning outcomes for students in both grades. Finally, the revision of the new Primary School Science Curriculum, which has not yet entered into force but has already been implemented in the Experimental Schools, proposing the abolition of the teaching of density in primary education, resulting in an abnormal transition to the concept of density directly in secondary education, which is confirmed by the literature **[15]**.

REFERENCES

[1] Rosalind Driver, "Theory into Practice II: A constructivist approach to curriculum development", in book: "Development and Dilemmas in Science Education", 1st ed. (Routledge, 1988): p. 133-149.
Url:https://books.google.gr/books?hl=el&lr=&id=V_pqPu_krF4C&oi=fnd&pg=PA133&dq=scott+wightman+1985&ots=Ec8tXBL2oJ&sig=G08E9eSEQ1vf0GafHB24NUM7HKE&redir_esc=y#v=onepage&q=scott%20wightman%201985&f=false

[2] Kiray, S., & Simsek , S. (2021, 6). Determination and Evaluation of the Science Teacher Candidates' Misconceptions About Density by Using Four-Tier Diagnostic Test. International Journal of Science and Mathematics Education(19), p. 935-955. doi:https://doi.org/10.1007/s10763-020-10087-5

[3] Graham Birley & Wendy Dewhirst, "It's soft and you can squeeze it: a study of six -year olds' understanding of materials", Research in Education, 44 (1) (November 1990): p.13-20. doi:https://doi.org/10.1177/003452379004400102

[4] Mariana Hewson, "The acquisition of scientific knowledge: Analysis and representation of student conceptions concerning density", Science Education, 70 (2) (1986): p.159-170. doi:https://doi.org/10.1002/sce.3730700210

[5] Chazbeck, B., & Ayoubi, Z. (2018). Resources Used by Lebanese Secondary Physics Teachers' for Teaching Electricity: Types, Objectives and Factors Affecting their Selection. Journal of Education in Science, Environment and Health, 4(2), p. 118-128. doi:https://doi.org/10.21891/jeseh.409487

[6] Borreguero, G., Naranjo Correa, F., Núñez, M., & Martín, J. (2018). Recreational Experiences for Teaching Basic Scientific Concepts in Primary Education: The Case of Density and Pressure. Eurasia Journal of Mathematics, Science and

Technology Education, 14(12). doi:https://doi.org/10.29333/ejmste/94571

[7] Anna Spyrtou, Anastasios Zoupidis & Petros Kariotoglou, "THE DESIGN AND DEVELOPMENT OF AN ICT-ENHANCED MODULE CONCERNING DENSITY AS A PROPERTY OF MATERIALS APPLIED IN FLOATING / SINKING PHENOMENA", in "Physics Curriculum Design, Development and Validation, Selected Papers" (GIREP INTERNATIONAL CONFERENCE, January 2008): p. 391-407.
Url:https://www.researchgate.net/publication/268439377_THE_DESIGN_AND_DEVELOPMENT_OF_AN_ICT-ENHANCED_MODULE_CONCERNING_DENSITY_AS_A_PROPERTY_OF_MATERIALS_APPLIED_IN_FLOATING_SINKING_PHENOMENA

[8] Ochs, A., Dee, J., Arnold, A., Barber, K., & Zovinka, E. (2023). Connecting Active Artwork to Chemistry: Leading Students in Inquiry-Based Learning of Density and Viscosity. Journal of Chemical Education, 100(9), p. 3703-3708. doi:https://doi.org/10.1021/acs.jchemed.3c00277

[9] Zenger, T., & Bitzenbauer, P. (2022). Exploring German Secondary School Students' Conceptual Knowledge of Density. Science Education International, 33(1). doi:https://doi.org/10.33828/sei.v33.i1.9

[10] Hashweh, M. (2015). The complexity of teaching density in middle school. Research in Science & Technological Education, 34(1), p. 1-24. doi:https://doi.org/10.1080/02635143.2015.1042854

[11] R.E. Yeend, Michael E. Loverude & Barbara L. Gonzalez, "Student understanding of density: a cross-age investigation", in book: "Conference: 2001 Physics Education Research Conference", (New York, July 2001). doi:https://doi.org/10.1119/perc.2001.pr.020

[12] Jean Piaget & Barbel Inhelder, "The growth of logical thinking from childhood to adolescence: An essay on the construction of formal operational structures", 1st ed., (London, Routledge, 1958).
Url:https://www.taylorfrancis.com/books/mono/10.4324/9781315009674/growth-logical-thinking-childhood-adolescence-jean-piaget-b%C3%A4rbel-inhelder

[13] Carol Smith, Joseph Snir & Lorraine Grosslight, "Using Conceptual Models to Facilitate Conceptual Change: The Case of Weight-Density Differentiation", Cognition and Instruction 9 (3), (1992): p.221-283. doi:https://doi.org/10.1207/s1532690xci0903_3

[14] Carol Smith, Susan Carey & Marianne Wiser, "On differentiation: A case study of the development of the concepts of size, weight, and density", Cognition 21 (3), (December 1985): p.177-237. doi:https://doi.org/10.1016/0010-0277(85)90025-3

[15] Zongo, I., Bougouma, M., & Moucheron, C. (2023). Proposal for a Didactic Tool on Teaching Practices Related to the Selective Sorting of Plastic Waste According to Relative Density in High Schools: Case Study in Burkina Faso. Journal of Chemical Education, 100(3), p. 1118-1127. doi:https://doi.org/10.1021/acs.jchemed.2c00629

[16] Xu, L. (2019). Relating Teaching and Learning of Science Through the Lens of Variation Theory. Scandinavian Journal of Educational Research, 63(1), p. 145-162. doi:https://doi.org/10.1080/00313831.2017.1357143

[17] J.A. Rowell & C.J. Dawson, "Teaching About Floating and Sinking: An Attempt to Link Cognitive Psychology with Classroom Practice", Science Education, 61(2), (April/June 1977): p.243-251. doi:https://doi.org/10.1002/sce.3730610215

[18] Seah, L., Clarke, D., & Hart, C. (2015). Understanding Middle School Students' Difficulties in Explaining Density Differences from a Language Perspective. 37(14), p. 2386-2409. doi:https://doi.org/10.1080/09500693.2015.1080879

[19] McMullen, J., & Van Hoof, J. (2020). The role of rational number density knowledge in mathematical development. Learning and Instruction, 65. doi:https://doi.org/10.1016/j.learninstruc.2019.101228

[20] Georgios Fassoulopoulos, "Students' perceptions of the relationship between intensive physical quantities and the quantity of the system and their implications for teaching", (Thessaloniki, Aristotle University of Thessaloniki, 2000). doi:http://dx.doi.org/10.12681/eadd/13630

[21] Eugene D. Gennaro, "Assessing Junior High Students' Understanding of Density and Solubility", School Science and Mathematics, (May/June 1981): p.361-448. doi:https://doi.org/10.1111/j.1949-8594.1981.tb09996.x

[22] Piet Lijnse, "Didactical structures as an outcome of research on teaching–learning sequences?", International Journal of Science Education, 26 (5), (February 2007): p. 537-554. doi:https://doi.org/10.1080/09500690310001614753

[23] Psillos, D., & Kariotoglou, P. (2016). Theoretical Issues Related to Designing and Developing Teaching-Learning Sequences. In D. Psillos, & P. Kariotoglou, Iterative Design of Teaching-Learning Sequences (p. 11-34). Dordrecht: Springer.

[24] Georgios Fassoulopoulos, Petros Kariotoglou, Panagiotis Koumaras & Dimitris Psillos, "Students' difficulties in understanding density", Pedagogical Review, 25, (October 1997) p. 161-176.
Url:https://www.researchgate.net/profile/Petros-Kariotoglou/publication/27376671_Dyskolies_ton_matheton_sten_katanoese_tes_pyknotetas/links/5775331408ae4645d60ba76c/Dyskolies-ton-matheton-sten-katanoese-tes-pyknotetas.pdf
[25] Anastasios Zoupidis, Dimitris Pnevmatikos, Anna Spyrtou & Petros Kariotoglou, "The gradual approach of the nature and role of models as means to enhance 5th grade students' epistemological awareness", in book: "Contemporary science education research: Learning and assessment", (Turkey, For Conference ESERA- Cakmakci & Tasar, January 2010): p. 415-423.
Url:https://www.researchgate.net/publication/251414648_Zoupidis_A_Pnevmatikos_D_Spyrtou_A_Kariotoglou_P_2010_The_gradual_approach_of_the_nature_and_the_role_of_models_as_means_to_enhance_5th_grade_students%27_epistemological_awareness_In_G_Cakmakci_MF_Tasar
[26] Savall-Alemany, F., Guisasola, J., Cintas, S., & Martínez-Torregrosa, J. (2019). Problem-based structure for a teaching-learning sequence to overcome students' difficulties when learning about atomic spectra. Physical Review Physics Education Research, 15(2), p. 020138. doi:https://doi.org/10.1103/PhysRevPhysEducRes.15.020138

ETHICAL STATEMENT

This study was approved by the Ethics committee of the Aristotle University of Thessaloniki (Protocol Number: 19960/19-01-2023). This research protocol was also approved by the Ministry of Education, Religious Affairs and Sports of Greece and the Institute of Educational Policy (Protocol Number: Φ15/7024/ΑΛ/9288/Δ1/26-01-2023). Participants were well noticed the research purpose and research methods. Signed consent was obtained for all participants and their parents.

DATA AVAILABILITY STATEMENT

Data will be supplied upon request (all in Greek).

Developing flipped classroom educational material in the Greek curriculum for Chemistry: Examples from 8th to 12th grade students

Nikolaos Giannakopoulos
Secondary Education Teacher – Chemist, Msc-MEd
Arsakeio School of Patras
giannakopoulos.n@e-arsakeio.gr

DOI: 10.62579/JAGC0007

Abstract
The present study aims to implement the flipped classroom teaching model in the Greek curriculum for chemistry from 8th to 12th grade students. Specifically, this involves designing and creating suitable educational material according to the flipped classroom methodology for targeted chemistry course units, which include laboratory exercises as well. The flipped classroom is a blended learning model, where students prepare by watching video lectures or other educational material at home, while homework is conducted in the classroom with the assistance of the teacher and students discussing and resolving questions. The teacher supports students exactly where they encounter difficulties, thus shifting their role from traditional lecturing to guiding, supporting, and individualizing.

Keywords
Learning science, flipped classroom, laboratory teaching

Introduction
The flipped classroom belongs to learning models, which focus on the student. In these models, the student actively and consciously participates in all stages of learning[1]. Additionally, it serves as a powerful catalyst, transforming the teacher into a guide in teaching rather than authority of knowledge and simultaneously transforming students into active learners who take on a more collective and self-directed role in the learning process[2].
Another advantage of the specific learning model allows the redistribution of time in class, facilitating the advancement of skills through collaborative work schemes and discussions. This, in turn, encourages students to teach and learn concepts from each other, always guided by teachers. Additionally, it enables students to actively participate in their own learning and to be proficient in mastering the knowledge they acquire[3]. It should also be emphasized that the flipped classroom is a blended learning model because it utilizes both face-to-face and distance learning methods[4].
In this study, a series of teaching interventions will be presented, which have been implemented by the undersigned during the academic years 2022-23 and 2023-24 at a specific Gymnasium and Lyceum school of Patras-Greece. These teaching interventions represent yet another way to share teaching tools that educators can use to enhance their instruction and strengthen their interaction with students in each area of study.

Theoretical Framework

Keypoints
21st-century students are often referred to as digital natives due to their familiarity with new technologies. According to McMahon and Pospisil (2005)[4], these students prefer learning environments that facilitate multitasking, collaborative activities, and social aspects of learning[5].
The flipped classroom represents an educational process where instruction shifts from group learning to individual, and the group space transforms into a dynamic, interactive learning environment where the educator guides students as they explore concepts and engage creatively with the subject matter. Therefore, education, especially in the field of Physical Sciences, plays a significant role as it follows the social constructivist approach, serving as a process of knowledge construction by students through individual and social processes[7]. The emphasis in teaching Physical Sciences should shift from one-way delivery of information through lectures to the construction of knowledge by the students themselves through collaborative activities in the classroom, with the teacher acting as a collaborator alongside the students[8].
In conventional teaching, classroom time is primarily devoted to the teacher presenting new knowledge, while students use their time at home to absorb and apply it through assigned tasks. Conversely, in the flipped classroom, students are tasked with studying and interacting with the content prior to class. Subsequently, during class,

they are tasked with applying the knowledge through active approaches, with the teacher serving as a guide in their efforts. The flipped classroom allows students to focus on higher levels of thinking during class time, in accordance with Bloom's cognitive taxonomy (e.g., apply, analyze, evaluate, create), as lower levels (remember, understand) have already been addressed before class[9].

Literature Review

The flipped classroom model gained worldwide recognition through the efforts of Bergmann and Sams[10]. In their attempt to assist students who were unable to attend their classes, they recorded PowerPoint presentations and uploaded them as videos on YouTube, making them accessible to absent students. Tucker[11] states that the flipped classroom model is based on the idea that students can study and prepare at home by watching interactive videos related to the lesson. Then, during class time, students can solve problems, advance concepts, and actively participate in the educational process through collaborative learning (see figure 1).

The flipped classroom model appeared to empower students to interact with educational content at their own pace, place, and time, taking responsibility for their learning and gaining greater autonomy and self-confidence[12]. Additionally, the implementation of active learning educational techniques such as discussions, problem-solving, case studies, etc., during classroom sessions allowed students to achieve deeper understanding, cultivate critical thinking, and attain higher academic performance. Furthermore, active student engagement in the learning process was observed[13], while collaborative approaches provided opportunities for students to interact, fostering communication and collaboration skills[14].The role of the teacher also appeared to change, transitioning to that of a facilitator helping students overcome challenges encountered during the knowledge-building process[15].

Methodology

Today, flipped classroom is implemented worldwide, across all levels of education and in various academic subjects (such as Physical Sciences, Mathematics, Humanities, and Social Sciences, etc.). Technology has enabled students to have easy access to digital media, particularly videos, through the internet. This has facilitated the online teaching of educational material in a remote setting, thereby enabling more interactive student participation during in class sessions. Moreover, especially in Greek educational community several educational videos that are been created for in class use usually replace the laboratory process. With the specific procedure that is been described below the provided video are being processed (with the website administrator's permission) in such a way that students interact with the provided material rather than being passive recipients of information[2].

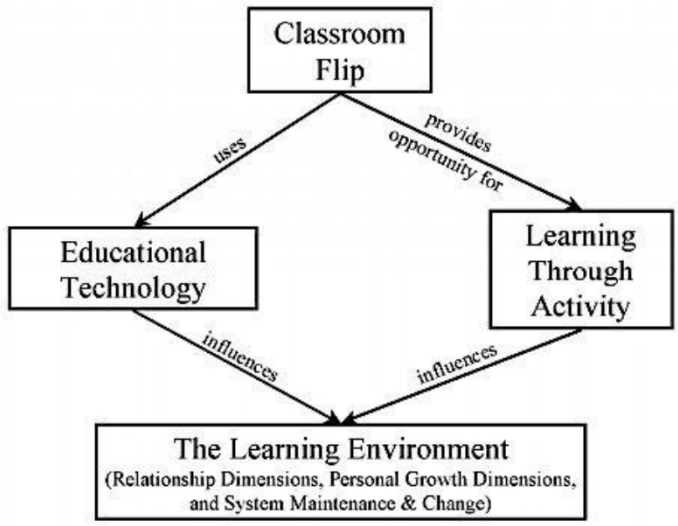

***Figure 1**: Theoretical framework of flipped classroom (taken from Strayer, 2007[30]).*

Although the implementation of the flipped classroom model may vary under different circumstances, it always relies on the following four pillars: a flexible environment, a learning culture, intentional content, and the professionalism of educators[16].

In the flipped classroom methodology, we can identify three main stages: the pre-class stage, the in-class stage and a third stage, after the class, which help students benefit more from the activities conducted in class as they can reflect on and consolidate their knowledge[17]. During the pre-class stage, students engage with the content through video lectures, podcasts, and other digital materials prepared by the educator and made available on a digital learning platform. This allows each student to interact with the

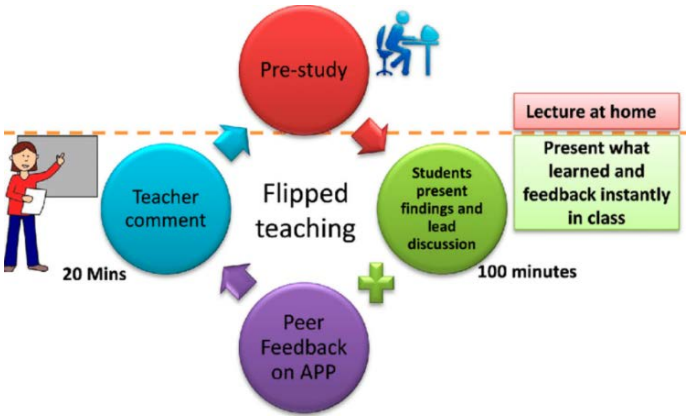

***Figure 2**: Stages of flipped classroom methodology (taken from Hsu, Ting, 2017[31])*

content according to their own learning style, pace, and preferred time and place[18]. Additionally, educators can use online assessments to identify students' prior knowledge and conduct an initial assessment of their understanding of the content, thus planning their next steps for the in-class stage accordingly[19]. It's worth noting that this initial engagement of students with the content focuses more on the lower levels of Bloom's taxonomy of cognitive objectives (remembering, understanding)[20]. Sharing content, aside from equipment (computers, tablets, etc.), requires a digital learning platform (Learning Management System) where course content is posted, access to the internet for students, and digital skills for interaction[21].

Learning management Systems (L.M.S)

Learning Management Systems (LMS) play a crucial role in facilitating the implementation of the flipped classroom model. An LMS enables the seamless sharing of educational content, including instructional videos, assessment quizzes, documents, and more. It provides educators with the means to upload materials and interact with students, while also allowing learners to access and engage with the content. Key features of an LMS include:

1. Content Sharing: Educators can upload multimedia resources, documents, and assignments for students to access.
2. Communication: LMS platforms facilitate communication between educators and students through direct messaging, email, and discussion forums.
3. Collaboration: Students can collaborate on projects, share ideas, and co-create content through features like wikis and group discussions.
4. Assessment: LMS systems support both formative and summative assessment methods, allowing educators to track student progress and evaluate learning outcomes.
5. Grading and Feedback: Educators can grade assignments, provide feedback, and monitor student performance using the built-in grading tools.
6. Organization: LMS platforms offer organizational tools for structuring content into units or modules, making it easy for students to navigate.

Overall, Learning Management Systems provide a comprehensive environment for teaching and learning, facilitating interaction, collaboration, assessment, and monitoring of student progress. They offer a range of features to support educators in delivering content and engaging students effectively in both traditional and flipped classroom settings.

In this study, some of the available Learning Management Systems were utilized, such as LAMS AI, e-me, and e-platform (exclusively for the students of the specific schools). These systems assist educators worldwide in designing and implementing online educational activities.

Purpose and Research

While an extensive body of research exists regarding theoretical framework in Greek literature[22] as well as several flipped based approaches in primary education[23] research highlighted the necessity of a series of teaching interventions in the educational field of Chemistry for the secondary education in Greece that will be used in future research as a guide to the impact of a teaching intervention that is based on the flipped classroom. Thus, the learning outcomes of these teaching interventions can be contrasted with the learning outcomes of teaching interventions that are based on the school science textbook used by Greek schools (traditional teacher-centered approach to flipped science learning).

Educational Material Implementation

For the needs of the teaching interventions that follow, planning and creation of educational material were carried out for 8th to 12th grade students in the conceptual areas of Chemistry that follow.

Example for 8th grade students

Conceptual Area: Preparation of a Solution with a specific %w/w concentration

Learning Management System: "e-platform"[28]

Number of participated students: Twenty-two (22)

Teaching Procedure:

Before Class: Students access the digital classroom on the e-platform from their homes using their login credentials, where specific materials and videos from the internet are posted. Then, they complete the provided worksheet questions and submit their answers.

During Class: Students work in groups to conduct the experiment proposed in their school textbook, under the guidance and supervision of the educator. In this case, the experiment titled "Preparation of a solution with a specific % w/w concentration" was implemented.

After Class: After completing the experiment at home, students return to the e-platform. They answer two additional exercises for reinforcement and then respond to a questionnaire or survey.

Example for 9th grade students

Conceptual Area: Neutralization – Salts

Learning Management System: "e- platform"

Number of participated students: Twenty-three (23)

Teaching Procedure:

Before Class: Students access the digital classroom on the

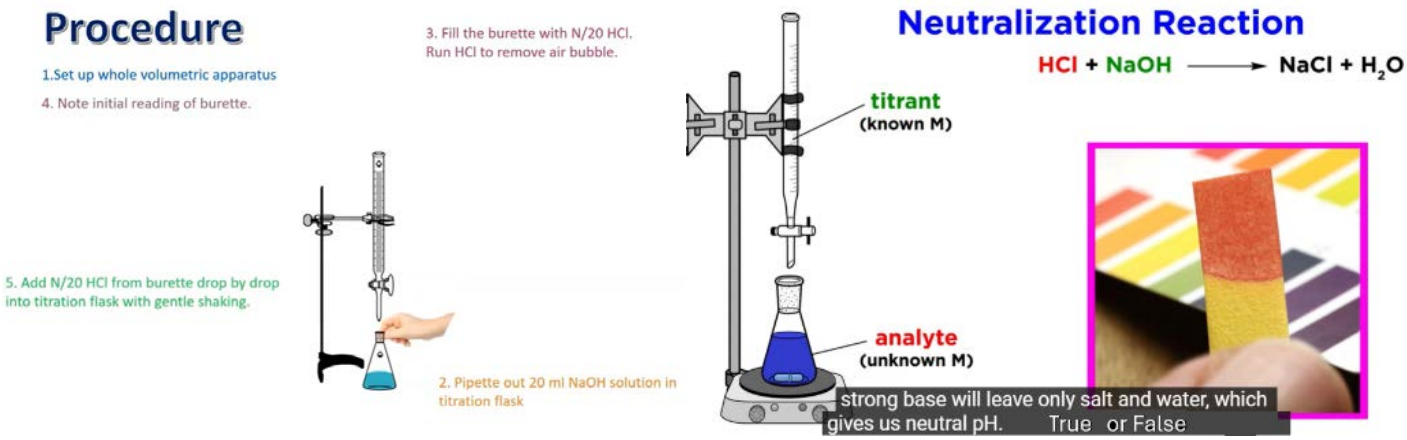

***Figure 3**: Attachment from the material distributed to students before class*

e-platform from their homes using their login credentials, where specific materials and videos from the internet are posted. Specifically, they watch a video titled "Successive neutralizations of acid solution with base using indicator." Then, they complete the provided worksheet questions and submit their answers. For the purpose of the specific paper a screenshot of the procedure is being presented on figure 3.

During Class: Students work in groups to conduct the experiment proposed in their school textbook, under the guidance and supervision of the educator. In this case, the experiment titled "Neutralization of hydrochloric solution from sodium hydroxide solution and preparation of sodium chloride" was implemented. In this particular case, students worked without the usual time pressure (due to the analytical Greek curriculum, chemistry is taught only for 1 hour per week), while the educator has the opportunity to delve into ion equations for salt formation.

After Class: After completing the experiment at home, students return to the e-platform. They answer two additional exercises for reinforcement and then respond to a questionnaire or survey.

Example for 10th grade students

Conceptual Area: Preparation of a Solution of Defined Concentration

Learning Management System: "e-me" electronic platform[27]

Number of participated students: Sixteen (16)

Teaching Procedure:

Before Class: Students access their private cell on the e-me platform from their homes using their login credentials, where specific materials and videos from the internet are posted. Specifically, they watch a video titled "Preparation of copper sulfate solution of defined concentration." Then, they complete the provided worksheet questions and submit their answers. For the purpose of the specific paper a screenshot of the procedure is being presented on figure 4.

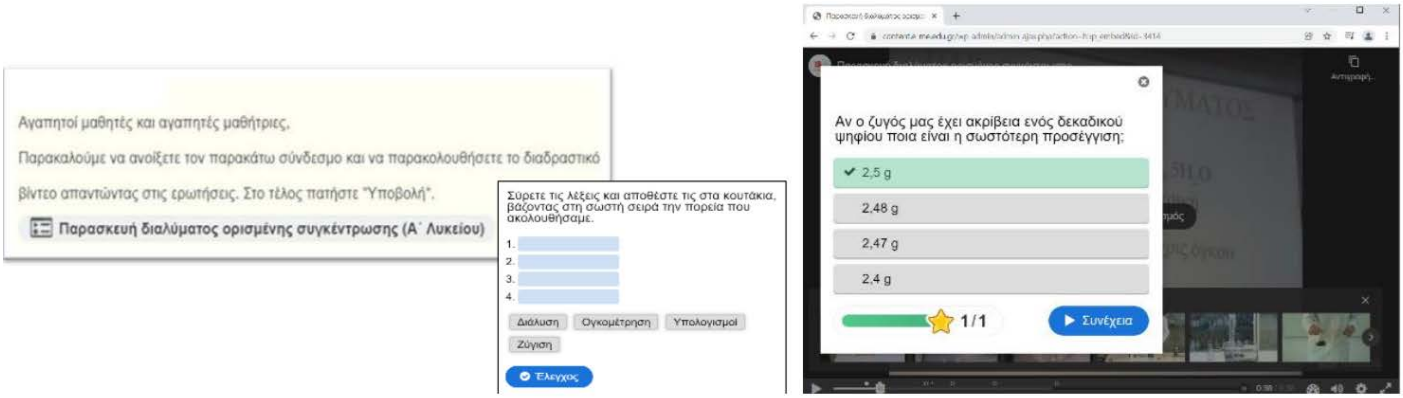

***Figure 4:** Attachment from the material distributed to students before class[24]*

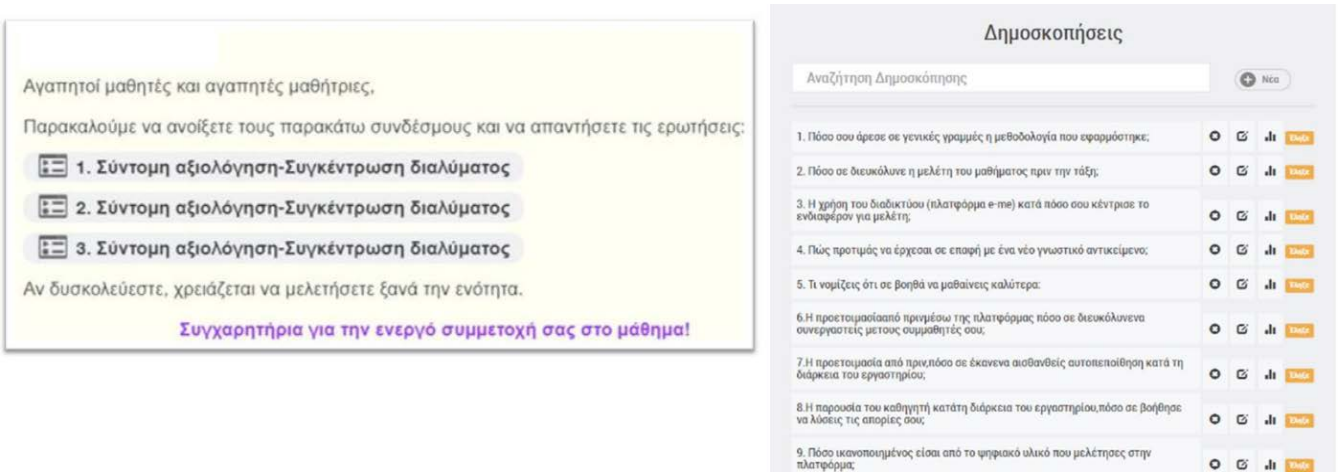

***Figure 5**: Attachment from the material distributed to students after class*

Firstly, the administrator explains the purpose of the educational material and asks from the students to view carefully the provided video and answer questions concerning the experiment like the one on figure 1 and translated below:
"If the scale has an accuracy of one decimal place, which of the following options is the most correct based on the video you watched"
During Class: Students work in groups to perform the experiment suggested in their laboratory guide under the guidance and supervision of the educator. In this case, the experiment titled "Preparation of a Solution of Defined Concentration" was implemented. The students worked more autonomously, with ample time, solving questions, remaining alert, and confident about what they were doing. They had time to discuss alternative ideas on how to conduct the experiment differently. They had time to improvise with successive dilutions, while the educator had the opportunity to delve deeper into the concepts of dilution and mixing solutions of the same substance.
After Class: The third part is digital, adapted for distance learning and includes a survey for evaluating the learning process and self-assessment activities. For the specific paper a screenshot of the procedure is being presented on figure 5.

More specific the administrator asks the students to open the provided links and complete the questions on a scale from 1 (Not at all) to 4 (Very much).
A few of the questions are been translated below:
"1. How much did you like the methodology that was followed?
6.How much did the prior preparation through the platform help you collaborate with your classmates?
9. How satisfied are you with the digital material you studied on the platform?"

Example for 11th grade students

Conceptual Area: Catalytic converters
Learning Management System: "e- platform"[28]
Number of participated students: Eighteen (18)
Teaching Procedure:
Before Class: Students, before the lesson, either from home or in the school computer lab (in-class flip scenario), log in with their personal codes to the digital classroom of the e-platform, where specific material and a video from the internet titled "How does a catalyst work?" are posted. They then complete the questions on the provided worksheet and submit their answers. For the specific paper a screenshot of the procedure is being presented on figure 6.

***Figure 6**: Attachment from the material distributed to students before class[25]*

Catalytic Converters
Part 1

A. Try to answer the following questions:

1. Which of the gases emitted by cars are toxic?

   .....
   .....
   .....

2. Where is the car's catalytic converter located?

   .....

3. Inside the catalytic converter, there is a porous material divided into two blocks. In the first one, there are the chemical elements ..... and ..... while in the second one ..... and .....

***Figure 7**: Attachment from the material distributed to students before class*[25]

Firstly, the administrator explains the purpose of the educational material and asks from the students to view carefully the provided video on figure 3. A part of the provided paragraph is being translated below:
"The aim is not to be evaluated, but to understand the use of a catalytic converter in cars"
Then students answer questions concerning the experiment like the one translated below (from the original Greek version) on figure 7.

In-Class: The second part takes place in the classroom and involves printed material supporting active student participation within the class structure and efficient use of teaching time according to the Chemistry II High School teaching guidelines for the school year 2022-23[29].

After Class: The third part is also digital, adapted for distance learning and includes practice and self-assessment activities, where students are informed of the results of the learning process. The teacher supports students precisely where they face difficulties, shifting their role from traditional lecturing to guiding, supporting, and personalizing. For the specific paper a screenshot of the procedure is being presented on figure 8.

More specific the administrator provides to students a digital working sheet showed on figure 5 (left side) for having feedback concerning the knowledge that students gained for the specific conceptual area and then asks the students to open the provided link and complete the survey on a scale from 1 (Not at all) to 4 (Very much).

A few of the questions showed on figure 5 (right side) are been translated below:
"1. How much did you like the methodology that was followed?
6.How much did the prior preparation through the platform help you collaborate with your classmates?
9. How satisfied are you with the digital material you studied on the platform?"

Example for 12th grade students
Conceptual Area: Acid-Base Titration (Acidimetry-Alkalimetry)
Learning Management System: e-platform – LAMS AI
It's a user-friendly and visually appealing environment for designing, managing delivery, and executing sequences of learning activities, essentially an electronic teaching and learning environment. The new generation of LAMS systems utilizes artificial intelligence and is called LAMS AI[26] (similarly to CHAT GpT).
Number of participated students: Fourteen (14)
Teaching Procedure:
Following the diagram below (figure 9) the lams proce-

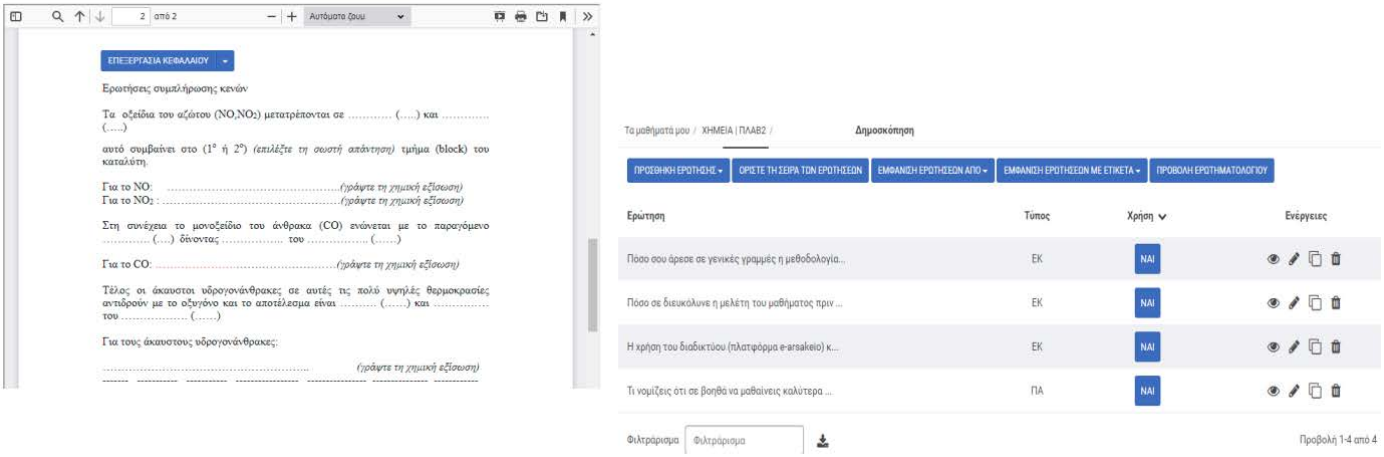

***Figure 8**: Attachment from the material distributed to students after class*

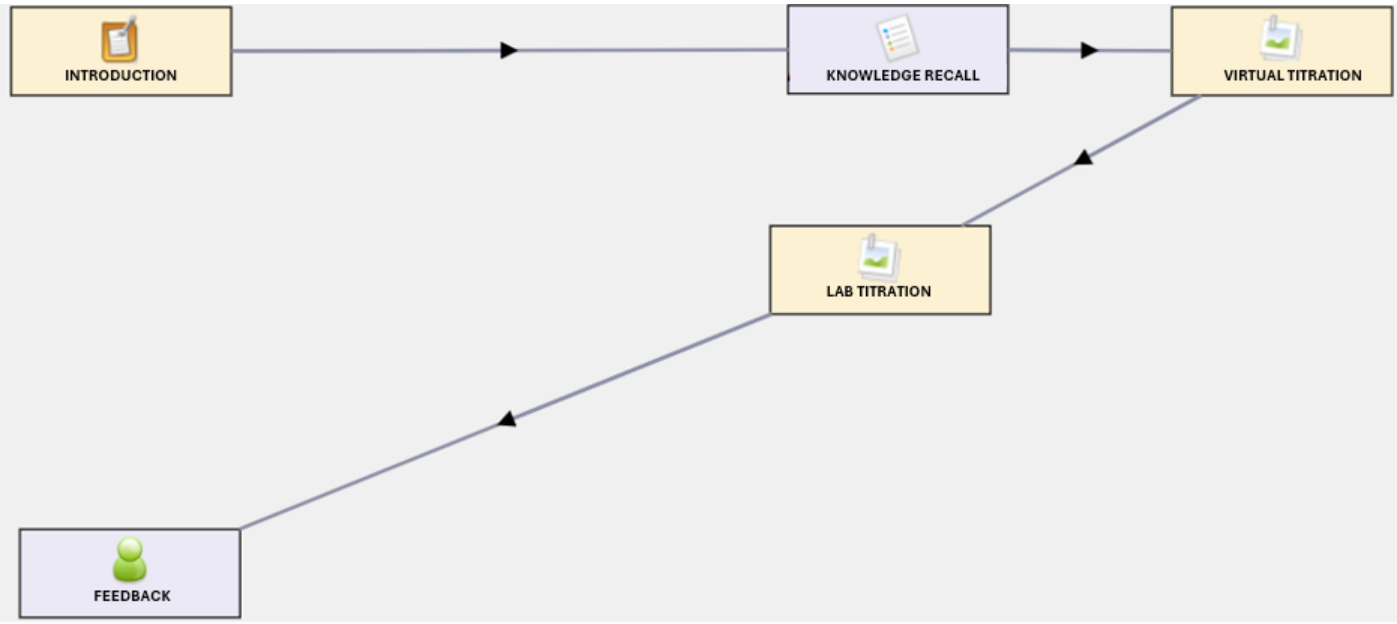

***Figure 9**: LAMS Diagram of Titration*

dure is been presented as a graph. Then the full procedure is been described.

Before Class: Students, prior to conducting the laboratory exercise, either from home or in the school computer lab (in-class flip scenario), log in with their codes to the digital classroom of the e-platform, where specific material and a video from the internet titled "Determination of the acetic acid content in vinegar" are posted (Alkalimetry). They then complete the questions on the provided worksheet and submit their answers (see figure 10 below).

In-Class: The second part takes place in the laboratory and involves determining the %w/w concentration of sodium hydroxide from a standard hydrochloric acid solution (Acidimetry). The teacher supports students precisely where they face difficulties. The teacher's role shifts from traditional lecturing to guiding, supporting, and personalizing (see figure 11 below).

***Figure 10:** In class flip scenario for 11th or 12th grade students*

After Class: The third part is also digital, adapted for in-class study, and includes practice and self-assessment activities, where students are informed of the results of the learning process.

Discussion and conclusions

From the analysis of the questionnaires for the assessment of the entire process, it was found that there are advantages as well as disadvantages mentioned in the sentences below:

Among the advantages of the method, standout are better time management and greater acceptance and engagement of students during the implementation of the laboratory exercise within the classroom. The teacher supports students precisely where they face difficulty (Teacher's role shifts from traditional lecturing to guidance, support, and personalization) Students are encouraged to invest their study time from their own space, at their desired pace and rhythm, autonomously, away from the classroom to some extent achieving lower levels of knowledge and understanding on their own.

There are also points highlight significant aspects of the digital learning landscape. Unequal access to technology underscores disparities in educational opportunities, potentially widening the gap between students with and without access to digital resources. Increased study time at home reflects a shift in learning dynamics, where students are expected to engage more independently outside traditional classroom settings. Similarly, educators

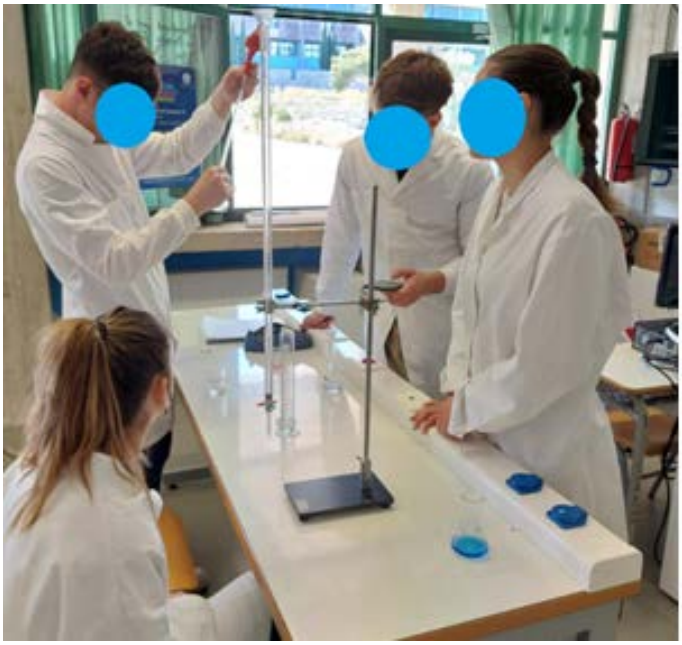
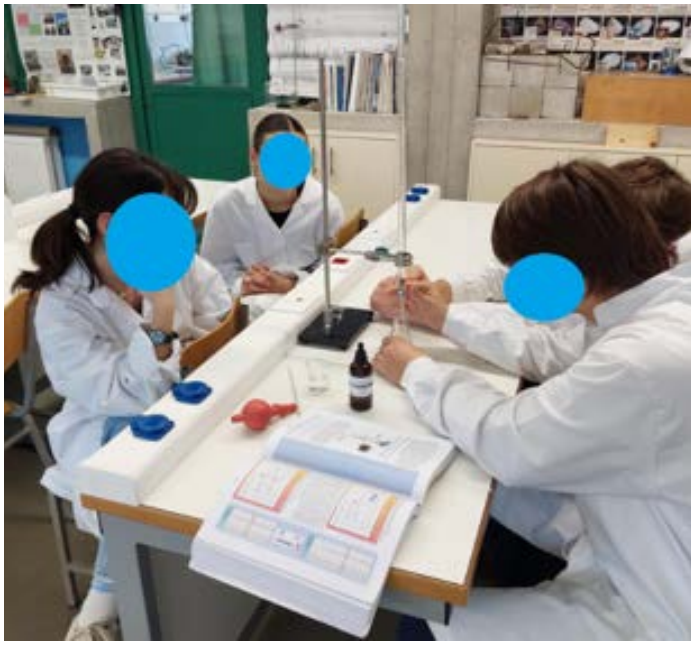

***Figure 11**: In class laboratory scenario for 12th grade students*

face the challenge of allocating additional time to prepare digital materials, adapting teaching strategies to online platforms. Ensuring the quality and reliability of digital materials becomes paramount, as their effectiveness directly influences the learning experience. Addressing these concerns is crucial for fostering equitable access to education and optimizing digital learning environments for all students.

Suggestions for future research

After recording the educational material and teaching interventions of this study, the suggestions for conducting future research in the specific conceptual areas follow:

a) The learning outcomes of this teaching intervention should be contrasted with the learning outcomes of a teaching intervention based on the instructional material of the school textbook that is used in all Greek middle schools.

b) In order to investigate whether the learning outcomes remain unchanged over time, it is proposed to implement a research study using the same teaching material and assessing the learning outcomes not only before and immediately after the teaching intervention, but also several months afterwards.

c) Carry out the same research on a larger sample of students of similar age and in General High Schools from different regions of Greece, to explore whether the learning outcomes can be generalized.

Acknowledgements

Many thanks to the Principals of Arsakeio Schools of Patras, Mr. Emmanouil Petrakis (Coordinator of Physical Sciences of the **Society for Promoting Education and Learning) and** Mr. Dimitrios Vlachodimitropoulos for granting permission to implement the particular teaching model at the school. Also, many thanks to Mr. Spyros Papadakis (Coordinator of Educational Informatics) and Mrs. Angeliki Gariou (Coordinator of Educational Activities in Physical Sciences) based at the Regional Directorate of Education of Achaia for their support and guidance.

References

1. Kiriazis, A. & Bakoyiannis, S. (2003). New Technologies in Education. Coexistence of Teaching Practice and Technology, Athens: Self edition, [In Greek].
2. Mascolo, M. F. (2009). Beyond student-centered and teacher-centered pedagogy: Teaching and learning as guided participation. Pedagogy and the human sciences, 1(1), 3-27.
3.Acedo, M. (2013) 10 Pros And Cons Of A Flipped Classroom. Link: http://www.teachthought.com/trends/10pros-consflippedclassroom, Accessed [15th June 2024], [In Greek].
4.Young, A. H., Gallagher, P., & Porter, R. J. (2002). Elevation of the cortisol-dehydroepiandrosterone ratio in drug-free depressed patients. *American Journal of Psychiatry*, *159*(7), 1237-1239.
5. McMahon, M., & Pospisil, R. (2005). Laptops for a digital lifestyle: Millennial students and wireless mobile technologies. *Proceedings of the Australasian Society for Computers in Learning in Tertiary Education*, *2*, 421-431.

6. Roehl, A., Reddy, S. L., & Shannon, G. J. (2013). The flipped classroom: An opportunity to engage millennial students through active learning strategies. *Journal of Family and Consumer Sciences*, *105*(2), 44.
7. Driver, R., Asoko, H., Leach, J., Scott, P., & Mortimer, E. (1994). Constructing scientific knowledge in the classroom. *Educational researcher*, *23*(7), 5-12.
8. King, A. (1993). From sage on the stage to guide on the side. *College teaching*, *41*(1), 30-35.
9. Gilboy, M. B., Heinerichs, S., & Pazzaglia, G. (2015). Enhancing student engagement using the flipped classroom. *Journal of nutrition education and behavior*, *47*(1), 109-114.
10. Bergmann, J., & Sams, A. (2012). *Flip your classroom: Reach every student in every class every day*. International society for technology in education.
11. Tucker, B. (2012). The flipped classroom: Online instruction at home frees class time for learning. *Education next*, *12*(1), 82-84.
12,22. Gariou, A. (2015). Investigation of the application of the "flipped classroom" model as a supplementary method of distance education in secondary education - Action Research. Diploma thesis, HOU. [Online] Available at: https://apothesis.eap.gr/handle/repo/29904, Accessed [15th June 2024], [In Greek].
13. Gariou, A., Makrodimos, N., Papadakis, S. (2021). Flipped Classroom: A blended learning model for all levels of education. Patras 2021, Gotsis. [Online] Available at: http://www.gotsis.net.gr/book.php?id=60dce8cf3a5d2 , Accessed [15th June 2024], [In Greek].
14. Pange, J. (2022). Online Student-to-Student Interaction: Is It Feasible? In *Innovations in Learning and Technology for the Workplace and Higher Education: Proceedings of 'The Learning Ideas Conference'2021* (pp. 250-256). Springer International Publishing. [In Greek]
15,18,19. Bishop, J., & Verleger, M. A. (2013, June). The flipped classroom: A survey of the research. In *2013 ASEE annual conference & exposition* (pp. 23-1200).
16, 23. Makrodimos, N., Papadakis, S., & Koutsouba, M. "Flipped classroom" in primary schools: a Greek case «Α α η η» η ό η ό ί, [In Greek].
17. Abeysekera, L., & Dawson, P. (2015). Motivation and cognitive load in the flipped classroom: definition, rationale and a call for research. *Higher education research & development*, *34*(1), 1-14.
20,21. Gilboy, M. B., Heinerichs, S., & Pazzaglia, G. (2015). Enhancing student engagement using the flipped classroom. *Journal of nutrition education and behavior*, *47*(1), 109-114.
24. Giannakopoulos, N., Gariou, A. (2019). Production and evaluation of educational material for "Solution Concentration" using the e-me platform of the Digital School. [Online] Available at: https://www.researchgate.net/publication/332781941_Paragoge_kai_axiologese_ekpaideutikou_ylikou_gia_te_Synkentrose_dialymatos_me_axiopoiese_tes_platphormas_e-me_tou_Psephiakou_scholeiou , Accessed [15th June, 2024]. [In Greek]
25. PEKES Western Greece. (2022). Scientific Symposium on Flipped Classroom. [Online] Available at: https://blogs.sch.gr/pekesde/archives/2683#prettyPhoto Accessed [15th June, 2024], [In Greek].
26. Papadakis, S. (2022). Webinar Innovation in Education: "Flipped Classroom" [Online] Available at: https://blogs.sch.gr/pekesde/archives/3280, Accessed [15th June, 2024].
27. e-me User Manual: https://e-me.edu.gr/s/eme/main/manual.html#e-me-hives Accessed [15th June, 2024], [In Greek].
28. e-arsakeio User Manual: https://www.e-arsakeio.gr/start [Online] Available at: http://events.di.ionio.gr/cie/imaes/documents21/CIE2021_OnLineProceedings/31CIE2021_Lampo_Final_P%20361-376.pdf, Accessed [15th June, 2024], [In Greek].
29. Chemistry teaching instructions for second grade of General High School for the school year 2023-24 https://iep.edu.gr/el/graf-b-yliko-2023-2024/geniko-lykeio-2023-2024 , Accessed [16th June, 2024], [In Greek].
30. Strayer, J. F. (2007). The effect of the classroom flip on the learning environment: A comparison of learning activity in a traditional classroom and a flip classroom that used an intelligent tutoring system. Ph.D. Thesis, Columbus, OH: Ohio State University.
31. Hsu, Ting. (2017). Behavioral sequential analysis of using an instant response application to enhance peer interactions in a flipped classroom. Interactive Learning Environments. 26. 1-15. 10.1080/10494820.2017.1283332.

Colorimetric analysis in Secondary Education, a simulation with portable electronic devices and food coloring substances.

P. Kotsikis
Secondary Education Teacher / Chemist, Msc
pKotsikis@sch.gr

2o General Lyceum Salamina (Greece)

DOI: 10.62579/JAGC0008

Abstract
Due to the widespread availability of smartphones with strong cameras and decent computing power, teachers are able to create innovative, experimental lesson plans. This study's primary goal was to use digital technologies, such cellphones, to the scientific process of colorimetry in chemistry and the Beer-Lambert law. Students made solutions using candy colors in varying quantities for this lab practice. They recorded the Hue (H) value on a white background using a cell phone that has software installed to measure color using the HSV model. They plotted the H color parameter against the quantity of droplets per 100 milliliters using these values. The outcome was a straight line, which effectively validated the method's underlying premise that is, the Beer-Lambert law. The solution used for the most recent measurement had an unknown concentration. The groups were able to accurately calculate the concentration of the unknown solution by using the reference curve they had generated. Students produced solutions, measured particulars, used software and smartphones as scientific instruments, made graphs, evaluated data, and came to scientific findings during this lab exercise.
Keywords: Smartphones, Colorimetry, School chemistry.

INTRODUCTION

People now use cellphones for a variety of purposes in their daily lives, making them omnipresent in society in recent years. Smartphones, however, have a great deal of potential as scientific instruments in addition to being communication and entertainment devices, especially in educational settings like schools. With its many capabilities, including internet access, high-resolution cameras, and a plethora of applications, smartphones may be extremely helpful tools for educators and students alike. They can help with data collection, analysis, and research for science. They can also improve critical thinking and increase scientific knowledge. One way to characterize smartphones is as versatile gadgets with the potential to completely transform scientific research and teaching. They can even be used for strictly scientific objectives, such taking pictures of bacterial colonies in a Petri dish or tracking changes in the temperature, using specific apps for virtual reality or educational activities in schools [1,2]. Research indicates that cellphones can function as dependable measuring devices, creating new avenues for data collecting and scientific investigation [3].There are opportunities for the quick and low-cost development of qualitative and quantitative methods due to the popularity and mobility of smartphones, the use of digital pictures, and the development of smartphone applications. Furthermore, a growing number of businesses, individuals, and governments are using digital picture colorimetry for various analytical processes, measurements, processing, and online result sharing [4].

1 METHODOLOGY

The goal of the experimental process outlined in this paper is to help students understand how a colored solution's color and concentration relate to one another and how this relationship can be used to determine the concentration of a solution containing the same substance but with an unknown concentration. In addition, it provides an introduction to the scientific method used in many analytical chemistry techniques and enables students to identify a legitimate scientific application for their mobile devices through the use of basic materials to measure things that appear to match actual chemical issues encountered in chemical analysis. The three elements that affect how an object appears to be colored are the type of lighting, the object's visual characteristics, and the eye's reaction. Either straight from the light source or after being reflected or absorbed by an object, light can enter the eye. The observer's

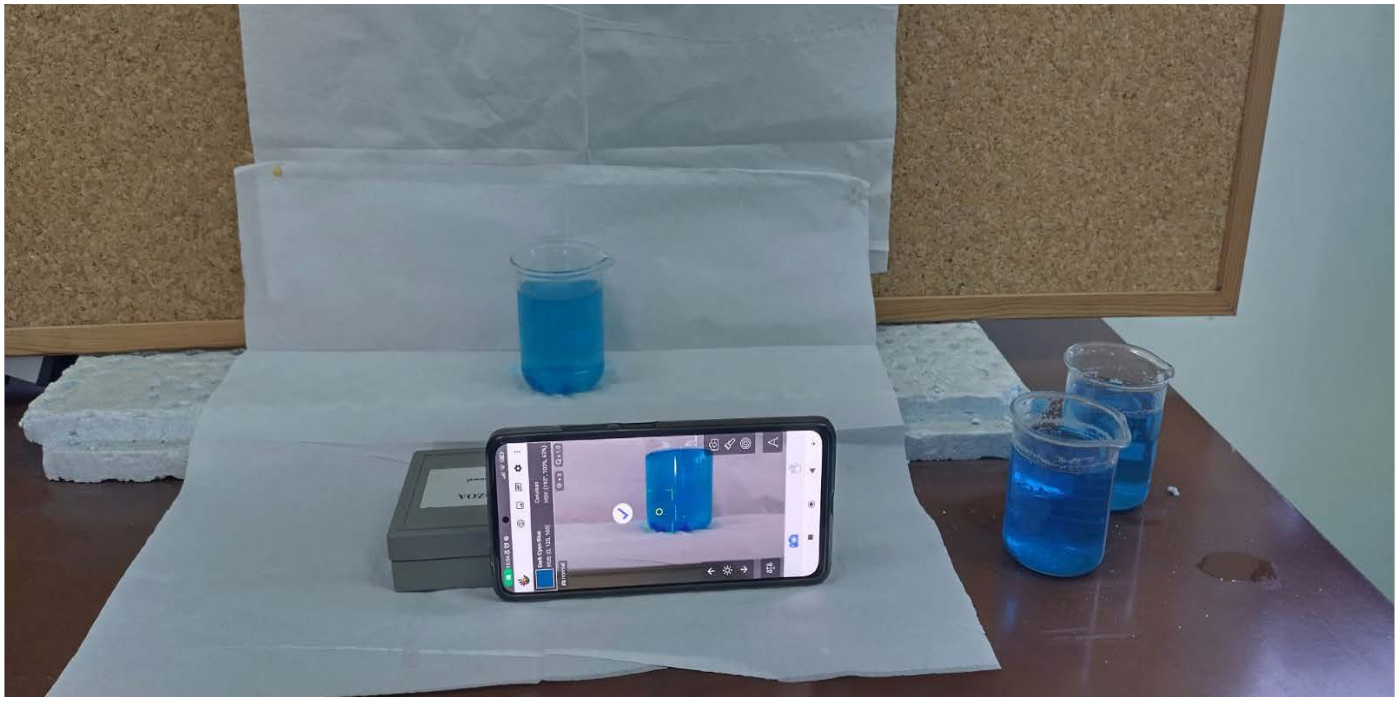

Figure 1. *Measuring the parameter H with Color Grab app for android.*

eye is exposed to this altered light, which evokes the sense of the material's hue. As a result, perception of color is subjective, and the observer must be considered [5].

Three variables can be used to fully characterize a color: i) hue, which is the color as it is perceived (e.g., red); ii) lightness, which is the color's brightness or darkness (e.g., bright or dark red); and iii) saturation, which is the color's intensity in relation to its associated spectral color (e.g., vivid or intense red) [6]. Color models like RGB, XYZ, L*A*B*, and L*C*H are frequently employed in order to precisely identify colors and quantify these parameters [5].

In colorimetric assays, a colorimeter (spectrophotometer) is used to measure a chemical compound's spectral absorbance at a certain wavelength in order to calculate the compound's concentration in a solution. A color is produced when the target substance and detecting chemical interact. Using a spectrophotometer to measure the color intensity, one can estimate the amount of the desired component. Colorimeters are low-cost, basic instruments that function by utilizing a range of filters. They work well in scenarios when a rapid estimate is wanted but high precision is not necessary. Colorimetric tests are quick, simple, and affordable, but they are not highly sensitive, and the pH and temperature of a solution can easily affect them [7].

The basis of quantitative spectroscopy is the Beer-Lambert equation, which states that the amount of radiation absorbed by a sample constituent, A (absorbance) ,is precisely proportional to the product of its molar absorptivity (e),route length (b), and concentration (c) for a homogeneous, non-scattering liquid sample. A = e*b*c is the formula for the Beer-Lambert law, where b for solution thickness [6].

In the context of optical sensors, the hue, or H component of the hue, saturation, and value (HSV) color space, has been investigated as a quantitative analytical parameter. Numerous variables, such as the sample concentration, the detector's spectral sensitivity, and the lighting, affect the accuracy of the H value. Studies that compare this metric to RGB absorption intensity and red, green, and blue (RGB) intensity have demonstrated its superiority. It can be used in commercial products like digital cameras and scanners because of its reliability and simplicity of computation. Moreover, it has enormous potential for a variety of uses, such as quality control, automated analysis, pharmaceutical analysis, imaging, and Lab-on-a-chip devices [8].

For paper-based applications, colorimetry, which makes use of picture resolution and RGB or HSV data is frequently employed in optical detectors and other complex devices [9]. The effects of chemical concentrations, such as ochratoxin A in beverage samples, have been studied using the color model HSV [10]. The absorbance of varying concentrations of the same solution is measured at the same wavelength in colorimetry in order to determine the concentration of a solution. The absorption of each solution at each known concentration is then graphically represented by a reference curve that is created using this data. By comparing the absorption of an unknown sam-

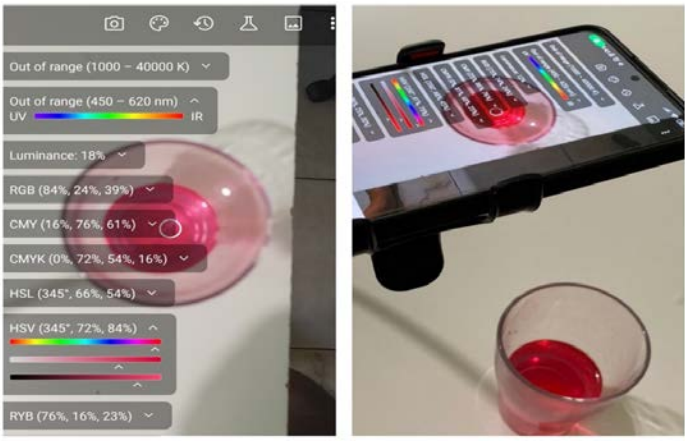

Figure 2 . *Vertical measurement with Color Picker app for android.*

ple to the reference curve, this method can be used to determine the sample's concentration [11]. The process of creating a reference curve will also take place in the school laboratory's experimental area, but absorption will be measured in place of another variable. The significance of improving pupils' problem-solving skills has increased in the modern era. Because they essentially practice with a simple methodology in the scientific method, students' problem-solving abilities in scientific fields depend not only on their ability to recall and apply the pertinent details of their subject and domain-specific knowledge, but also on their analytical thinking abilities [12]. This paper aims to address these issues.

In the school laboratory, the pupils are first split up into groups of four to five individuals. Phase I involves projector-slide presentations on how color is viewed by humans and how transparent solutions, like $KMnO_4$ or $CuSO_4$, seem colored in a lab setting. Phase II describes the hue, saturation, and value (HSV) color model parameters because the subsequent experiment will use a smartphone to measure parameter H. A webpage called CSS HSL Colors (https://www.w3schools.com/css/css_colors_hsl.asp) is also provided, where students can manipulate values in the H variable to observe changes in color and intensity [13].

Phase III involves the graphic presentation of a colorimeter in conjunction with an online movie (https://youtu.be/yTabfxvMdCM?si=EiSv4yxkKOnUV7LY) that provides a basic explanation of the analytical method's principle. Every group in the fully experimental Phase IV receives a distinct color of food coloring. The hues that are readily available are blue, red, and yellow, all of which are accessible from any grocery. Using a volumetric cylinder, they transfer 100 milliliters of water into three transparent plastic cups. Next, they add one, two, and four drops of the specified dye, respectively. When building the calibration curve, these solutions will be used as the reference solutions to be measured.

A whiteboard is supported on a bench that has been installed at a certain location in the lab. The solution to be measured is put in front of and slightly away from the white background. In addition, the program is used to measure the desired variable by placing the mobile phone in front of the sample [14] (Fig.1).

An alternative would be to use a stationary arm to hold the mobile device vertically while the sample to be examined was positioned directly below the camera at a location determined by the application's focus point (Fig 2).

A color detection program that measures colors using the HSV model is loaded on each group member's smartphone. Smartphones running iOS and Android have a wide variety of applications available. An online converter (such as https://colordesigner.io/convert/hextohsv) can be used to convert HEX color values used by the mobile application to HSV values. Of course, an iPad or tablet can also be used to take the measurements.

2 RESULTS

Each solution is positioned in relation to the smartphone camera at a fixed, modest distance, and the phone marks the same spot for each measurement. The mobile phone might be secured by the steady arm, guaranteeing the reference point's stability. Following sample placement, the attention is moved to a specific location inside the solution, and the parameter H value is measured using the mobile application. The results are then recorded in a computer program called Numbers (macOS) or a comparable spreadsheet program (like Excel) in order to generate a graphical depiction of the data and build the reference curves (Fig. 3, 4, 5). The values are functions of the droplet per 100ml of solution.

2 .1 The measurements of Hue (H)

2.1.1 The measurements of the blue dye

Measurements of the value H for three solutions with varying concentrations in drops of blue dye are displayed in the table (Table 1) below. A reference curve (Fig.3) is created using these data.

Table 1. Measurements - Blue coloring drops / 100 ml - Hue(H)

drops/ 100mL	*Hue(H)*
One	196
Two	199
Four	208

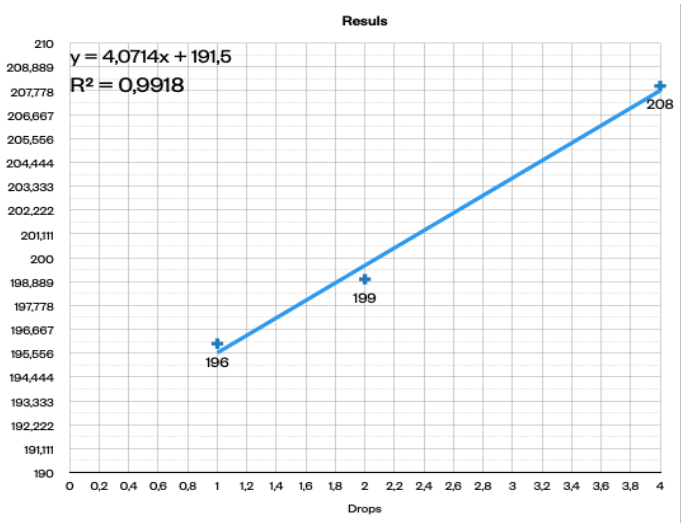

Figure 3. *Reference Curve of Blue coloring*

2.1.1 The measurements of the Red Dye

Below in the table (Table 2) , measurements of the value H are shown for three solutions of different concentrations in drops of blue dye. Using these values, a reference curve (Fig.4) is constructed.

Table 2. Measurements - Red coloring drops / 100 ml - H

drops/ 100mL	*Hue(H)*
One	355
Two	356
Four	358

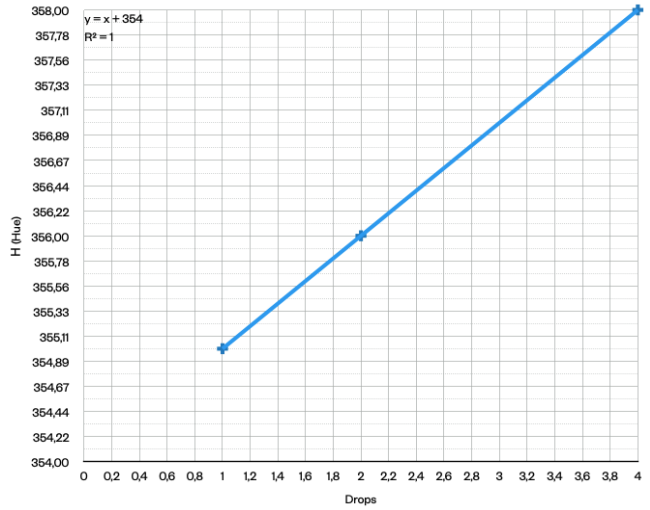

Figure 4.*Reference Curve of Red coloring.*

2.1.3 The measurements of the Yellow Dye

Below in the table (Table 3) , measurements of the value H are shown for three solutions of different concentrations in drops of blue dye. Using these values, a reference curve (Fig.5) is constructed.

Table 3. Measurements - yellow food dye drops / 100 ml - H

drops/ 100mL	*Hue(H)*
One	56
Two	55
Four	53

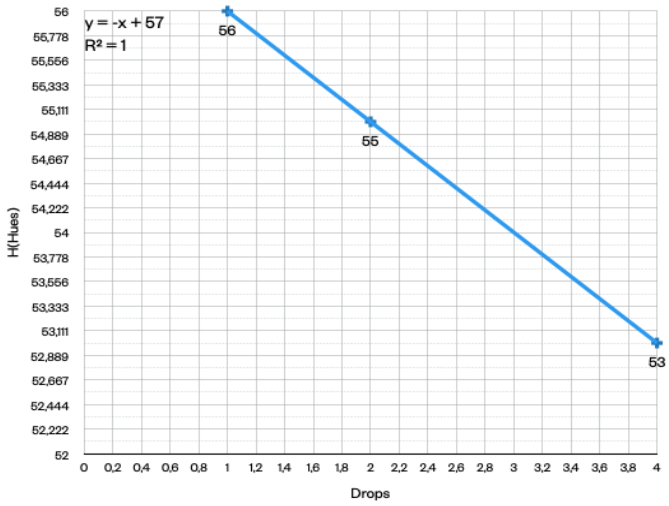

Figure5. *Reference Curve of Yellow coloring.*

2.2 Presentation of the results

The graphical representations that each group produces are showcased during the class assembly. The way the results are presented makes it very plain that the dye concentration in drops with different color shades is linear. These findings are consistent with the link between concentration and colored solution absorption provided by the Beer-Lambert equation. For the yellow dye, there is a discernible variation in the gradient, though (Fig. 5). The analysis of the color model will reveal the solution. Students consult the website [7], where they can alter the values for the yellow dye and see that our eyes' ability to perceive color declines as the dye's H value rises.

2.3 The "unknown" concentration

Each group receives a solution with an undetermined dye concentration in terms of the quantity of drops during the final stage. This solution had three drops per 100 milliliter for every dye. Students' goal is to determine how many drops are in the unknown sample by utilizing the reference curve they have developed. For instance, a group studying the blue dye discovered that the unknown sample had a value of 212. By using the straight line equation, it can be ascertained that the sample had 3.2 drops in it. Considering that the dyes are added with a dropper that isn't very precise, the accuracy of the determination is fairly high, but it mostly aligns with the experiment's objectives,

which were to demonstrate the connection between the solution's color and concentration and the practical application of analytical methods to real-world chemical problems like determining a solution's concentration.

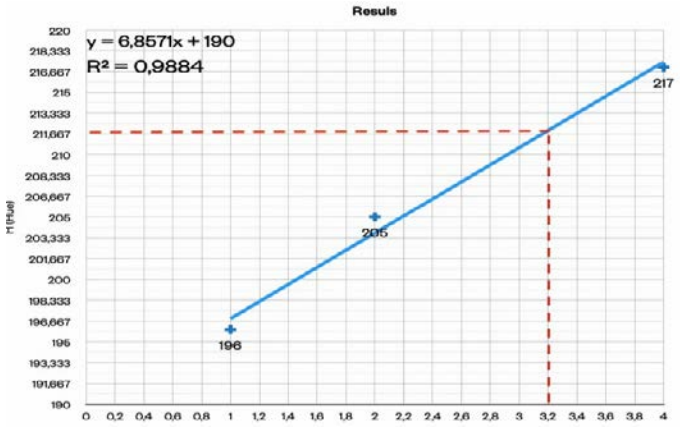

***Figure 6**. The value H (212) for the unknown sample is determined from the reference curve and corresponds to 3.2 drops /100mL .*

3 DISCUSSION

Wanting to compare the linearity provided by measurements using the paremeter Hue of the HSV model, measurements were made in the final stage of the study using the RGB model, measuring a different parameter each time (Red - Green - Blue). The measurements were made with the same software, in solutions with different amounts of Red dye (Figure 7) and Bue dye (Figure 8), and the graphical representations were made on the same diagram. From the calculation of R^2, it is evident that parameter H provides better results .

4 CONCLUSIONS

Students learn about the scientific methods of inorganic chemical analysis, including colorimetry, through the aforementioned process. The relationship between color intensity and solution concentration is ultimately ascertained by applying the scientific approach of chemical analysis with reference curves. This method's simplicity is important since it employs readily prepared solutions, making it possible to take a lot of measurements from various colored solutions. Naturally, the mobility that cellphones offer allows for flexibility in terms of where tests may be conducted. Lastly, students prepare solutions, take measurements and make graphical representations, draw conclusions, and solve chemical issues using smartphones as scientific tools. It is an experimental method that defies the clichés of classroom laboratory activities and sparks students' curiosity about chemistry as a subject that offers solutions to practical issues.

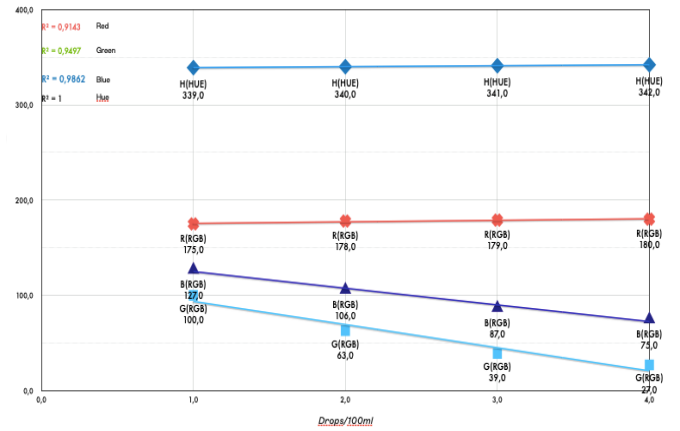

***Figure 7**: Measurements of different parameters with the number of Red dye drops per 100ml.*

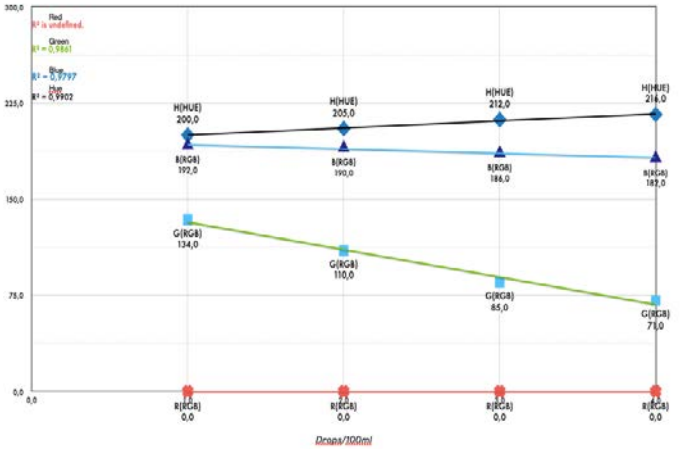

***Figure 8:** Measurements of different parameters with the number of Blue dye drops per 100ml.*

REFERENCES

[1] Odenwald, Sten. "Smartphone Sensors for Citizen Science Applications: Light and Sound." *Citizen Science: Theory and Practice*, vol. 5, July 2020, p. 13, https://doi.org/10.5334/cstp.254.

[2] "Smartphones in Science Teaching | Science on Stage Europe." Science on Stage Europe, www.Science-on-Stage.Eu/Smartphones. (Last accessed 30 Aug. 2023)

[3] González-Pérez, Alberto, et al. "Using mobile devices as scientific measurement instruments: Reliable android task scheduling." *Pervasive and Mobile Computing*, vol. 81, Apr. 2022, p. 101550, doi:10.1016/j.pmcj.2022.101550.

[4] Resende, Lívia Maria Braga, et al. "Optimization and validation of a smartphone-based method for the determination of total sterols in selected vegetable oils by digital image colorimetry." *Journal of Food Composition and Analysis*, vol. 117, Apr. 2023, p. 105111, doi:10.1016/j.jfca.2022.105111.

[5] Gilchrist, Alison, and Jim Nobbs. 'Colorimetry, Theory'. *Encyclopedia of Spectroscopy and Spectrometry*, Elsevier, 2017, pp. 328–333, https://doi.org10.1016/b978-0-12-803224-4.00124-2.
[6] Chandra, Shaneel, and Mani Naiker. 'Chapter Three - Applications of Infrared Spectroscopy in Environmental Contamination'. *" In Infrared Spectroscopy for Environmental Monitoring*, edited by Daniel T-Comprehensive Analytical Chemistry Cozzolino, vol. 98, Elsevier, 2022, pp. 77–90.
[7] Cooper, J. A., et al. '4 - Assays for Determining Cell Differentiation in Biomaterials'. *In Woodhead Publishing Series in Biomaterials*, Woodhead Publishing, 2013, pp. 101–137.
[8] Cantrell, K., et al. 'Use of the Hue Parameter of the Hue, Saturation, Value Color Space as a Quantitative Analytical Parameter for Bitonal Optical Sensors'. *Analytical Chemistry*, vol. 82, no. 2, American Chemical Society (ACS), Jan. 2010, pp. 531–542, https://doi.org10.1021/ac901753c.
[9] Soda, Yoshiki, and Eric Bakker. 'Quantification of Colorimetric Data for Paper-Based Analytical Devices'. *ACS Sensors*, vol. 4, no. 12, American Chemical Society (ACS), Dec. 2019, pp. 3093–3101, https://doi.org10.1021/acssensors.9b01802.
[10] Bueno, Diana, et al. 'Colorimetric Analysis of Ochratoxin A in Beverage Samples'. *Sensors (Basel, Switzerland)*, vol. 16, no. 11, Nov. 2016, https://doi.org10.3390/s16111888.
[11] "Standard Curve Generation for Colorimetric Assay in the Kinetic or Basic Eppendorf BioSpectrometer®".https://www.news-medical.net/whitepaper/20160218/Standard-Curve-Generation-for-Colorimetric-Assay-in-the-Kinetic-or-Basic-Eppendorf-BioSpectrometer.aspx.(Last accessed 7 June 2024)
[12] Sutherland, Louise. 'Developing Problem Solving Expertise: The Impact of Instruction in a Question Analysis Strategy'. *Learning and Instruction*, vol. 12, no. 2, Elsevier BV, Apr. 2002, pp. 155–187, https://doi.org10.1016/s0959-4752(01)00003-2
[13] "CSS HSL Colors." *CSS HSL Colors*, www.w3schools.com/css/css_colors_hsl.asp. (Last Accessed 30 Aug. 2023)
[14] 'Coloured Chemistry With Smartphones: Test the Beer-Lambert Law With Blue Copper Solution | Science on Stage Europe'. *Science on Stage Europe*. https://www.science-on-stage.eu/material/coloured-chemistry-with-smartphones (Last accessed 30 Aug. 2023)

Commercial industrial synthesis of Naproxen

Krokou Charalambia (email: chakrok@chem.ihu.gr),
Koutsoyianni Konstantina (email: kokotts@chem.ihu.gr),
Kotanidou Christina (email: chrkota@chem.ihu.gr),
Kalafatas Angelos (email: agkalaf@chem.ihu.gr)

DOI: 10.62579/JAGC0009

Summary
Naproxen, a derivative of α-aryl propionic acid, belongs to the class of Non-Steroidal Anti-Inflammatory Drugs NSAIDs and is commercially available under the name "Aleve". It is the first Non-Steroidal Anti-Inflammatory NSAID that was isolated in its pure form as the S enantiomer by the Pope -Peachy method. The synthetic processes that have taken place in the industry in recent years are the subject of extensive scientific research and analysis with the aim of improving them to find a more "green", efficient, economical and short process. In this context, a thorough historical review of naproxen is presented, focusing on its development from its commercial application in the early 1970s to its current position. Its synthesis began in 1970 by Syntex with beta-naphthol as a raw material and a production of 500 kg. It was also commercialized by Syntex in 1976. The present industrial synthesis took place in the period 1984-1993, with a yield of 90% using the Pope-Peachy method and a recovery of N-alkylglucamine in each cycle of 98%. A brief reference is made to the chemical structure of the molecule, its pharmacodynamic and pharmacokinetic profile as well as its mechanism of action in order to understand at a later stage the mechanism as well as the catalytic system of the predominant industrial synthesis of naproxen, highlighting the chemical reactions. Through a detailed flow chart, the exact synthesis process is presented, describing each step of the process in technical detail. Finally, statistical data on naproxen's patents and formulation publications are presented, highlighting its global influence and importance in the field of the pharmaceutical industry.

SUBJECT AREA: Industrial Synthesis of Naproxen

KEYWORDS: Naproxen, industrial synthesis, Pope-Peachy, Syntex, historical review, mechanism, catalysts, statistics

LIST OF FIGURES

CATALOG OF IMAGES

LIST OF TABLES

1. Introduction

The purpose of the paper is to present the predominant production process of naproxen on an industrial scale, but

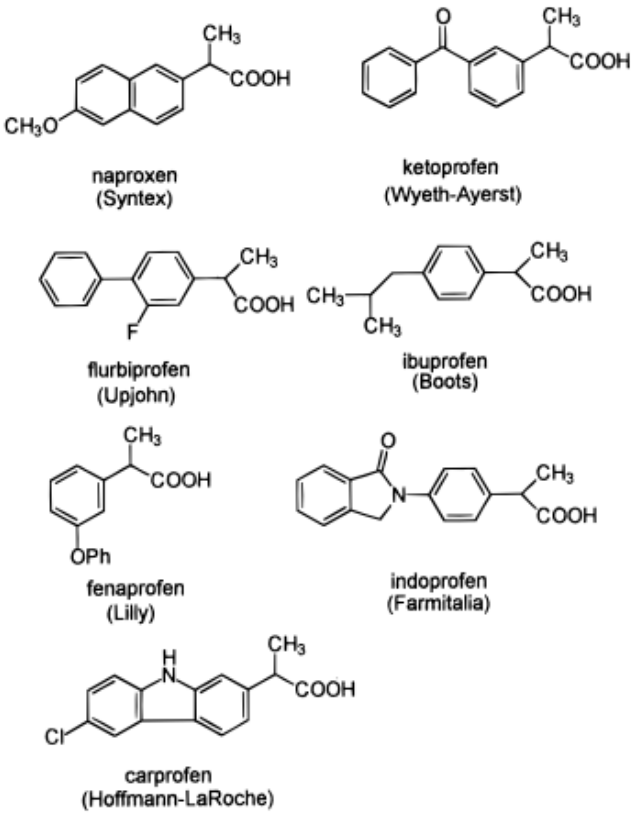

***Picture 1**. Non-Steroidal Anti-Inflammatory Drugs.*

also older methods of its synthesis by the pharmaceutical company, Syntex. Therefore, a brief historical review of naproxen is made from its first large-scale synthesis in 1970 to its second large-scale synthesis in the period 1976-1993.[3] Naproxen is marketed in its pure form, S enantiomer. Figure 1 (below) shows seven of the most well-known Non-Steroidal Anti-Inflammatory drugs, of which only naproxen is found in its pure form.[3]

The choice to study the composition of the particular drug lies in several reasons. Primarily, naproxen is an over-the-counter drug used to treat pain, inflammatory conditions such as rheumatoid arthritis, and fever. It is also available as a generic drug.[1-2] Studies have shown an increased demand for anti-inflammatory drugs, which makes improving the production formulation of naproxen especially important.[4]

At a later stage, continuous efforts to improve the production process of naproxen were identified in the literature which contributed to the improvement of efficiency, production costs but also to the minimization of catalysts or to finding more environmentally friendly catalysts.[3] In 1991, before the patent expired, (S)-naproxen was the fourth best-selling optically pure drug, based on Table 1 (below). Also on the list were the blockers enalapril (first),

pharmaceutical	sales ($ million)
enalapril	1745
captopril	1580
lovastatin	1090
naproxen	971
diltiazem	912
lisinopril	630
simvastatin	400

***Table 1**. World market for optically clear pharmaceuticals in 1991.[3]*

captopril (second) and lisinopril (sixth), the lipid-lowering drugs lovastatin or mevinolin (third) and simvastatin (seventh), and the calcium antagonist and vasodilator diltiazem (fifth) [3] .It becomes clear, therefore, that huge industrial interests derive from the composition of this particular drug.

The methodology of this work is mainly focused on gathering and analyzing existing information and data from the literature and other sources. In other words, the creation of an integrated theoretical framework related to the industrial synthesis of naproxen is sought. First, a historical review of Syntex's drug compositions is carried out with an emphasis on the dominant composition, then the chemical structure and characteristics of the molecule, its mechanism of action and its pharmacokinetic profile are examined. Emphasis is placed on the mechanism of the catalytic reaction but also on the characterization of the catalytic system. Then, a flow diagram of the specific chemical process is presented, but also information related to the industrial application of naproxen; producing countries, plant capacity, and its uses are listed. Finally, various related publications are presented regarding the use of naproxen around the world as well as patents for its composition.

1.1 Historical Review

The first large-scale synthesis of naproxen produced 500kg of material in 1970 by Syntex (Figure 1).[5] Friedel-Crafts acylation of 2-methoxynaphthalene gave 2-acetyl-6-methoxynaphthalene (MAN), which was converted to naphthylacetic acid by the Willgerodt reaction. A-methylation yields the d,l-acid, which can be efficiently resolved using cinchanonidine. This process had several undesirable characteristics. First, the Friedel-Crafts acylation was not regioselective, also producing the 1-isomer, which can be removed by crystallization. Second, aluminum hydroxide waste was produced in significant quantity and buried. Third, there were a number of unwanted reagents in the sequence: nitrobenzene (used in the acylation), ammonium sulfide (used in the Willgerodt reaction), sodium hydride, and methyl iodide.[3]

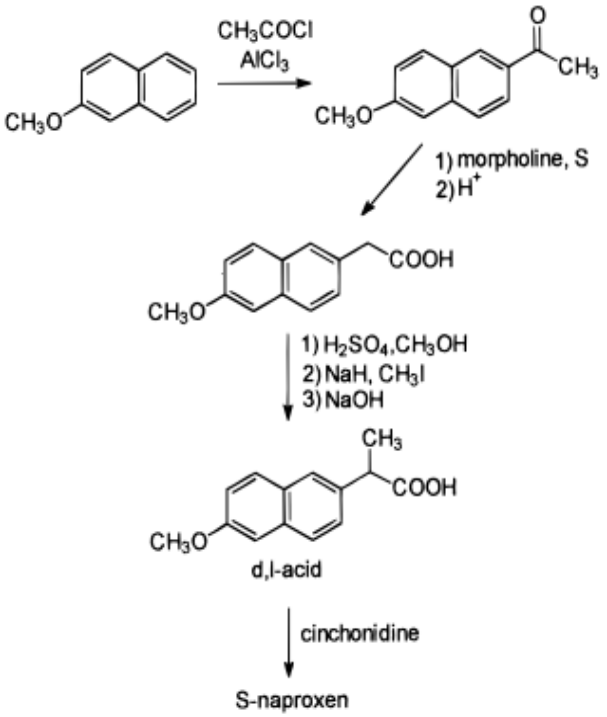

Figure 1. *First large-scale synthesis of naproxen (500 kg).[3]*

All of these issues were addressed and the first naproxen manufacturing process, implemented in 1972-1975, was dramatically different (Figure 2). Naphthol was brominated in methylene chloride to produce 1,6-dibromonaphthol. Bromine at position 1 was removed with bisulfite. The resulting 2-bromo-6-hydroxynaphthalene (BHN) was methylated with methyl chloride in water-2-propanol. The yield of 2-bromo-6-methoxynaphthalene (BMN) was 85-90% from β-naphthol. BMN was converted to a Grignard reagent, which was transmetallated with zinc chloride,

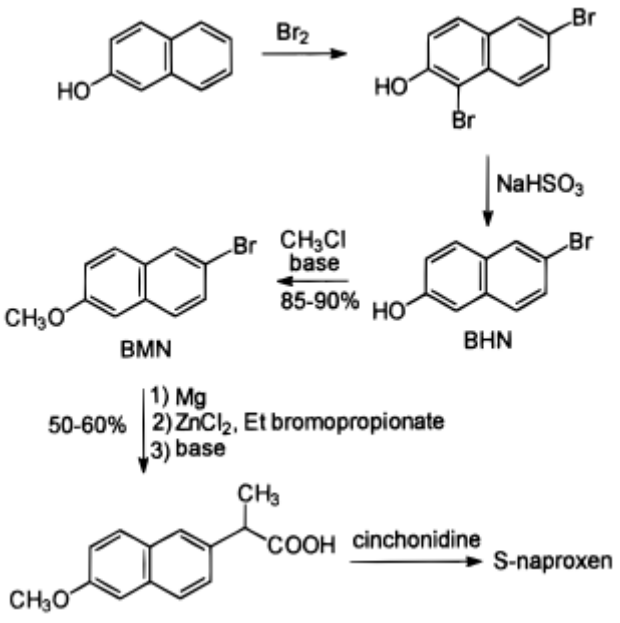

Figure 2. *First large-scale production process 1972-1975.[3]*

and then naphthylzinc was coupled with ethyl bromopropionate. Hydrolysis of the ester gave d,l-acid. The yield from BMN to d,l-acid was 50-60%. Again, the cinchonidine assay was effective (95%).[3]

But there were significant problems with this synthetic course as well. First, a stoichiometric amount of zinc chloride was required for the naphthyl-zinc coupling reaction. Large volumes of zinc hydroxide were filtered and landfilled. Second, the yield in the coupling reaction was low. Third, there were two undesired side products in the coupling reaction. The reduction produced 2-methoxynaphthalene, which is volatile and has a "sweet grape" odor - complaints from the local community were common. A radical coupling reaction produced a highly insoluble dinaphthyl "dimer". Unacceptably large quantities of dimer were landfilled with the zinc waste.[3]

The main problems of this first production process were related to the naphthyl-zinc coupling reaction. An alternative coupling to the second manufacturing process, implemented in 1976-1993, eliminated zinc waste and minimized the formation of nerolin and dimers (Figure 3, below). BMN was converted to a Grignard reagent, which was directly coupled to a bromopropionic acid salt. As might be expected, this coupling reaction produced d,l-acid as a component of a complex mixture. In fact, production yields in 1984 were less than 50%. A series of process improvements introduced over the last 10 years have increased efficiency to over 90%! Cinchonidine was replaced by an N-alkylglucamine. Again, the assay was efficient (>95%).[3] The Pope-Peachy method was applied to this industrial synthesis and a 98% recovery of N-alkylglucamine was achieved in each cycle. N-alkylglucamine, usually prepared by reductive amination of D-glucose, is both cheap and readily available.[6]

In 1988, staff at the Syntex Technology Center in Boulder were tasked with evaluating all naproxen synthesis technologies and then developed and implemented the lowest cost naproxen process. At that time, one-third of the total production cost of naproxen was related to the racemic acid, and two-thirds of the production cost (mainly labor) was related to the analysis-racemization. They concluded that reducing the cost of d,l-acid had little benefit. The real savings will come from a more refined resolution or asymmetric technology.[3]

As mentioned above, the pharmaceutical company Syntex dealt with the synthesis of naproxen. It is a company founded in Mexico City in January 1944 by Russell Marker, Emeric Somlo and Federico Lehmann with the aim of man-

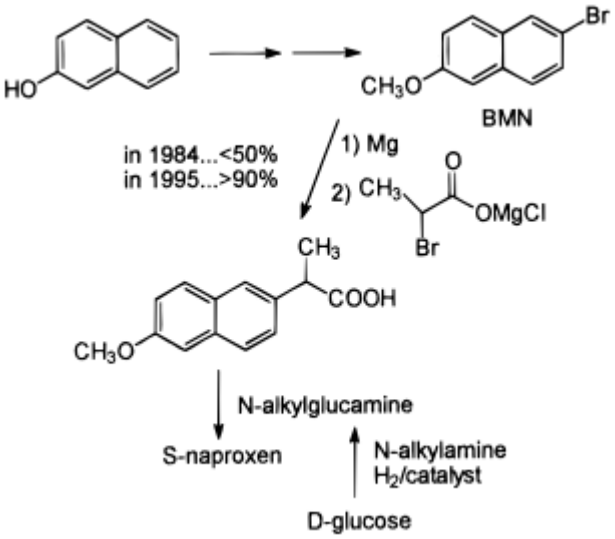

***Figure 3**. First large-scale production process 1976-1993.[3]*

ufacturing therapeutic steroid drugs.[7] In 1959, Syntex moved its headquarters to Palo Alto, California and grew into a multinational corporation. After 1959, Syntex was founded in Panama - management, research and marketing were conducted from Palo Alto - steroid production remained in Mexico - and also produced final drugs in factories in Puerto Rico and the Bahamas.[8] Syntex agreed to be acquired by the Roche Group in May 1994.[9]

George Rosenkranz: The "father" of naproxen

George Rosenkranz (1916-2019) was born in Budapest to middle-class Jewish parents. His childhood was marked by an appreciation for the arts, music, theater and education. Although he showed a talent for modern languages, he was particularly drawn to scientific studies, especially chemistry.[11]

In 1933 he left his family home to continue his studies at the Swiss Federal Institute of Technology in Zurich. There, he enrolled in an organic chemistry course taught by future Nobel laureate Lavoslav (Leopold) Ružička. Rosenkranz was deeply influenced by Ružička, who was involved in the synthesis of the male sex hormone testosterone. He sought to continue his studies under the guidance of Ružička. In 1937, Rosenkranz became a doctoral student of Ružička, receiving his degree in 1940. At that time, the Axis countries rose to power. Ružička protected Rosenkranz and his other Jewish colleagues from the Nazis in Zurich, but they decided to leave the city, not wanting to endanger their mentor.

Through connections, Rosenkranz secured a professorship in Ecuador. The plan was to travel to Cuba via Spain and then Ecuador. He made it all the way to Havana, but then the attack on Pearl Harbor caused a world panic and his transfer to Ecuador never took place. Stranded in Cuba, Rosenkranz made the best of the situation and began looking for work. He was hired by the company Vieta-Plasencia Laboratorios, where he developed successful treatments for venereal diseases.[11]

His years at Syntex

In 1945, Rosenkranz received an invitation to interview at a company called Syntex in Mexico City. Syntex was a synthetic hormone research company founded just a year earlier by chemist Russell Marker and two others.[10] They were trying to make synthetic hormones from diosgenin, a natural plant hormone found in wild Mexican sweet potatoes.[11]

Rosenkranz impressed the interviewers and was immediately offered the position of chief chemist. After a brief re-

Picture 2. *Dr George Rosenkranz at his home in Mexico.[13]*

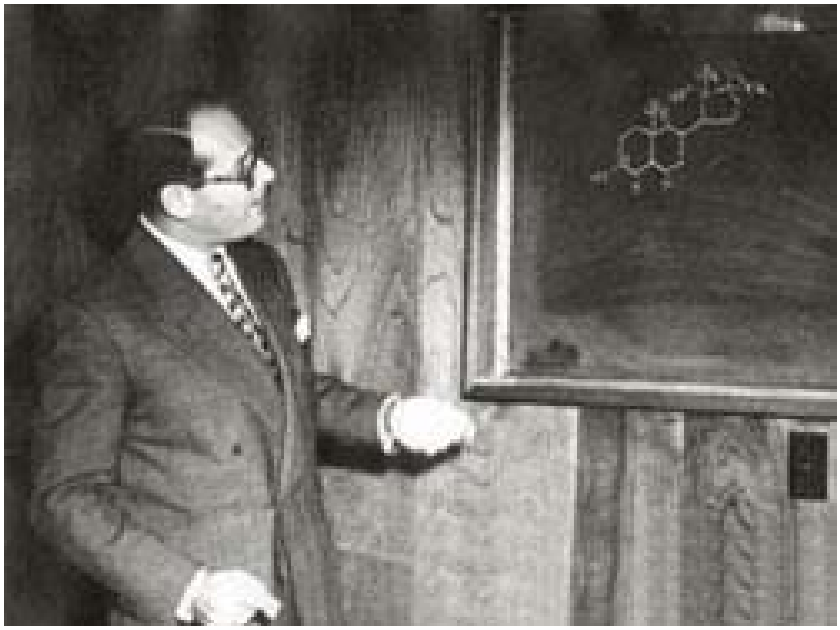

Picture 3. *Dr George Rosenkranz in 1950 draws the structure of a steroid drug.[14]*

Picture 4. *Dr George Rosenkranz and his research team at Syntex.[15]*

turn to Havana, Rosenkranz moved to Mexico to begin his tenure at Syntex. He remained with the company throughout his career, occupying the roles of chief executive officer and chairman of the board for a significant part of that period. Retired from Syntex in 1981.[11]

Rosenkranz was able to recruit leading organic chemists, including Carl Djerassi and Alejandro Zaffaroni. Their collaboration proved fruitful. During his career, Rosenkranz and his numerous colleagues developed and refined pioneering advances in the understanding and production techniques of steroid drugs, using native Mexican plant sources as raw materials.[11]

In 1951, Syntex synthesized the first effective oral contraceptive (norethindrone). During his tenure, the company expanded its operations to become the leading supplier of the oral contraceptive pill (commonly referred to as "the pill") and other corticosteroids, permanently changing social structures.

Having succeeded in the field of steroid research, Rosenkranz recognized the need to diversify the company's operations. He and a team of researchers began investigations into the potential of a nonsteroid anti-inflammatory drug for the systemic treatment of rheumatoid arthritis and osteoarthritis. The result of this research was the development of another drug, Naproxen. In the following years, the FDA granted approval for Naproxen for use in the treatment of a wide range of diseases, including osteoarthritis and juvenile arthritis. In 1980, naproxen sodium was introduced to the US market as Anaprox. By 1983, the two drugs had become the best-selling non-steroidal anti-inflammatory drugs in the world. Both products contributed to a significant increase in Syntex's annual sales, which in 1987 reached $1 billion. Alleve, a pain reliever used for conditions such as arthritis, muscle pain, and menstrual cramps, was then launched a few years later, completing Syntex's transformation into a major pharmaceutical company.[12]

Continued Influence and Recognition

Rosenkranz's legacy continues to be recognized and influential, with his name associated with over 150 patents and over 300 published research articles on steroid hormones. After his retirement, he continued to hold numerous roles in the industry, including as a member of the New York Academy of Sciences and on the boards of Tel Aviv University, the Weizmann Institute of Science, Digital Gene Technologies, and ICT Mexicana. The National Academy of Medicine of Mexico awarded Rosenkranz the distinction of honorary member in recognition of his dedication to scientific work and to the education of his Mexican colleagues at Syntex.[11]

In 2004, Rosenkranz was jointly honored with Alejandro Zaffaroni with the Winthrop-Sears Medal of the Chemists' Club. In 2013, the Biotechnology Innovation Agency and the Chemical Heritage Foundation (now the Institute for the History of Science) presented him with the Biotechnology Heritage Award, recognizing him as a pioneering biopharmaceutical entrepreneur and the mastermind behind Syntex and "the pill".[11]

In addition, Rosenkranz was a highly successful bridge player who authored 15 books on bridge and won.[11]

1.2 Chemical Structure and Molecule characteristics

Naproxen is an arylalkanoic acid, an aromatic derivative of propionic acid.

IUPAC name:(2S)-2-(6-methoxynaphthalen-2-yl) propanoic acid[16]

Trade names:Aleve, Naprosyn[16]

Listed below are some basic characteristics of the molecule as well as some of its physical and chemical properties:[16]

Molecular weight:230.26 g/mol

XLogP3:3.3

Number of hydrogen bond donors:1

Number of hydrogen bonds accepted:3

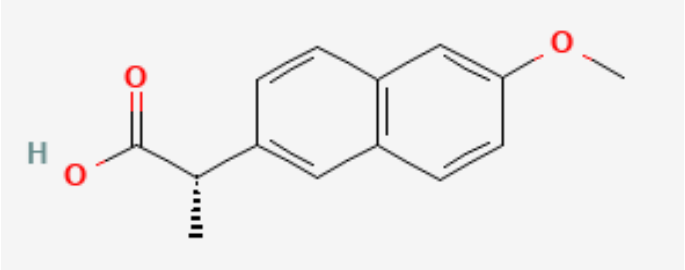

Figure 4. *Chemical structure of naproxen molecule.[16]*

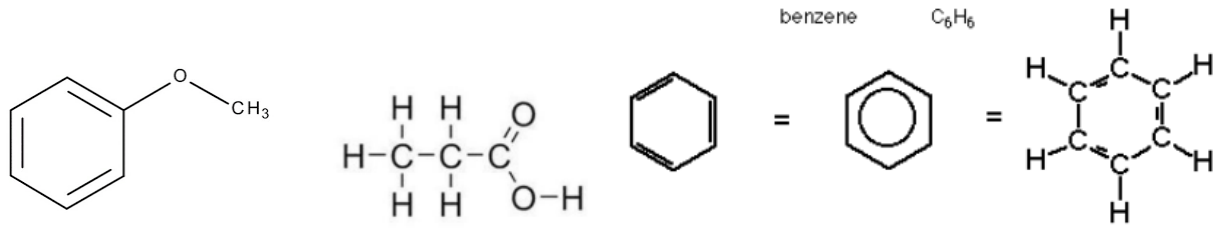

***Picture 5**. Chemical groups that make up the naproxen molecule.*

Referring to the experimental properties of the molecule, its physical description in the literature is a solid, colorless, crystalline stable powder, with a characteristic odor. Its boiling point is at 402-404°C and melting point at 152-154°C. Naproxen is readily soluble in most organic solvents and very soluble in ethanol, 55 mg/mL.[17]

1.3 Mechanism of Action

Naproxen is a non-narcotic drug with strong anti-inflammatory and antipyretic properties. These properties have been proven in human clinical trials and classic animal studies. Anti-inflammatory effects have also been observed in adrenalectomized animals, indicating that its effects are not determined by the adrenal-pituitary axis.

As with other anti-inflammatory drugs, the exact mechanism of action of naproxen is unknown. Naproxen does not inhibit the CNS and does not induce enzyme production. [17] More specifically, naproxen works by reversibly inhibiting COX-1 and COX-2 enzymes as a non-selective coxib. This results in inhibition of prostaglandin synthesis. Prostaglandins act as signaling molecules in the body, causing inflammation. Thus, by inhibiting COX-1/2, naproxen produces an anti-inflammatory effect.[18]

1.4 Pharmacokinetic profile

Naproxen is freely soluble in water and is rapidly and completely absorbed from the gastrointestinal tract after oral administration.

Rapid and complete absorption results in significant plasma concentrations and analgesic effects within 20 minutes of administration. After each administration, peak plasma concentrations are reached after 1 to 2 hours, depending on the amount of food consumed. Steady-state plasma concentrations develop after 4-5 doses. The biological half-life is approximately 13 hours. At therapeutic levels, more than 99% is bound to plasma proteins.

About 95% of a single dose of naproxen is excreted in the urine as unchanged drug. The rate of excretion has been found to approximately correspond to the rate of disappearance of the drug from the plasma.

2. Catalytic system and mechanism

2.1. Catalytic system characterization

Catalysis is the phenomenon in which certain substances, called catalysts, change the rate of a chemical reaction, usually increasing it, without themselves being consumed and without changing the point of chemical equilibrium predicted by chemical thermodynamics under certain conditions. Catalysis is distinguished into homogeneous, heterogeneous and heterogenised homogeneous catalysis. Regarding the first two categories, it is true that in homogeneous catalysis, the catalyst and reactants are in the same phase, usually in solutions. In heterogeneous catalysis, the catalyst is usually a solid body, while the reactants are in the liquid or gas phase. Because in this case the reaction takes place on the surface of the solid, heterogeneous catalysis is also called surface catalysis. In homogeneous catalysis the catalyst is some well-defined species (molecule, ion, ion complex, enzyme), while in heterogeneous catalysis the catalytic action manifests itself in only certain positions of the catalytic surface, the active sites, whose concentration, and much more the nature , very difficult to determine.[18]

According to the picture above, in which the industrial synthesis of naproxen is presented we notice that β-naphthol was brominated to produce 1,6-dibromo-2-naphthol. The labile bromine at the 1-position was then removed with bisulfite and the resulting 6-bromo-2-naphthol (BHN) was methylated with methyl chloride. The yield of 2-bromo-6-methoxynaphthalene (BMN) was 85-90% from β-naphthol.

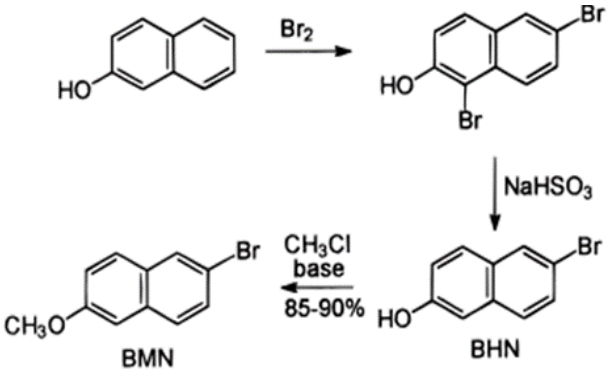

***Figure 5**: Initial phase of industrial synthesis of naproxen.*

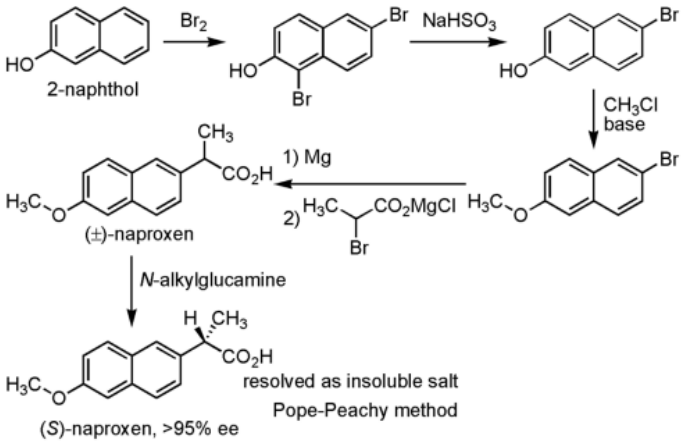

***Figure 6**: Industrial synthesis of naproxen.*

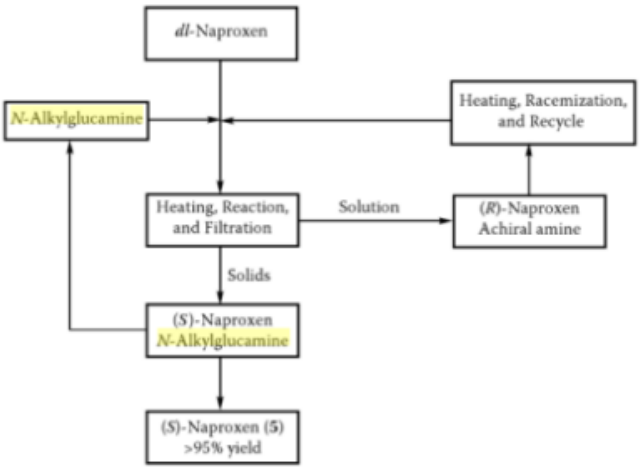

***Figure 7**. Flow chart of the naproxen assay procedure.*

BMN was converted to a Grignard reagent in the presence of Mg (Magnesium), which was directly coupled to a bromopropionic acid salt. As expected, this coupling reaction produced d,l-acid (racemic mixture) as one component of a complex mixture. At the end of the specific industrial synthesis of naproxen is added N-alkylglucamine (Usually prepared by reductive amination of D-glucose and is both a cheap and readily available reagent), which acts as a solubilizing agent[19] to obtain (S) enantiomer of naproxen with 95% enantiomeric excess.[20] It is generally true that, of the two possible enantiomers, only the (S) enantiomer is used for therapeutic purposes. The majority of known synthetic routes, as happens in this particular case, require the preparation of the racemic mixture, the separation of the (S) enantiomer, racemization of the (R) enantiomer, further separation of the (S) enantiomer, and so on. [21] This process for the separation of the S enantiomer is consistently efficient, with a theoretical yield greater than 95%, and is also much more efficient due to the low cost of the separating agent.[20]

The production of S-naproxen requires continuous improvements of the analytical process in order to achieve dramatic cost reductions. The innovation comes from the in-process racemization and recycling of the by-product, i.e. R-naproxen, and the recovery of the solubilizing agent. In this new and efficient assay procedure, racemic naproxen is reacted with half an equivalent of chiral N-alkylglucamine and another half equivalent of a non-chiral amine. Theoretically, there should be an equilibrium of four different salts in this mixture: the salt of the chiral amine with S-acid, the salt of the achiral amine with S-acid, the salt of the chiral amine with the R-acid, and the salt of the non-chiral amine with the R-acid. However, only the salt of the chiral amine with the S-acid is insoluble in the system and crystallizes. This process drives the equilibrium towards the complete formation of S-naproxen - N-alkylglucamine which is collected by filtration and upon acidification liberates S-naproxen. The mother liquor, which contains the unwanted acid and the achiral amine, is heated. The amine base catalyzes the racemization of the R-acid—the resulting salt of racemic naproxen and the achiral amine is then recycled through the assay loop in continuous operation. Although each individual run of the assay yields the diastereomer in 45-46%, the overall result of continuous operation produces S-naproxen with 99% ee in greater than 95% yield from the racemic mixture. The recovery of the dissolving agent, N-alkylglucamine, is greater than 98% per cycle. This efficient combination of analysis, racemization, and recycling of both the undesired enantiomer and the analysis agent dramatically increases throughput, reduces cost, and reduces the waste stream, making it ideal for Pope -Peachy analysis. Despite the availability of so many asymmetric and chiral synthetic tank processes, the optimized analytical procedure still proves to be the most cost-effective route for the preparation of S-naproxen. This example demonstrates that classical analytical technology, when combined with appropriate process engineering, can be a superior method for the preparation of chiral industrial chemicals.[22]

Important reagents

During the first step in the synthesis of naproxen, in order to introduce the bromine into the aromatic ring (benzene), the creation of a Lewis acid, iron tribromide $FeBr_3$, is required. Iron tribromide, as can be seen from the mechanism below, is regenerated during the second stage of the bromination of benzene, so it is understood that it is not consumed during the reaction and thus it is also a catalyst for the benzene-bromine reaction. Br_2 first reacts with Fe to form a catalytic amount of $FeBr_3$.

$$3\ Br2 + 2\ Fe \rightarrow 2\ FeBr3$$

***Picture 6**: Reaction of bromine and iron.*

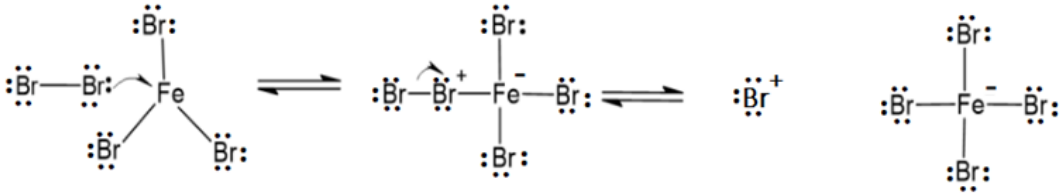

Figure 8. *Reaction between bromine and iron tribromide.*

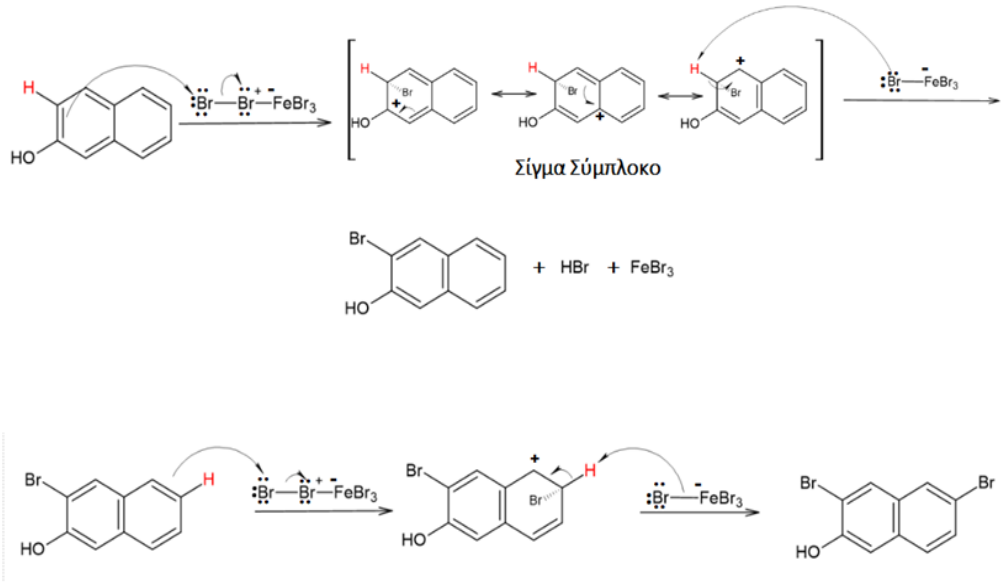

Figure 9. *Sequence of steps for synthesis of 6-Bromo-2-naphthol.*

In the presence of $FeBr_3$, Br_2 can then brominate the aromatic compound through the formation of a complex that serves as an electrophile, so that nucleophilic attack of the complex from the aromatic ring follows.[23]

2.2. Catalytic reaction mechanism

The mechanism for the industrial synthesis of naproxen is not a known and published subject. Below is a simplified and possible version of it, which is very likely in need of improvement and further analysis.

According to the above total composition of (S) Naproxen it is observed that during the first stage of the mechanism β-Naphthol was brominated to form 1,6-Dibromo-2-naphthol. In order to introduce bromine into the aromatic ring, bromine must first react with iron to form iron tribromide. This is because the bromine atom is sufficiently electrophilic to react with the alkene, but not electrophilic enough to react with the benzene. The presence of iron in the reaction mixture enhances the electrophilic character of the bromine atom. Iron tribromide is a Lewis acid and specifically reacts with Br_2 to form a complex that reacts as if it was Br+. This complex, as shown below, serves as an electrophilic medium that achieves the bromination of the aromatic ring, as shown in the following images.

Regarding the bromination of the benzene ring, in the first step the aromatic ring acts as a nucleophile and attacks the electrophilic medium creating a positively charged intermediate called the Sigma Complex or Arenium Ion, which is stabilized through coordination structures. This stage requires an increase in energy, because it involves a momentary loss of aromatic stabilization. The loss of stabilization occurs because the sigma complex is not aromatic - it does not possess a continuous system of overlapping p orbitals. In the second step of the mechanism, the sigma complex is deprotonated thus restoring aromaticity and regenerating the Lewis acid (FeBr3).[23]

The bromine present at the 1-position was then removed with bisulfite ($NaHSO_3$). The reason that the bromine in position 1 is removed is because it is in the benzene ring, in contrast to the bromine in position 6, which is the most stable aromatic ring, while at the same time in benzene there is also the hydroxyl which is a strong activator with the result to increase the stability of the ring so that it is not affected by the removal of the specific bromine atom. The resulting product, 6-Bromo-2-naphthol (BHN), was methylated with methyl chloride and base (indicatively NaOH was used to design the mechanism).

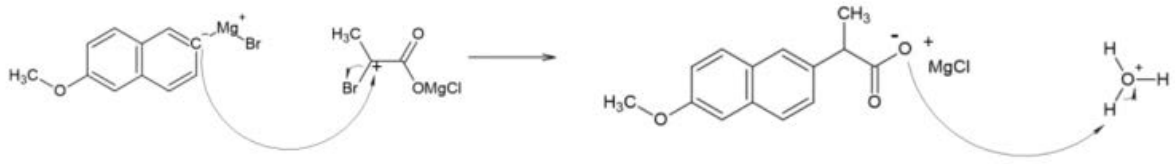

***Figure 10**. Formation of racemic-acid mixture.*

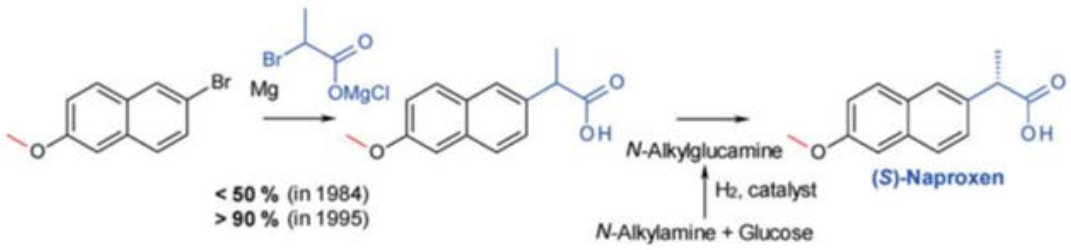

***Figure 11**. Formation of S-naproxen.*

In a next step, Mg is added to form the Grignard reagent. As mentioned above, carbon is more electronegative than magnesium and thus attracts electrons from magnesium by induction. This fact results in the appearance of a negative charge on the carbon atom, with the result that the carbon acts as a nucleophile and is able to attack an electrophile.

What is then formed is a racemic acid mixture of the two enantiomers of naproxen. This racemic acid reacts with 0.5 equivalents of an achiral amine and 0.5 equivalents of an enantiomerically pure amine (the N-alkylglucamine). The chiral amine salt with (S)-naproxen is precipitated and filtered. The salt of (R)-naproxen with the pure amine remains in the mother liquor and is racemized under heating. The racemic mixture is then subjected to the assay cycle again. In this way the performance in the analysis exceeds 95%.[27]

3.Chemical Process Flow Chart

3.1 Importance of Flow Chart

A flowchart (or PFD in this case, process flow diagram) is a visual representation of the flow of a particular system or process that is widely used in many fields, such as information technology, engineering, business management and industry, to analyze, design and process understanding. It uses specific symbols and arrows to show the sequence of steps or decisions that must be made to complete a process. The basic types of symbols used in a flowchart include terminals, processes, decisions, connections, and inputs/outputs. Each symbol has a specific meaning and is used to represent a specific step. It is therefore an important tool in process analysis, as it presents the various steps of a process in sequential order. It can be adapted to cover a wide range of purposes and describe various processes, such as production, administration, services or project plans. In the case of Industrial synthesis, the flowchart is used to:

1. Analyze the production process of a particular product based on the flow of reactants in the appropriate reactors.
2. Visualize the sequence of actions required for the production of the selected product, as it provides a complete picture of the production or operation processes of an industry, facilitating the understanding of the process, i.e. the workflow process and the connection of the various stages and extend the identification of possible points of improvement.
3. Predict process efficiency, detect potential problems and improve production performance.
4. Be used as a training tool to train new employees or retrain staff in different processes.[28]

3.2 Flow Chart of Industrial Catalyzed Synthesis of S-Naproxen

The industrial production of S-Naproxen as shown in the diagram above is a process of several steps. In terms of equipment, a series of reactors and separators are used which serve respectively to carry out reactions and to recycle the reactants back to the reactors in order to achieve the maximum possible efficiency with the least consumption of raw materials. Suitable containers and gas bottles have been chosen to store the necessary reagents, while electronic valves are adapted to reactant containers, specifically in the step of adding the Grignard reagent, as the reaction must take place in the same reactor but with a controlled flow of reactants. In the final stage, the device has a Mixer that creates the appropriate stirring conditions required to form the desired product and store it in the final tank.

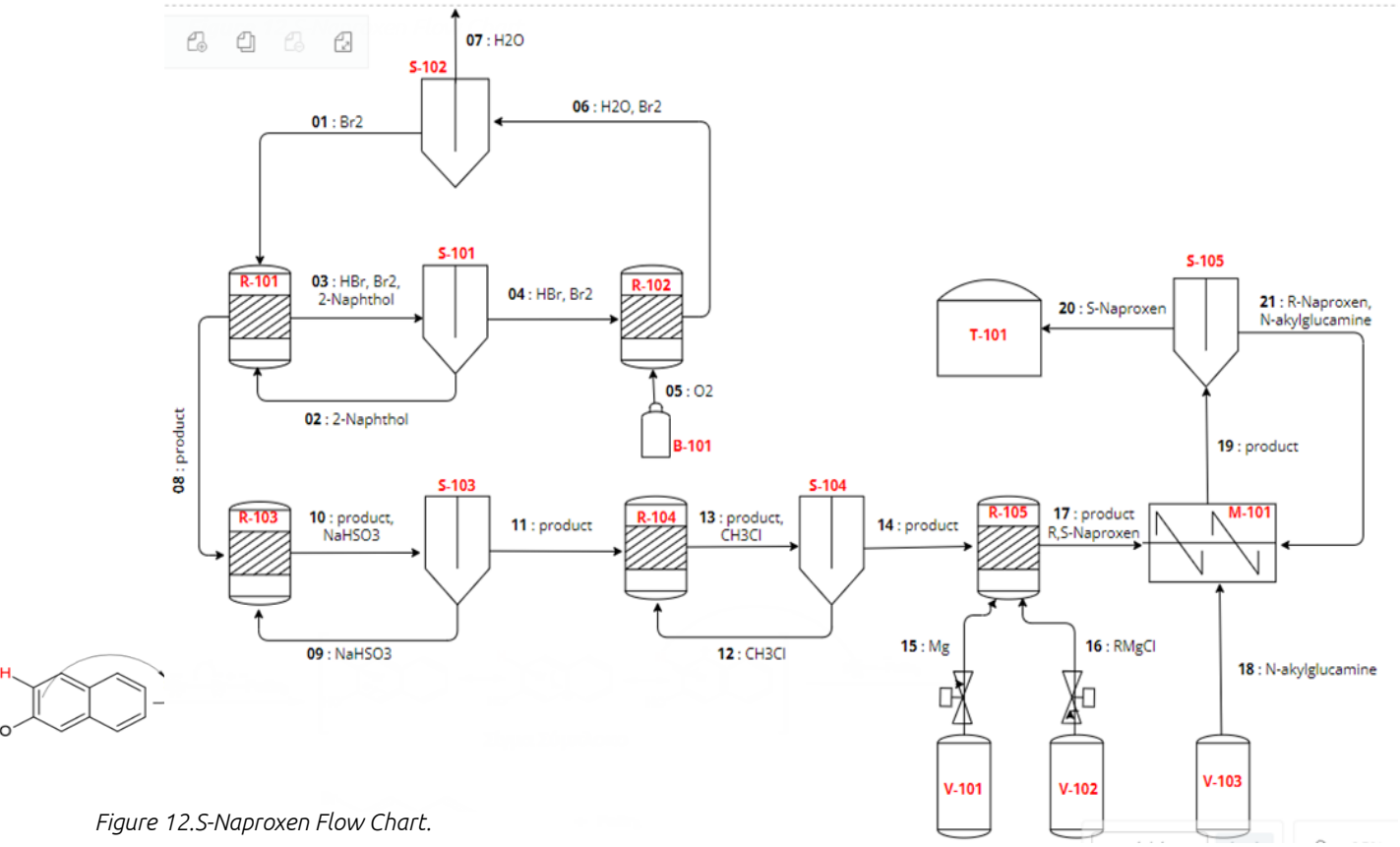

Figure 12.S-Naproxen Flow Chart.

Regarding the raw materials used, the Grignard reagent has the role of reactant while the Br2 introduced during the first stage. In addition, it is important to mention that in the given composition the N-alkylglucamine compound is used as a solvent in the last step. This is a relatively new technique known as the Pope - Peachey method, where the previously mentioned solvent, which in its preparation uses reduction by hydrogen, manages to separate the racemic mixture of naproxen formed when the Grignard reagent is added. S-Naproxen is about 28 times more effective than its R-enantiomer, which justifies the desire to separate them. S-Naproxen can be obtained by enantioselective synthesis but this is expensive and time consuming. The racemic mixture can be readily prepared using a well-developed and optimized method (see PFD Diagram) on a large scale. Currently, most of the enantiopure drug is prepared from the analysis of R,S-Naproxen. R,S-Naproxen is a racemic mixture. It consists of the two enantiomers, R-Naproxen and S-Naproxen, which have identical physical properties and cannot be separated. Therefore, the recovery process (Resolution) is performed by the Pope -Peachey method, an analytical technique based on the formation of diastereomeric salts. The original separation method developed by Pope- Peachey involved adding the separation solvent and a non-chiral auxiliary (achiral base in this case) to the racemic mixture, each in half-equivalent amounts. The separating solvent formed a compound, typically a salt, preferably with one of the enantiomers and caused precipitation of (S-Naproxen). The achiral base increased the solubility of the unreacted mixture of enantiomers and thus the precipitated compound could be removed by simple filtration. However, the now modified method omits the achiral base, relying on the solubility difference between the solvent separation-enantiomer compound and the unreacted enantiomers. In this case N-alkylglucamine is used, a selected base (separation solvent) ideal for the enantiomeric acids (R-Naproxen & S-Naproxen) which will react giving as products of this neutralization reaction (acid + base reaction), salts. The salts formed are no longer enantiomers but diastereoisomers, so they have different physical properties and can reasonably be separated. With this method, not only can the two enantiomers be separated by simultaneously recycling the solvent in each step, but the “unwanted” enantiomer (R) is converted to the desired (S), instead of being discarded, effectively doubling the yield of the product (>95% ee).

4. Industrial application

4.1 Production countries, unit capacity

Naproxen is produced in large quantities and marketed by many pharmaceutical companies worldwide. The largest producers are in India, China and the United States. The

production capacity of these companies ranges from a few tons per year to several thousand tons per year, depending on the size of the company and the demand for the product. Some of the major naproxen producers and their production capacities are as follows:

- Bayer (Germany): 2,500 metric tons per year
- Pfizer (USA): 2,000 metric tons per year
- Yung Shin (Taiwan): 600 metric tons per year
- Almirall (Spain): 250 metric tons per year
- Mylan (USA): 200 metric tons per year

It is important to note that some information may not be available to the public as it may be proprietary information held by the companies that produce and use the particular compound. [29]

According to Volza's global export data, Naproxen export shipments from the world are 21.7 thousand, exports from 1,335 Global Exporters to 2,385 Buyers. Globally most of Naproxen is exported to the United States, India and Bangladesh. The top 3 exporters of Naproxen are India with 14,869 shipments, followed by Mexico with 1,716 and the United States in 3rd place with 1,275 shipments.

According to Volza's global import data, Naproxen import shipments in the world totaled 21.7 thousand, imported by 2,385 Global Importers from 1,335 Suppliers. Globally most Naproxen is imported from India, Mexico and the United States. The top 3 importers of Naproxen are the United States with 6,768 shipments followed by India with 2,682 and Bangladesh in 3rd place with 979 shipments. [30]

According to data obtained from the US Department of Customs, $194,571,772 worth of Naproxen has been exported to 74 countries. The average export price for naproxen was $0.46. The United States was the largest importer of naproxen accounting for 60.5% of total naproxen exports. The United Kingdom was the second largest importer of naproxen accounting for 7.3% of total naproxen exports. The month of June 2016 represented the highest number of export shipments. There are 192 naproxen exporters and 69 naproxen importers.[31]

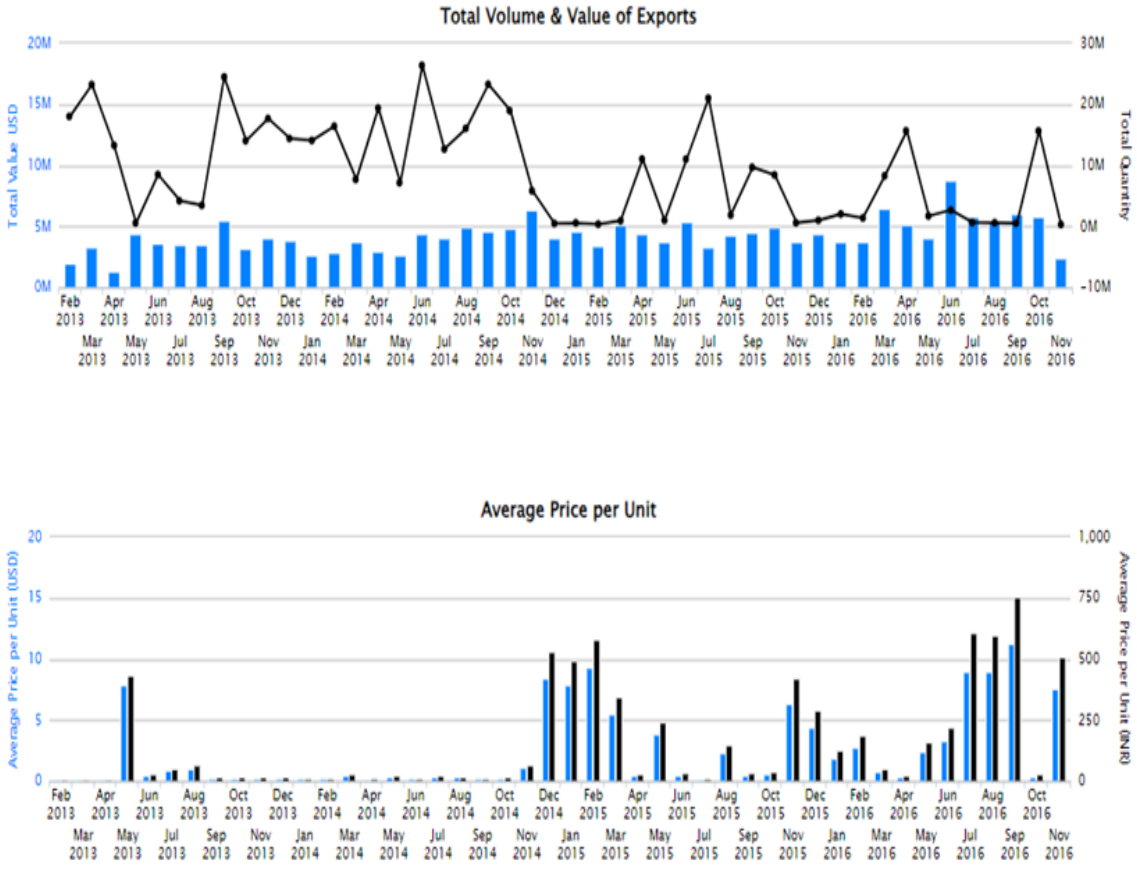

***Figure 13**. Naproxen export volume per month as well as its corresponding value.*

United States	60.5%
United Kingdom	7.3%
Canada	6.2%
Spain	4.9%
Bangladesh	3.1%
Mexico	2.8%
Russia	2.6%
Germany	1.9%
Malta	1.5%
Turkey	1.4%
Iran	1.3%
Philippines	1.1%
Australia	1.1%
New Zealand	0.8%
Ireland	0.8%
Argentina	0.7%
Pakistan	0.7%
Finland	0.7%
Poland	0.6%

***Table 2**: Total value of exports by country.*

United States	86.0%
United Kingdom	11.7%
Malta	1.0%
Canada	0.3%
Honduras	0.1%
Gautemala	0.0%
Australia	0.0%
El Salvador	0.0%
Peru	0.0%
Spain	0.0%
New Zealand	0.0%
Bangladesh	0.0%
South Africa	0.0%
Mexico	0.0%
Philippines	0.0%
Russia	0.0%
Afghanistan	0.0%
Germany	0.0%
Iran	0.0%

Table 3: The quantity of Naproxen exported by country.

4.2. Forms and uses

Naproxen is mainly used as an analgesic and anti-inflammatory drug. It belongs to the class of non-steroidal anti-inflammatory drugs (NSAIDS). NSAIDs are drugs that reduce inflammation, pain and fever with Naproxen being among the three most common along with Aspirin and Ibuprofen. NSAIDs are available in the following four forms: [32]

1)Tablets or capsules
2)Liquid
3)Gels and creams
4)Assumptions

Naproxen in its pure form is mainly found as tablets or capsules [33] and as a liquid. [34] In addition, it is also available in the form of suppositories,[35] while in gel form it is mainly contained as an ingredient (eg Naprosyl gel) and not as pure Naproxen gel.[36]

Naproxen is a structural element in the composition of pharmaceutical products, agrochemicals and perfumes. It is also used in the manufacture of polypropylene fibers and other materials, as well as in the production of polymers and plastics. However, its most widespread use is found in the Pharmaceutical Industry, since as mentioned above it is classified among the widespread NSAIDs. Health care providers use NSAIDs to treat a wide range of symptoms, from headaches and toothache to arthritis and muscle stiffness. Naproxen is primarily used to treat: [37]

- Muscle pains
- Arthritis
- Tendonitis
- Back pain
- Folliculitis
- Toothache
- Menstrual cramps

In conclusion, Naproxen has a wide range of uses in both the medical and industrial fields, with the former being the most widespread, making it a versatile and important chemical compound.

5. Statistical analysis of publications and patents of naproxen

The composition of naproxen has been the subject of numerous scientific publications around the world. After a search of the "ScienceDirect" database, a significant increase in the number of scientific articles related to the synthesis of naproxen in the science of pharmacology was found during the last decade. [42] In 2010, approximately 500 publications were recorded on this topic, but this number has tripled to date. Now that is, the publications that have as their main topic the synthesis of

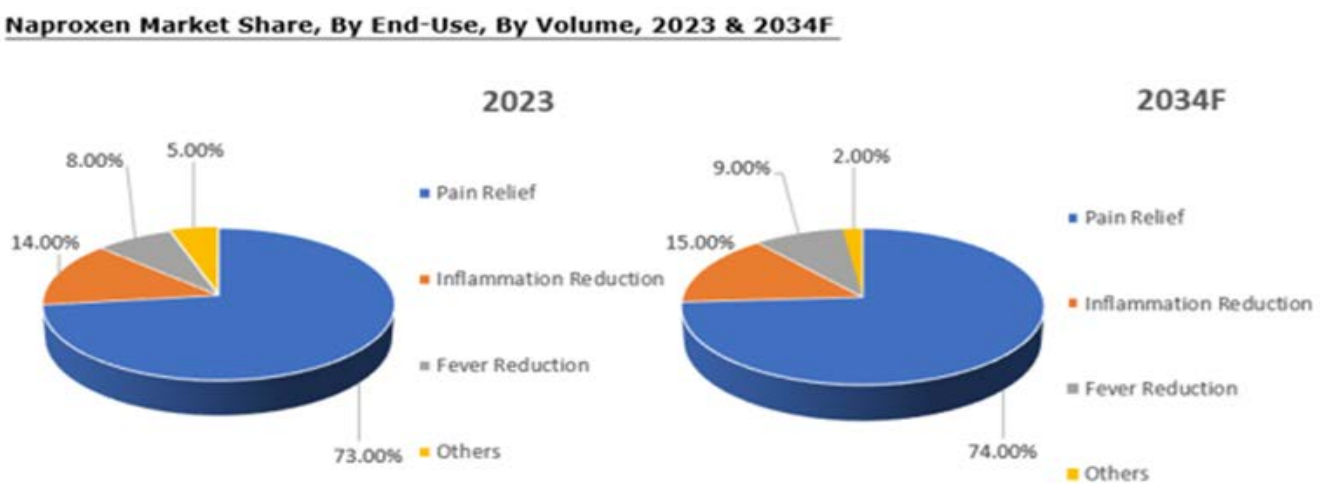

***Figure 14**. The value of naproxen in the market, by use and by volume by decades*

naproxen, have exceeded 1,500. [38] Geographically, the United States holds 30% of all publications, China 20%, India 15% while Europe as a whole holds 25% of publications. The remaining 10% is scattered mainly in the African Continent.[38].

Regarding the distribution of publications, there are significant changes over the years, with China showing the fastest growth rate, from 50 publications in 2010 to 300 publications in 2020. [41,42] Furthermore, 60% of publications are research articles. , while the remaining 40% consists of reviews, discussions and comments. These publications cover a wide range of topics, such as synthesis methodologies (40% of publications), elucidation of naproxen mechanisms of action (25%), naproxen activity (20%), and applications of naproxen in pharmacological research and synthesis new medicinal substances (15%). [41,42]

The industrial formulation of naproxen has also led to an increase in patents worldwide. Patent databases such as those of the United States Patent and Trademark Office (USPTO) and the European Patent Office (EPO) reveal a remarkable escalation of patent applications related to methods of naproxen synthesis. In particular, from 2019 to 2024, the number of patents on naproxen saw an exponential increase in which 500 patents exceeded 2,000 patents worldwide. [39,40,43]

Novartis, Pfizer and GlaxoSmithKline collectively hold approximately 40% of the total patents granted, indicative of their continued research and development. These patents include a wide range of innovations, such as new synthesis techniques (representing 55% of the patents), ways to create more active and pure naproxen (25%), new ways of drug delivery for increased bioavailability (20%). [40, 43]

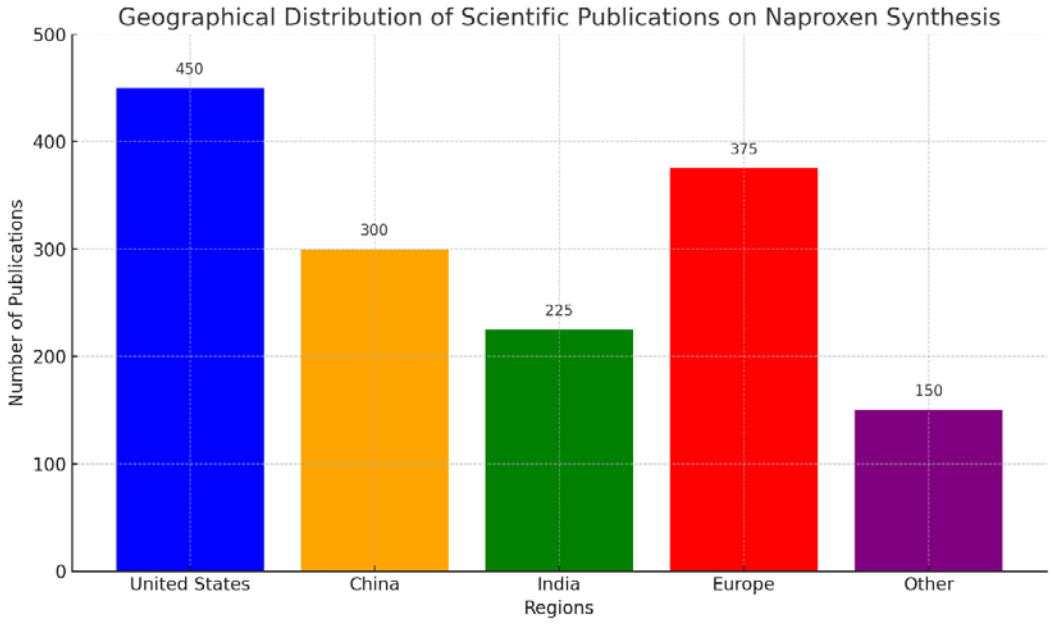

***Figure 15**. Naproxen publication numbers worldwide.*

6. Conclusions

At present study of the pharmaceutical preparation "S-Naproxen" highlighted its important pharmacological action as well as the ways in which this therapeutic substance is prepared. The historical course from the discovery of naproxen to its widespread use today was examined. The production process of the medicinal substance and the importance of active catalytic centers in this process were fully analyzed. This understanding of the mechanism consequently contributes to the design of new effective drugs against each disease.

Furthermore, the analysis of statistical data on publications and patents reveals the wide range of research conducted around naproxen, as well as the competition that characterizes the pharmaceutical industry market. It is anticipated that even more publications and patents will be issued in the future to further optimize this drug. In this way, the practice of medical science will be effectively applied, with the aim of treating patients and improving their quality of life.

However, there is an urgent need to carry out more literature reviews on the medicinal substance of naproxen. The side effects of the drug and all its effects on the human body can be thoroughly studied, in order to highlight the correct health and safety rules for this drug. It is also good to investigate in detail how it affects the tricarboxylic acid cycle of cells, the metabolic pathway of glycolysis, platelet activating factor and cholesterol synthesis and storage in organisms. Based on these investigations, useful conclusions will be drawn, which will help people to understand the correct way to administer the medicine, based on their individual physical characteristics. Various unwanted reactions of the drug in the body will therefore be avoided and the health of consumers will be protected to the highest degree.

7. Bibliography

All websites accessed in April-May 2024

1. Drugs.com. (n.d.). Naproxen Monograph for professionals. https://www.drugs.com/monograph/naproxen.html
2. Ong, C. K. S., Lirk, P., Tan, C., & Seymour, R. A. (2007). An evidence-based update on nonsteroidal anti-inflammatory drugs. *Clinical Medicine & Research, 5*(1), 19–34. https://doi.org/10.3121/cmr.2007.698
3. Harrington, A. P. J., & Lodewijk, E. (1997). Twenty years of Naproxen technology. *Organic Process Research & Development, 1*(1), 72–76. https://doi.org/10.1021/op960009e
4. Harrison, I. T., Lewis, B. M., Nelson, P. A., Rooks, W. H., Roszkowski, A. P., Tomolonis, A. J., & Fried, J. H. (1970). Nonsteroidal anti-inflammatory agents. I. 6-Substituted 2-naphthylacetic acids. *Journal of Medicinal Chemistry, 13*(2), 203–205. https://doi.org/10.1021/jm00296a008
5. Central Business Informatics Journal. (2012). Research Paper 5. https://cbijournal.com/paper-archive/jan-feb-2012-vol-1/Research-Paper-5.pdf
6. Gereffi, G. (1983). *The pharmaceutical industry and dependency in the third world* (2017 reprint ed.). Princeton University Press. ISBN 9781400886227.
7. Freudenheim, M. (1994, May 3). Roche set to acquire Syntex. *The New York Times.*
8. Chemical Heritage Foundation. (2013). George Rosenkranz receives Biotechnology Heritage Award. https://web.archive.org/web/20160712193832/http://www.chemheritage.org/about/news-and-press/press-releases/2013-04-21-george-rosenkranz-biotechnology-heritage-award.aspx
9. Pan American Health Organization. (n.d.). The contribution of PAHO/WHO in the development of the pharmaceutical industry. https://www3.paho.org/English/DD/PIN/Number13_article4_5.htm
10. Science History Institute. (n.d.). George Rosenkranz: Scientific Biographies. https://www.sciencehistory.org/education/scientific-biographies/george-rosenkranz/
11. Pan American Health Organization. (n.d.). The pharmaceutical industry in Latin America. https://www3.paho.org/English/DD/PIN/Number13_article4_1.htm
12. Pan American Health Organization. (n.d.). The pharmaceutical industry: A complex reality. https://www3.paho.org/English/DD/PIN/Number13_article4_2.htm
13. Pan American Health Organization. (n.d.). Pharmaceutical production in the region. https://www3.paho.org/English/DD/PIN/Number13_article4_3.htm
14. National Center for Biotechnology Information. (n.d.). PubChem: Naproxen. https://pubchem.ncbi.nlm.nih.gov/compound/Naproxen#section=2D-Structure
15. Cayman Chemical Company. (n.d.). Naproxen (CAS 22204-53-1) - Product insert. https://cdn.caymanchem.com/cdn/insert/70290.pdf
16. Hawkey, C. J., Langman, M. J. S., Harper, S. E., Thompson, C., Lanas, A., & Logan, R. F. A. (2000). Comparative inhibitory activity of rofecoxib, meloxicam, diclofenac, ibuprofen, and naproxen on COX-2 versus COX-1 in healthy volun-

teers. *Journal of Clinical Pharmacology, 40*(10), 1109–1120. https://doi.org/10.1177/009127000004001005
17. Galinos. (n.d.). Naproxen: Pharmacology. https://www.galinos.gr/web/drugs/main/substances/naproxen/pharmacology
18. Hagen, J. (2015). *Industrial Catalysis: A Practical Approach*. https://doi.org/10.1002/9783527684625
19. Acetti, D., Brenna, E., Fronza, G., & Fuganti, C. (2008). Monitoring the synthetic procedures of commercial drugs by 2H NMR spectroscopy: The case of ibuprofen and naproxen. *Talanta, 76*(3), 651–655. https://doi.org/10.1016/j.talanta.2008.04.009
20. Harrington, A. P. J., & Lodewijk, E. (1997). Twenty years of Naproxen technology. *Organic Process Research and Development, 1*(1), 72-76. https://doi.org/10.1021/op960009e
21. European Patent Office. (1985). Process for preparing naproxen. *EP 0163338 A1*. https://patentimages.storage.googleapis.com/32/89/4c/b5ba37c57d44e0/EP0163338A1.pdf
22. Ager, D. (2005). *Handbook of Chiral Chemicals*. CRC Press by Taylor & Francis Group.
23. Klein, D. (2015). *Organic Chemistry* (2nd American ed., 1st Greek ed.). Johns Hopkins University.
24. Drapeau, M. P., Lafantaisie, M., & Ollevier, T. (2013). Iron(III) Bromide. *Encyclopedia of Reagents for Organic Synthesis*. https://doi.org/10.1002/047084289x.rn01568
25. Deng, Q., Shen, R., Ding, R., & Zhang, L. (2016). Bromination of aromatic compounds using bromine in a microreactor. *Chemical Engineering & Technology, 39*(8), 1445–1450. https://doi.org/10.1002/ceat.201400723
26. Wang, W., Lu, K., Qin, Y., Yao, W., Yuan, D., Pullarkat, S. A., Xu, L., & Ma, M. (2020). Grignard reagents-catalyzed hydroboration of aldehydes and ketones. *Tetrahedron, 76*(18). https://doi.org/10.1016/j.tet.2020.131145
27. Schaefer, B. (2015). *Natural Products in the Chemical Industry*. Springer.
28. Kemper, B., De Mast, J., & Mandjes, M. (2009). Modeling process flow using diagrams. *Quality and Reliability Engineering International, 26*(4), 341–349. https://doi.org/10.1002/qre.1061
29. World Health Organization. (2023). WHO Model List of Essential Medicines - 23rd list, 2023. https://www.who.int/publications/i/item/WHO-MHP-HPS-EML-2023.02
30. Volza. (2023). Naproxen exports from world - Export data with price, buyer, supplier, HSN code. https://www.volza.com/p/naproxen/export/
31. Zauba. (n.d.). Export data and price of Naproxen. https://www.zauba.com/export-naproxen-hs-code.html
32. Cleveland Clinic. (n.d.). NSAIDs (Nonsteroidal Anti-Inflammatory Drugs). https://my.clevelandclinic.org/health/treatments/11086-non-steroidal-anti-inflammatory-medicines-nsaids
33. Deep Heat Australia. (n.d.). Pain relief naproxen liquid capsules. https://www.deepheat.com.au/products/pain-relief-naproxen-liquid-capsules
34. Electronic Medicines Compendium. (n.d.). Naproxen 500mg tablets - Summary of product characteristics (SmPC). https://www.medicines.org.uk/emc/product/14308/smpc#gref
35. Familiprix. (n.d.). Pms Naproxen 500mg suppository – Medication guide. https://www.familiprix.com/en/medications/pms-naproxen-500mg-suppository-02017237
36. Minerva Pharmaceutical. (n.d.). Naprosyn gel. https://www.minervapharmaceutical.gr/product/naprosyn-gel/
37. Cleveland Clinic. (n.d.). NSAIDs (Nonsteroidal Anti-Inflammatory Drugs). https://my.clevelandclinic.org/health/treatments/11086-non-steroidal-anti-inflammatory-medicines-nsaids

*Process Flow Diagram Software. (n.d.). Visual Paradigm. https://www.visual-paradigm.com/features/flowchart-software/

38. Brutzkus, J. C., Shahrokhi, M., & Varacallo, M. (2023). Naproxen. In *StatPearls* [Internet]. Treasure Island (FL): StatPearls Publishing. PMID: 30247840.
39. European Patent Office. (n.d.). Search results for naproxen synthesis. https://www.epo.org/en/results?search_type=website&q=naproxen%2Bsynthesis&filters=%5B%5D&sortField=&sortDirection=&tab=all_results
40. Google Patents. (n.d.). Search results for naproxen synthesis. https://patents.google.com/?q=%28naproxen%2Bsynthesis%29
41. Ha, M. W., & Paek, S. M. (2021). Recent advances in the synthesis of ibuprofen and naproxen. *Molecules, 26*(16), 4792. https://doi.org/10.3390/molecules26164792
42. ScienceDirect. (n.d.). Search results for naproxen synthesis. https://www.sciencedirect.com/search?qs=naproxen+synthesis
43. U.S. Patent and Trademark Office. (n.d.). Search results for naproxen synthesis. https://www-search.uspto.gov/WWW-search.html

Creating augmented reality objects and using them as a teaching tool utilizing zappar software

Theokleia Gkatzianidou[1*], Evangelia Parisopoulou[2], Panagiotis Giannakoudakis[3]
[1] PhD Candidate, Secondary school teacher, Fryganiotis Schools, Greece
[2] PhD in Chemistry Secondary school teacher, Fryganiotis, Schools, Greece
[3] Professor Department of Chemistry, Aristotle University of Thessaloniki, Greece
*Corresponding author's email: theokleiaga18@gmail.com

DOI: 10.62579/JAGC0010

ABSTRACT
This paper presents the construction of augmented reality objects with the aim of studying the three-dimensional structure by middle school students. Traditional methods of teaching chemistry face challenges due to the sub-microscopic nature of chemical structures. Augmented reality provides tools to visualize and interact with them, encouraging student interest and engagement, while providing motivation. Augmented objects depicting 3D molecular models can be created using Zappar software. However, their use requires appropriate infrastructure and teacher training. A balanced approach must be maintained to enhance learning while avoiding common teaching misconceptions, making education more dynamic and interesting.

Keywords: Augmented reality, 3D molecular models, Teaching tools.

INTRODUCTION AND BACKGROUND

Teaching chemistry faces challenges due to the sub-microscopic nature of chemical structures. Students often have difficulty understanding the structure and behavior of atomic, molecular, and ionic compounds. As a result, many alternative concepts occur about the three-dimensional (3D) behavior of them [1]. The phenomenon is intensified when studying subatomic particles and various models or the structure of the atom. Getting students to understand that a molecule is so small that it cannot be observed but has volume and yet remains structured in three dimensions, is a challenge. Teachers try to close the gap between the macroscopic and sub-microscopic world using analogies with experiences from everyday life and the behavior of the compounds, but that can also result in alternative frameworks in students' minds [2].

The initial attempt to bridge this gap in teaching was through modeling with plastic or other materials, which allow teachers to demonstrate chemical structures. The use of plastic models is considered of great help in enhancing students' spatial awareness, but has limitations too. This approach then evolved into electronic simulations, made accessible via the internet [3]. According to research, utilizing both physical and virtual models can help students better understand the concepts in question [4]. However, augmented reality offers a more dynamic and realistic experience.

AUGMENTED REALITY

Augmented Reality (AR) is an innovative technology that has focused on enhancing the real user experience by adding virtual elements to the physical environment [5]. For an experience to be classified as augmented not only it has to provide a connection between physical and virtual reality, but it should be three-dimensional, and the user can interact with it in real time [6]. The portal that connects the two worlds can be accessed through scanning a Qr Code unique to each AR object [7].

In recent years, education has been shifting from teacher-centered transfer of knowledge to more student-centered approaches that are more in line with constructivist learning theory [8]. According to constructivism, knowledge is the result of experiences gained by the individual and is built on pre-existing knowledge by constructing mental models that represent the new knowledge [9], [10]. The use of augmented reality in education is inextricably linked to these trends, as it helps students build mental models.

According to research, the use of augmented reality in the educational process significantly improves the overall performance of students. This is achieved through the motivation it provides to students, causing active participation in the learning process, as well as through its ability to facilitate the understanding of complex concepts and problems [11].

Through it, students can interact with the sub-microscopic level of chemical structures in a way that was previously impossible [12]. They can explore the structures of mol-

ecules and ionic compounds, rotate them, and observe their behavior in space [13]. They can also study the way macromolecules such as proteins and nucleic acids are structured in space and observe bond lengths and angles. This interactive feature provides students with a more comprehensive understanding of chemical structures and can help minimize the appearance of alternative concepts about them [14].

However, the use of augmented reality in the teaching of chemistry is not limited to the subatomic world. There are apps that leverage AR to study concepts like the properties of chemical elements and the periodic table or nomenclature. In addition, augmented reality enables the creation of virtual laboratories, where students can perform experiments and observe the effects of changing parameters in real time. This interactive approach fosters engaging and immersive learning.

Zappar software is a great tool for creating augmented reality content in the education sector. Through ZapWorks Studio, educators can create augmented objects that leverage 3D models and provide information about them, while providing the ability to interact in 3D space. This technology is a valuable tool for chemistry education, enhancing students' understanding and interest.

ZAPPAR SOFTWARE

In the field of augmented object creation there are a variety of platforms and software that support the creation, and implementation of AR, including Unity 3D, BlippAR and Metaverse Studio [15]. For this particular project, the Zappar software was chosen, which was developed in Cambridge in 2011. The main reasons for this choice include ease of use and management, as well as the relatively low cost of obtaining a license [16].

Zappar provides end-to-end AR solutions that appeal to a variety of user groups, from ordinary citizens who want to get familiar with the technology, educators who want to integrate AR into their classroom, and businesses looking to create immersive experiences for their customers. This software offers a range of tools that allow the user to create custom objects with the desired content, as well as servers that ensure access to the material by scanning a simple pointer.

Through the use of Zappar software, simple pointers can be created that lead to AR objects, products and packaging that offer augmented experiences, as well as online augmented reality (WebAR) material. For material creation, there are two main platforms: ZapWorks Designer online and ZapWorks Studio desktop application.

ZapWorks Studio is an advanced application that offers a wide range of capabilities for creating augmented reality (AR) material, going beyond the functionality of Designer, and offering additional options. However, its use is more advanced and requires more technical familiarity. This application allows the creation of AR material without the constraints of being connected to a specific real-world object or person. In addition, it provides the possibility to create animations and timelines that allow the presentation of the object in motion. Although Studio provides all these features without the need for programming knowledge, users with a programming background have the ability to create even more complex experiences, such as games and content that dynamically adapts to each user's needs. This enables the creation of customized and layered AR experiences, offering a wide range of applications in various fields, from education to entertainment and entrepreneurship.

DEVELOPMENT OF THE TEACHING TOOL

In this paper, three augmented objects are presented which contain a total of 13 3D molecular models. For each 3D model, the name and chemical symbol of the element or molecular formula of the compound is provided.

For the development of the augmented reality objects, ZapWorks Studio was used, which allows the import of 3D models produced using modeling software. It is important to note that only specific types of 3D model format can be supported in Zappar [17]. The one more accessible to chemists without virtual 3D modeling knowledge is the Object format (files with extension .obj). These files can be saved from websites such as ChemSpider that use Jmol software to visualize 3D molecular models [18]. Each model is imported into Studio along with the .mtl file generated when it is exported from Jmol. At this stage, the size and position of the molecule is adjusted in the space defined by the application for viewing on the user's smart device. In addition, with the appropriate commands the user can have the ability to rotate and enlarge each model, a characteristic necessary for a more substantial understanding of the three-dimensional structure.

Studio gives the ability to enter parameters of appearance/disappearance, movement, and rotation of the molecule as well as any other object that is imported. In this way buttons can be inserted which are activated by the user's touch. Each button activates a series of commands (timeline) which displays the elements required each time and eliminates all the rest. In the objects created for this paper, the buttons enable the display of the 3D molecular model, return the user to the main menu, or display additional information about the compounds.

Another interesting feature of the application is the accelerometer tool that allows the content of the screen to

adapt to the direction in which the user's mobile is facing. By using the two possible orientations, vertical (portrait) and horizontal (landscape) and appropriate adjustment of the elements inside the screen, the user can see the model in any orientation he wishes.

At each stage of the creation of the object, the Studio provides the possibility of viewing and checking through the preview feature, which creates a temporary Qr Code each time. When the construction of the augmented reality object is complete, it can be published through Zappar and is available to any user who has access to the Qr Code or Zap Code generated by the application. This is done with the scanner present on the smart device giving permission to use the camera, or through the dedicated Zappar app available for Android and iOS.

The augmented material that appears after scanning the Qr or Zapp Code for each object is depicted on the respective figures below each object.

AUGMENTED OBJECTS

The first object is about visualizing Carbon, both in its compounds and its allotropic forms. It contains four (4) common chemical compounds that contain carbon:

- Carbon Dioxide
- Carbon Monoxide
- Methane
- Butane

And two (2) forms of pure Carbon and their 3D structures:

- Diamond
- Graphite

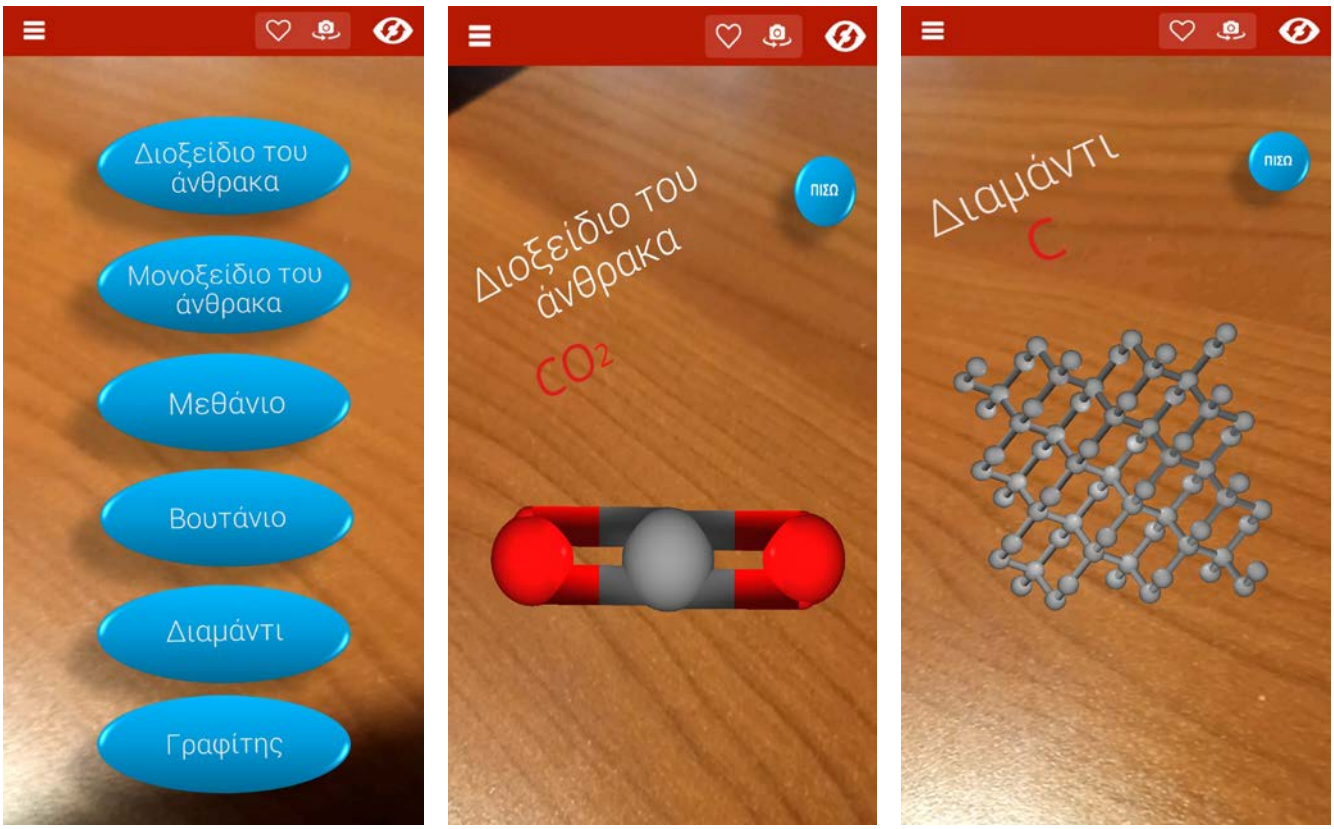

***Figure 1**: Compounds – Forms of carbon.*

***Figure 2**: Qr and Zapp Codes for Compounds – Forms of carbon.*

The second item shows two (2) ionic compounds and their crystal lattice structures:

- Barium sulfate
- Sodium chloride

In the main menu of this object the user has the opportunity to learn some additional information about salts (in Greek) via a link to the ChemNoesis website [19]. Alongside the sodium chloride crystal, there is an info button that activates the state that contains additional information about table salt and a picture of crystals in the microscope.

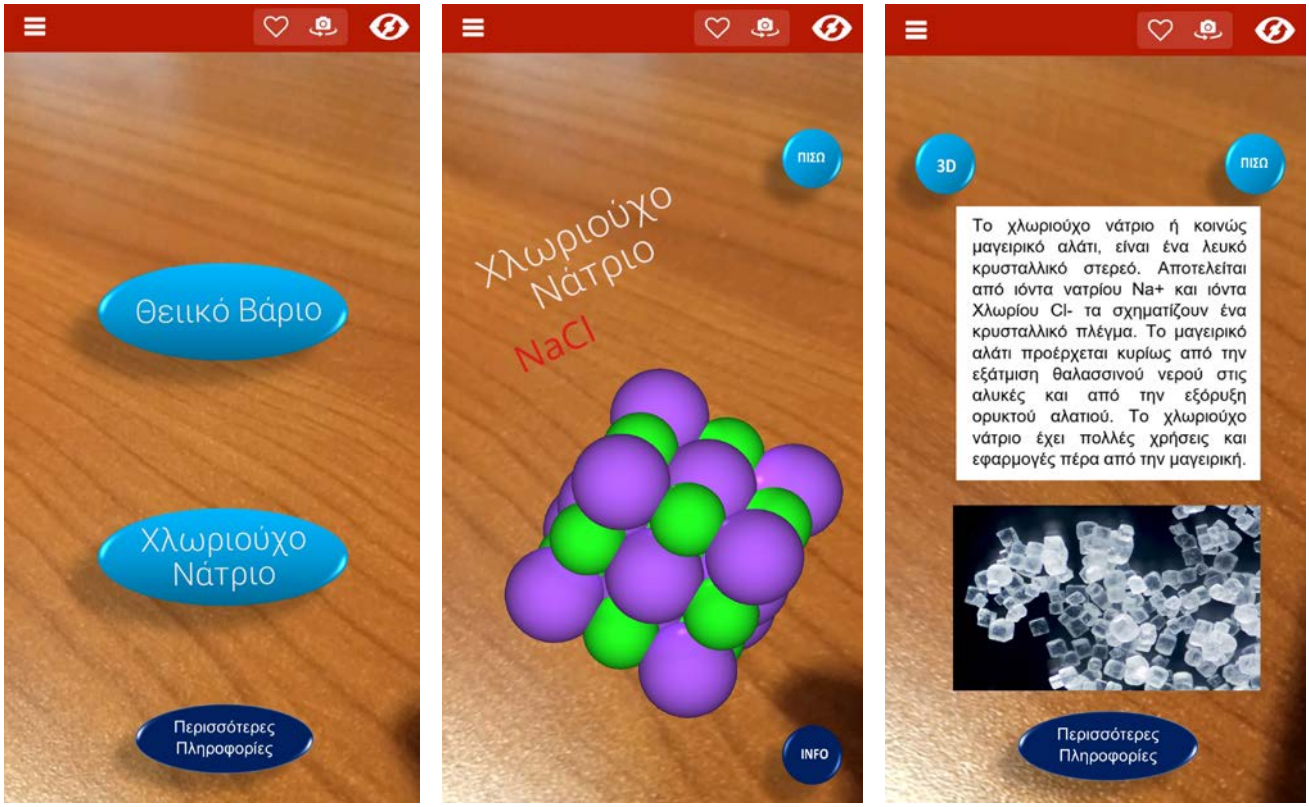

***Figure 5**: Covalent Compounds*

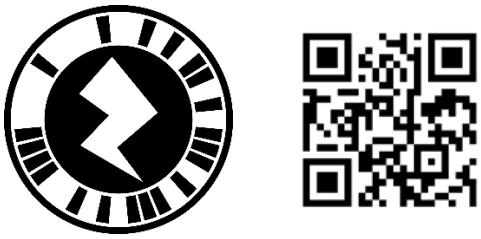

Figure 4: Qr and Zapp Codes for Ionic Compounds

The third object presents five (5) Covalent compounds and their 3D molecules:

- Hydrochloride
- Water
- Nitric acid
- Acetic acid
- Ammonia.

The three objects provide 3D structures for compounds used in everyday life and can all be used in teaching both middle and high school students. In the middle school curriculum, they can be applied in teaching about molecules and ionic compounds in second grade. In the third grade, the first object can be used as supplementary material in teaching about carbon and its properties. High school students can use the second and third object to better under-

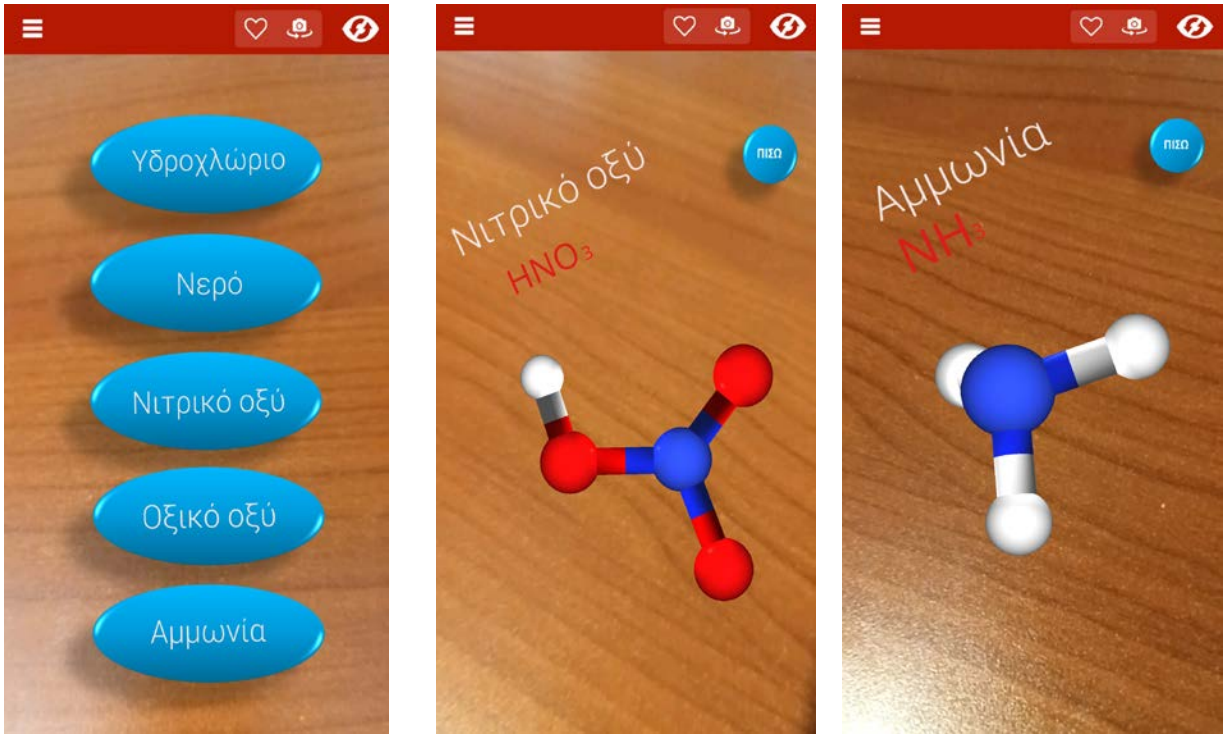

***Figure 5**: Covalent Compounds*

***Figure 6:** Qr and Zapp Codes for Covalent Compounds*

stand the ionic and covalent bonds in first grade. The application of the AR objects can be studied farther in all grades of middle and high school to help students understand more about the sub microscopical level of chemistry.

RESULTS

The augmented objects were utilized in teaching students that are in the second grade of middle school and there was a significant increase in the students' motivation to participate. In general, the use of mobile phones during the educational process arouses the interest of students as they are now a large part of their everyday life. The students reacted positively to the whole teaching approach, although some technical problems regarding the simultaneous use of augmented reality in a large group of students arose during the application. The problems concern access to a fast wireless network and familiarity with the use of the software.

The ability to view and rotate the 3D molecular models proved to help significantly in the more effective understanding of the existence of 3D structure of the compounds in space and reduced to a satisfactory extent the misconceptions that appear when studying these concepts with conventional teaching methods. Students were able to see how atoms are connected, the differences in size that exist in chemical elements, and the angles that exist between atoms. As a result, they understood more efficiently and faster concepts concerning atoms, molecules, and chemical compounds.

CONCLUSIONS

Augmented reality is a modern approach to technology that seeks to integrate virtual elements into the real world.

While this technology holds great promise in the field of education, its limitations should not be overlooked. One of the main limitations is the need for personal devices, such as smartphones or tablets, and access to wireless internet. At the same time, access to the internet via a wireless network is necessary, which is not available in all school units. This type of equipment is not always available in all educational units, causing problems of accessibility and equity in the educational process.

In addition, the successful adoption of AR also requires the training of teachers. Familiarizing them with new technologies, as well as understanding their function, are essential to be able to use it effectively in the educational process. Howev-

er, it is observed that many educators express apprehension or fear towards the technology, which may negatively affect the adoption and effective use of AR in educational practice.
In addition, using augmented reality in an irresponsible way can lead to cognitive load problems for students. Excessive use of images and models can create confusion rather than enhance understanding. Therefore, the successful use of AR requires a balanced approach that takes into account students' needs and abilities, as well as teacher supervision to ensure effective learning.
Overall, augmented reality provides a valuable opportunity to improve the educational process, but its successful adoption requires well-designed approaches and adequate training of teachers and students.

REFERENCES

[1] Kapici, H. O. (2023). From symbolic representation to submicroscopic one: Preservice science teachers' struggle with chemical representation levels in chemistry. *International Journal of Research in Education and Science (IJRES),* 9(1), 134-147. https://doi.org/10.46328/ijres.3122

[2] Taber, K. S. (2017). Teaching and learning chemistry. In *SensePublishers eBooks* (pp. 325–341). https://doi.org/10.1007/978-94-6300-749-8_24

[3] Savec, V.F., Vrtacnik, M., Gilbert, J.K. (2005). Evaluating the Educational Value of Molecular Structure Representations. In: Gilbert, J.K. (eds) Visualization in Science Education. *Models and Modeling in Science Education,* vol 1. Springer, Dordrecht. https://doi.org/10.1007/1-4020-3613-2_14

[4] Chinthammit, W., Yoo, S., Parker, C., Turland, S., Pedersen, S., & Fu, W. (2015). MolyPoly: A 3D Immersive Gesture Controlled Approach to Visuo-Spatial Learning of Organic Chemistry. In *Lecture notes in computer science* (pp. 153–170). https://doi.org/10.1007/978-3-319-16940-8_8

[5] Gutiérrez, J. M., & Fernández, M. D. M. (2014). Applying augmented reality in engineering education to improve academic performance & student motivation. *International Journal of Engineering Education*, *30*(3), 625–635. https://dialnet.unirioja.es/servlet/articulo?codigo=7372823 (accessed May 22, 2024).

[6] Azuma, R. T. (1997). A survey of augmented reality. *Presence*, *6*(4), 355–385. https://doi.org/10.1162/pres.1997.6.4.355

[7] Τσιμούρης, Κ. (2021). Ανάπτυξη Εφαρμογής Επαυξημένης Πραγματικότητας (Augmented Reality) Για Την Οπτικοποίηση Μοριακών Ενώσεων Στο Μάθημα Της Χημείας. *Master Thesis*, National and Kapodistrian University of Athens. https://pergamos.lib.uoa.gr/uoa/dl/object/2937209/file.pdf (accessed May 2, 2024).

[8] Ertmer, P. A., & Newby, T. J. (2013). Behaviorism, cognitivism, constructivism: Comparing critical features from an instructional design perspective. *Performance Improvement Quarterly*, *26*(2), 43–71. https://doi.org/10.1002/piq.21143

[9] Merrill, M. D. (1991). *Constructivism and instructional design*. Learning & Technology Library (LearnTechLib). https://www.learntechlib.org/p/170732/ (accessed June 22, 2024).

[10] Wiesen, G. (2024, March 2). *What is Multimedia Learning?* Practical Adult Insights. https://www.practicaladultinsights.com/what-is-multimedia-learning.htm

[11] Cabero-Almenara, J., Fernández-Batanero, J. M., & Barroso-Osuna, J. (2019). Adoption of augmented reality technology by university students. *Heliyon*, *5*(5), e01597. https://doi.org/10.1016/j.heliyon.2019.e01597

[12] Phon, D. N. E., Ali, M. B., & Halim, N. D. A. (2014). Collaborative Augmented Reality in Education: a review. *Proceedings - 2014 International Conference on Teaching and Learning in Computing and Engineering*, 78–83. https://doi.org/10.1109/latice.2014.23

[13] Wang, Y., & Chen, N. (2019). Application of Augmented reality technology in chemistry experiment teaching. *Proceedings of the 5th International Conference on Economics, Management, Law and Education (EMLE 2019)*. https://doi.org/10.2991/aebmr.k.191225.223

[14] Saidin, N. F., Halim, N. D. A., & Yahaya, N. (2015). A review of Research on Augmented Reality in Education: Advantages and Applications. *International Education Studies*, *8*(13). https://doi.org/10.5539/ies.v8n13p1

[15] Βολιώτη Ο. (2021). Η επαυξημένη πραγματικότητα στην εκπαίδευση: συγκριτική μελέτη. *Master Thesis, University of West Attica*. https://doi.org/10.26265/polynoe-1293 (accessed May 2, 2024).

[16] Zappar. (n.d.). *Zappar: World-leading Augmented Reality solutions since 2011*. Zappar. https://www.zappar.com/ (accessed June 1, 2024).

[17] *Supported formats and requirements*. (n.d.). https://docs.zap.works/studio/3d-models/supported-3d-formats/ (accessed June 1, 2024).

[18] *ChemSpider | Search and share chemistry*. (n.d.). https://www.chemspider.com/Default.aspx (accessed May 19, 2024).

[19] *Αρχική*. (n.d.). CHEMNOESIS. https://chem.noesis.edu.gr/ (accessed May 10, 2024)